DEVELOPMENT OF LECITHOTROPHIC TROCHOPHORE-LIKE *PILIDIUM NIELSENI* FOUND IN FIVE LINEIFORM SPECIES (LINEIDAE; HETERONEMERTEA; PILIDIOPHORA; NEMERTEA) FROM OREGON

by

MARIE KATHERINE HUNT

A THESIS

Presented to the Department of Biology
and the Graduate School of the University of Oregon
in partial fulfillment of the requirements
for the degree of
Master of Science

June 2016

THESIS APPROVAL PAGE

Student: Marie Katherine Hunt

Title: Development of Lecithotrophic Trochophore-like *pilidium nielseni* Found in Five Lineiform Species (Lineidae; Heteronemertea; Pilidiophora; Nemertea) from Oregon

This thesis has been accepted and approved in partial fulfillment of the requirements for the Master of Science degree in the Department of Biology by:

Dr. Svetlana Maslakova	Advisor
Dr. Richard Emlet	Member
Dr. Kelly Sutherland	Member

and

Scott L. Pratt	Dean of the Graduate School

Original approval signatures are on file with the University of Oregon Graduate School.

Degree awarded June 2016

THESIS ABSTRACT

Marie Katherine Hunt

Master of Science

Department of Biology

June 2016

Title: Development of Lecithotrophic Trochophore-like *pilidium nielseni* Found in Five Lineiform Species (Lineidae; Heteronemertea; Pilidiophora; Nemertea) from Oregon

The pilidium larva is an idiosyncrasy defining the Pilidiophora. Its development is unique, and conserved even in derived pilidia; the juvenile is formed via a series of invaginations of the larval epidermis (imaginal discs), then bursts through the larval body while simultaneously consuming it in catastrophic metamorphosis. *Pilidium nielseni* is a lecithotrophic pilidium with two circumferential ciliary bands reminiscent of the "prototroch" and "telotroch" of a trochophore larva, the ancestral larval form of spiralians. However, *pilidium nielseni* represents a convergence on this larval form, not the resurgence of the ancestral larva, and typical pilidial development is conserved. In this thesis, I describe the development of *pilidium nielseni*, and determine it has converged on its body plan at least twice, independently.

CURRICULUM VITAE

NAME OF AUTHOR: Marie Katherine Hunt

GRADUATE AND UNDERGRADUATE SCHOOLS ATTENDED:

University of Oregon, Eugene
Coe College, Cedar Rapids, IA
National University of Ireland Galway, Galway, Ireland

DEGREES AWARDED:

Master of Science, Biology, 2016, University of Oregon
Bachelor of Arts, Psychology and Creative Writing, 2009, Coe College

AREAS OF SPECIAL INTEREST:

Larval biology and evolution
Marine invertebrate zoology

PROFESSIONAL EXPERIENCE:

Graduate Teaching Assistant, Oregon Institute of Marine Biology, University of Oregon, Charleston, Oregon, 2015-2016

Graduate Research Assistant, Oregon Institute of Marine Biology, University of Oregon, Charleston, Oregon, 2013-2014

Substitute Special Education Paraprofessional, San Francisco United School District, San Francisco, California, 2011-2013

One-on-One Autism Paraprofessional, Viola Gibson Elementary, Cedar Rapids, Iowa, 2010-2011

Writing Consultant, Coe College Writing Center, Cedar Rapids, Iowa, 2005-2009

Archivist, Coe College Heritage Club, Cedar Rapids, Iowa, 2007-2008

GRANTS, AWARDS, AND HONORS:

Student Support, Society for Integrative and Comparative Biology, 2016

Robert C. Terwilliger Scholarship, University of Oregon, 2013

Presidential Academic Scholarship, Coe College, 2005-2009

Coe College Writing Scholarship, Coe College, 2005-2009

Writing Center Fellowship, Coe College, 2005-2009

Inducted into Mortar Board Crescent Chapter, Coe College 2008

Writing Fellowship, Coe College, 2008

Coe College Music Scholarship, Coe College, 2005-2007

Inducted into Alpha Lambda Delta, Coe College, 2006

Most Contribution by a Non-Major Music Award 2006

Member Iowa All-Star Band 2005 & 2006

PUBLICATIONS:

Hunt, M. & Maslakova, S.A. 2016. Development of a non-feeding trochophore-like pilidium. *ICB* 56:e1-e250.

Hiebert, T.C. & Hunt, M. 2015. *Cerebratulus californiensis*. In: Oregon Estuarine Invertebrates: Rudys' Illustrated Guide to Common Species, 3rd ed. T.C. Hiebert, B.A. Butler and A.L. Shanks (eds.). University of Oregon Libraries and Oregon Institute of Marine Biology, Charleston, OR.

Hiebert, T.C. & Hunt, M. 2015. *Ramphogordius sanguineus*. In: Oregon Estuarine Invertebrates: Rudys' Illustrated Guide to Common Species, 3rd ed. T.C. Hiebert, B.A. Butler and A.L. Shanks (eds.). University of Oregon Libraries and Oregon Institute of Marine Biology, Charleston, OR.

ACKNOWLEDGMENTS

First, I thank my advisor, Dr. Svetlana Maslakova, for taking a chance on a psych and writing major. I am grateful for her guidance and encouragement both in and out of lab, and appreciative of the time and careful consideration she invested in me and my work. I also thank Dr. George von Dassow for introducing me to microscopy, and for saving the day on numerous occasions with his troubleshooting advice. I am grateful to them both for creating a supportive environment in lab, and for reminding us that we can laugh while we work, and to take a break and go outside every once in awhile. I also want to thank the other members of the Maslakova lab; Brittney Dlouhy-Massengale, who was the first to welcome me to OIMB, Terra Hiebert and Laurel Hiebert, for their patience with my many questions, especially when I was first starting, and Nicole Moss and Kara Robbins, for willing to be my test audience as I put my defense and this thesis together, and whose company has helped me make it through these last few terms.

I also thank my committee members, Dr. Richard Emlet and Dr. Kelly Sutherland, for their feedback, advice, and encouragement on this project. In particular, I'd like to thank Richard for making me think about why, not just what and how, and Kelly for giving me a home in her lab on main campus. I am also grateful to Dr. Poh Khen Loi in the Histology Facility, for her hospitality, and for instructing me in my histology work. This project was supported by grant IOS-1120537, awarded to Svetlana Maslakova by the National Science Foundation, and I appreciate the opportunity it has provided.

Thank you to Maren Dent, Colin Nickerson, and Jessica Scales, who worked with me on this project during our Molecular Marine Biology class. I am also thankful for the worm hunters who braved the rain, cold, and "trail" to Middle Cove during my winter collecting season; Anders Hansen, Ashley Hueckstaedt, Kunica Kosugi, Will Pischel, Carly Otis, and Marcel Rockwell.

I want to thank my fellow grad students for their camaraderie, and for all their help along the way. Thanks to Amy Burgess, Keats Conley, Marco Corrales-Ugalde, Marley Jarvis, Ella Lamont, Caitlin Plowman, Cate Pritchard, Leif Rasmuson, Rose Rimler, Carly Salant, Jenna Valley, and Sam Zeman.

I am grateful to the Graduate Teaching Fellows Federation for their efforts to reach out to and include OIMB, for the community they've built and welcomed us into, and for their passionate commitment to safety and fairness.

Finally, I want to acknowledge that I have been lucky to encounter so many excellent teachers on my way here. I want to thank Country Meadows Montessori School for teaching me to follow my curiosity, and take responsibility for my education, Mrs. Drews and Ms. Monahan at O'Plaine School, Mr. Neal and Ms. Stohl at Viking Middle School, Mr. Triveline and Mr. Leathem at Warren Township High School, Dr. Bob, Chuck, Gordon, Dr. Leonardo, Dr. Sanchini, Dr. Baker, and Dr. Burke at Coe College, and Cheli and Allen at Laney College, for guiding me all the way here. I also want to thank my music teachers and band directors, whose teaching has shaped me as a person and musician; Miss Suzie, Mrs. Mulligan, Heidi, Mr. Worth, Jamey, Mr. Bandman, and Mr. Beckwith.

For my dad, Dr. Edmund Hunt

TABLE OF CONTENTS

Chapter Page

I. INTRODUCTION 01

II. DEVELOPMENT OF A NON-FEEDING TROCHOPHORE-LIKE PILIDIUM, *pilidium nielseni* 09

Introduction 09

Materials and Methods 20

Collection 20

Obtaining Gametes and Rearing Larvae 22

Light Microscopy 23

Flourescent Labeling and Confocal Microscopy 23

Results 25

Developmental Timeline of *pilidium nielseni* 25

Development of the Juvenile Rudiments 38

Anterior Invaginations – Homologues of Anterior Pilidial Axils? 40

Ciliary Band Formation 41

Larval Musculature 41

Juvenile Musculature 44

Juvenile Nervous System 44

Digestive System 45

Discussion 45

III. A MULTIFACETED APPROACH TO DELIMITING SPECIES BEARING *pilidium nielseni* LARVAE 53

Chapter Page

Introduction 53
Methods 59
Larva Collection and Documentation 59
Adult Collection and Documentation 60
Histology of Adult Specimens 61
Flourescent Labeling and Confocal Microscopy 64
Molecular Analysis 65
Alignment and Phylogenetic Analysis 67
Results 69
Phylogenetic Analysis 69
Barcoding Gap 79
Species Delimitation Based on Larval Morphology 81
Species Delimitation Based on Adult Morphology 85
Adult Ecology 87
Discussion 89
IV. CONCLUSION 98
APPENDIX: SPECIMENS AND SEQUENCES USED IN THIS STUDY 100
REFERENCES CITED 112

LIST OF FIGURES

Figure Page

2.1. *Pilidium nielseni* is found in five different pilidiophoran species from Southern Oregon 15

2.2. Adult morphology of *Micrura* sp. “dark”. 16

2.3. Lecithotrophic development of *Micrura* sp. “dark” 26

2.4. Invagination of cephalic and trunk discs in *Micrura* sp. “dark” 28

2.5. Anatomy of the “pileus” stage of *Micrura* sp. “dark” 30

2.6. Anatomy of the torus stage of *Micrura* sp. “dark” 31

2.7. Anatomy of the hood stage of *Micrura* sp. “dark” 33

2.8. Development of the ciliary bands in the *pilidium nielseni* of *Micrura* sp. “dark” 34

2.9. Complete juvenile formed within *pilidium nielseni* of *Micrura* sp. “dark” 36

2.10. Larval muscles in *pilidium nielseni* of *Micrura* sp. “dark” 37

2.11. Development of the juvenile nervous system in *Micrura* sp. “dark” 39

2.12. Juvenile muscle development of Micrura sp. “dark” 43

3.1. Adult morphology of *Micrura* sp. “albocephala” 55

3.2. (A-E) Bayesian analyses of “trochonemertes” and Pilidiophora; (A) Bayesian phylogeny of 16S sequences of the “trochonemertes” species; (B) 16S Bayesian phylogeny of the Pilidiophora supports the monophyly of the four “trochonemertes” species; (C) COI Bayesian analysis of “trochonemertes” species; (D) COI Bayesian phylogeny of the Pilidiophora supports the monophyly of the four “trochonemertes” species; (E) 28S Bayesian analysis of “trochonemertes” species; (F) 28S Bayesian phylogeny of the Pilidiophora supports the monophyly of the four “trochonemertes” species 71

3.3. Larval pore and cirrus of three morphotypes of *pilidium nielseni* 84

LIST OF TABLES

Table Page

2.1. Comparison of juvenile rudiment development in lecithotrophic larvae and one typical planktotrophic larva 12

2.2. Timeline of developmental stages of *Micrura* sp. "dark" *pilidium nielseni* based on developmental milestones 27

3.1. A comparison of results between different species delimitation methods 70

3.2. Average uncorrected *p*-distances showing intra- and interspecific variation in the 16S gene region, COI gene region, and 28S gene region 80

3.3. Range of divergence of inter- and intraspecific variation as uncorrected *p*-distances 80

3.4. Average measurements of each *pilidium nielseni* morphotype 82

CHAPTER I

INTRODUCTION

Nemerteans are a phylum of primarily marine worms, also known as ribbon worms, characterized by an eversible proboscis within a rhynchocoel. Despite their fascinating diversity, and ecological, evolutionary, and phylogenetic significance, nemerteans are frequently overlooked and understudied, and remain relatively unknown even among biologists.

Though they are predators with a significant influence over the infaunal communities in which they live, Nemerteans are often ignored in biodiversity studies, or, if included at all, are listed under the dismissive category of "Nemertean sp." (McDermott and Roe, 1985; Ambrose, 1991; Thiel and Kruse, 2001; Schwartz and Norenburg, 2001). In part, this is due to the difficulty inherent in identifying soft-bodied animals with few distinctive external characteristics (e.g. Schwartz and Norenburg, 2001; Turbeville, 2002; Tholleson and Norenburg, 2003; Sundberg, 2015). Fortunately, this challenge can be overcome by incorporating genetic analysis into biodiversity studies, and using techniques like DNA barcoding to identify and delimit species (e.g. Hebert et al., 2003; Tholleson and Norenburg, 2003; Barber and Boyce, 2006). Currently, there are about 1,300 described nemertean species (Kajihara et al., 2008), but this is likely a gross underestimate. Even along the coast of the Pacific Northwest, one of few regions where nemerteans were thought to be thoroughly catalogued, DNA sequence data recently revealed nearly twice as many species as were previously

documented for the area, including a number of undescribed species (T. Hiebert, 2016). Nemerteans are not alone; by some estimates, up to 90% of marine species are undescribed (Mora et al., 2011; Appeltans et al., 2012). It is important to detect and describe diversity in any group before it disappears, but nemerteans are of particular interest because they are extraordinarily diverse, and can provide insight into patterns of evolution.

Nemerteans group with the Trochozoa (within the Spiralia/Lophotrochozoa), and are closely related to coelomate protostome phyla which have spiral cleavage and trochophore larvae, such as annelids and mollusks (Turbeville et al., 1992; Turbeville, 2002; Andrade et al., 2014). Spiralian development is highly conserved, but spiralians have produced a wide array of body plans and life histories. This makes them ideal for studying evolutionary trends (Turbeville, 2002; Andrade et al., 2012; Henry, 2014). Nemerteans, like most benthic marine invertebrates, have a biphasic life history with benthic adults and planktonic larvae; though their larvae can be divided into two basic larval types, the planuliform larvae and the pilidia, these categories encompass a diverse array of larval types.

Planuliform larvae are named for their superficial resemblance to cnidarian planulae, and are found in the Hoplonemertea and the Palaeonemertea (Norenburg and Stricker, 2002; Thollesson and Norenburg, 2003; Andrade et al., 2014). Their development is comparatively "direct," with the larva gradually becoming more worm-like as it transitions into its adult form. The monophyletic clade

Pilidiophora (Thollesson and Norenburg, 2003), which includes the Heteronemertea and the family Hubrechtidae (formerly considered part of Palaeonemertea), is named for its distinctive pilidium larva, which typically resembles a deer-stalker cap with the earflaps pulled down (from Greek *pilos (πῖλος),* or *pilidion (πιλίδιον)* — a type of brimless conical cap). Their development is "maximally-indirect" (Davidson et al., 1995). The juvenile is formed by a series of discrete, paired invaginations of the larval epidermis, called imaginal discs, as well as unpaired juvenile rudiments possibly derived from the mesenchyme (Maslakova, 2010a and references therein). The discs and other rudiments gradually fuse together around the larval gut, forming the complete juvenile. Development culminates in a dramatic catastrophic metamorphosis wherein the juvenile emerges from—while it simultaneously ingests—the larval body (Maslakova, 2010a). It is thought that the ancestral nemertean larva is more similar to the planuliform larva of the basal Palaeonemertea, while the pilidium represents a highly derived larval form (Thollesson and Norenburg, 2003; Maslakova et al., 2004a, 2004b; Maslakova, 2010a, 2010b).

The basic elements of pilidial development are conserved in all pilidia; each one develops via a sequence of imaginal discs and rudiments and undergoes a dramatic metamorphosis (Schwartz, 2009; Maslakova and T. Hiebert, 2014). However, the shape of the pilidium, the reported number and sequence of rudiments, and the orientation of the juvenile anteroposterior (AP) axis relative to the larval AP axis can vary. Examples include the sock-like *pilidium recurvatum,*

and the mitten-like *pilidium auriculatum* (Maslakova, 2010b; T. Hiebert et al., 2013; Maslakova and T. Hiebert, 2014). Other pilidia deviate even further, altering both larval morphology and feeding mode.

Just in the past decade, the number of known (or suspected) non-feeding pilidiophoran larvae has increased from three (i.e. Desor's larva, Schmidt's larva and Iwata's larva) to twenty (Maslakova and T. Hiebert, 2014; T. Hiebert, 2016). Some of these are uniformly ciliated, while others, in addition to a complete covering of short cilia, have one or two circumferential ciliary bands of longer cilia, which superficially resemble the prototroch and telotroch of some annelid trochophore larvae (Schwartz and Norenburg, 2005; Schwartz, 2009; Maslakova and von Dassow, 2012; Maslakova and T. Hiebert, 2014).

The suspiciously trochophore-like pilidiophoran larva with two transverse ciliary bands was dubbed *pilidium nielseni* in honor of Claus Nielsen, for his theories on the evolution of marine larval forms, in which the trochophore larva plays a central role (Maslakova and von Dassow, 2012). Its discovery is significant. Until 2004, when a vestigial prototroch was discovered in a palaeonemertean, *Carinoma tremaphoros,* convincing evidence for a nemertean trochophore was strikingly absent; nemerteans were the only phylum within the Trochozoa without a trochophore larva (Maslakova et al., 2004a, 2004b). If *pilidium nielseni* were a nemertean trochophore, it would represent a reversion to the hypothetical ancestral trochozoan larval form.

The morphology of the ancestral trochophore has been a matter of some debate. Some theorize that the ancestral trochophore would have two ciliary bands, a prototroch and metatroch, used in opposed band feeding (Nielsen, 1987), while others propose that it had one pre-oral ciliary band, the prototroch, derived from the primary trophoblasts (Rouse, 1999). *Pilidium nielseni* is akin to neither; it undergoes a catastrophic metamorphosis unmistakably similar to that of a typical pilidium (Maslakova and von Dassow, 2012), and, as I show here, its development closely parallels that of a typical planktotrophic pilidium. Rather than a reversion to the hypothetical ancestral trochophore, *pilidium nielseni* represents a remarkable convergence upon a successful larval body plan, the trochophore, and offers insight into the larval evolution and development of nemerteans and lophotrochozoans in general (Maslakova and von Dassow, 2012; Maslakova and T. Hiebert, 2014).

To compare the lecithotrophic *pilidium nielseni* to the typical planktotrophic pilidium and further distinguish it from a trochophore, I tracked and documented its development in laboratory culture with light and confocal microscopy. This is one of the first studies of non-feeding pilidiophoran development using modern methods, i.e. confocal microscopy, rather than histology (Schwartz, 2009; von Döhren, 2011; Martîn-Durán et al., 2015). I show that *pilidium nielseni* develops much like the classic pilidium, despite its unconventional appearance. It forms its juvenile from three pairs of imaginal discs and two unpaired rudiments, all of which fuse together around the vestigial larval gut. Early in development,

pilidium nielseni even takes on the hat-like appearance of a typical pilidium, developing highly reduced transient lobes and lappets, and the initial arrangement of the ciliary bands is also very similar. However, as a lecithotrophic larva, its development is predictably accelerated, and ultimately, its external morphology does deviate from that of a typical pilidium. Even so, the modification in body shape, arrangement of ciliary bands, and accelerated development, is not particularly surprising, as similar alterations have been previously observed in other non-feeding pilidia (Iwata, 1958; Schwartz and Norenburg, 2005; Schwartz, 2009; Maslakova and T. Hiebert, 2014; L. Hiebert and Maslakova, 2015; Martîn-Durán et al., 2015).

Pilidium nielseni represents a novel larval type, illustrates the evolution of a lecithotrophic larva from a planktotrophic ancestor, and serves as an example of convergence upon a common larval body plan (Maslakova and von Dassow, 2012). When the species bearing *pilidium nielseni* are defined and described, and their relationships with other pilidiophorans are established, this will contribute to a larger story about the evolution of novel larval types, the history of lophotrochozoans, and the nemerteans' place in that history (Turbeville, 2002; Thollesson and Norenburg, 2003; Andrade et al., 2004; Henry, 2014). But first, the number of species producing *pilidium nielsen*i larvae needs to be determined, and boundaries between those species need to be defined. Delimiting the species producing *pilidium nielseni* larvae will provide a more complete account of nemertean biodiversity, help determine whether larval morphotypes have

phylogenetic significance, and facilitate further study (Dawydoff, 1940; Chernyshev, 2001; Maslakova and T. Hiebert, 2014).

Traditionally, systematists classified organisms based on characters of adult morphology, but this has been problematic for nemerteans. These soft-bodied worms have few external features that can be evaluated objectively (especially in preserved material), so systematists focused on internal characters reconstructed from serial histological sections (Schwartz and Norenburg, 2001; Strand and Sundberg, 2005; Sundberg et al., 2009). Unfortunately, cladistic studies show that many of these features have no phylogenetic significance (e.g. Schwartz and Norenburg, 2001; Maslakova and Norenburg, 2001; Thollesson and Norenburg, 2003; Sundberg and Strand, 2010). Consequently, most nemertean species are currently lumped into non-monophyletic mega-genera (e.g. *Lineus*, *Cerebratulus*, *Micrura*, *Amphiporus, Tetrastemma*), while many others are placed into monotypic genera (Thollesson and Norenburg, 2003). Genetic data can help refine these relationships, and reveal unknown diversity (Barber and Boyce, 2006; T. Hiebert, 2016).

Genetic data determined the original *pilidium nielseni* (Maslakova and von Dassow, 2012) belonged to an undescribed pilidiophoran species from Southern Oregon, but data from subsequent collections revealed at least four other co-occurring species that produce such larvae, three of which are closely related to the original, and one which is not (Maslakova and T. Hiebert, 2014; this study). Each appears to produce its own variation of the basic, trochophore-like form of

pilidium nielseni. To test whether each larval morphotype corresponds with a different species, I used several sequence-based species delimitation methods, and compared their results to morphological differences (e.g. larval size, the position of ciliary bands, position and length of larval ciliary cirrus). Phylogenetic analyses of sequence data from multiple gene regions resulted in five reciprocally monophyletic clades representing each of the five species. The presence of "barcoding gaps" led to the same conclusion, which was further supported by larval morphology. A unique *pilidium nielseni* morphotype was associated with each species. All together, the four closely-related species formed a monophyletic clade within the Pilidiophora, which is characterized by the *pilidium nielseni*, while the fifth, which is not included in this clade, is related to other pilidiophorans with lecithotrophic development (T. Hiebert, 2016; this study). This indicates that larval synapomorphies, combined with adult morphology and sequence data, are useful in identifying and distinguishing clades, and can further resolve nemertean phylogeny (Maslakova and T. Hiebert, 2014; T. Hiebert, 2016). This project also demonstrates the advantages of collecting and sequencing both larvae and adults, the effectiveness of barcoding, and the benefits of using the congruence of multiple methods to classify organisms.

CHAPTER II

DEVELOPMENT OF A NON-FEEDING TROCHOPHORE-LIKE PILIDIUM, *pilidium nielseni*

Introduction

The pilidium larva is an idiosyncrasy defining one clade of nemerteans, the Pilidiophora. It is unique to nemerteans, and its development is rather eccentric. In a typical planktotrophic pilidium, the juvenile forms from a series of isolated rudiments. Invaginations of the larval epidermis form three paired imaginal discs in a predictable sequence; first the cephalic discs, then the trunk discs, and later the cerebral organ discs. An unpaired proboscis rudiment, possibly mesenchymal in origin, appears at the same time as the cerebral organ discs, and the last rudiment to appear, is the unpaired dorsal rudiment, which is also thought to be mesenchymal in origin. These structures eventually fuse together around the larval stomach, forming a complete juvenile with an anteroposterior (AP) axis roughly perpendicular to the larval AP (which corresponds to the apical-vegetal) axis. Finally, the juvenile will erupt through and ingest the larval body in catastrophic metamorphosis (Maslakova, 2010a).

To avoid ambiguity, I use the term "imaginal discs" only to describe the paired discs which invaginate from the larval epidermis. The term "juvenile rudiments" applies to the paired imaginal discs, as well as the dorsal and proboscis rudiments, which do not appear to invaginate from the larval epidermis in typical pilidia, and are possibly derived from the mesenchyme (Maslakova, 2010a). In literature describing the pilidium, imaginal discs and juvenile rudiments are often used interchangeably, or imaginal discs

are mentioned exclusively without defining the term (e.g. von Döhren, 2011; Bird et al., 2014). In the latter case, "imaginal discs" could be interpreted as juvenile rudiments in general, or imply that only those rudiments which invaginate from the epidermis are being discussed. The inconsistency of the terminology is likely due to the historical understanding of pilidial development. Until recently, it was thought that the typical pilidium developed via seven imaginal discs, all of which invaginated from the epidermis (Norenburg and Stricker, 2002; Maslakova, 2010a). The distinction in terms was unnecessary unless the described pilidium deviated from the usual pattern of development (e.g. Iwata, 1958). However, Maslakova (2010a) suggests that the dorsal disc does not form as an epidermal invagination, and also identifies a second unpaired rudiment, the proboscis rudiment (Maslakova, 2010a). This brings the total number of juvenile rudiments formed during typical pilidial development up to eight, but drops the number of imaginal discs *sensu stricto* to six. Distinguishing between these terms is important because they indicate tissue origin and formation, which is key to understanding pilidial development and distinguishing divergent pilidia.

The classic planktotrophic hat-shaped pilidium larva is widespread throughout Pilidiophora, but there are many variations on this larval form. It is not uncommon for pilidia to differ in shape (e.g. Dawydoff, 1940), and reported number and sequence of imaginal discs, and the orientations of their larval and juvenile axes (Iwata, 1958; Schwartz, 2009; Martîn-Durán et al., 2015). In pilidia, larval and juvenile morphogenesis are dissociated, which may contribute to this flexibility (L. Hiebert and Maslakova, 2015). Unorthodox planktotrophic pilidia, such as the sock-like *pilidium recurvatum* and

the mitten-like *pilidium auriculatum*, likely arose independently from an ancestral planktotrophic pilidium (T. Hiebert et al., 2013; von Dassow et al., 2013). Considering the difference in shape of the *pilidium recurvatum,* it may not be surprising that the AP axis of the juvenile is not perpendicular to the larval AP axis, as in the typical pilidium, but instead corresponds with the larval AP axis (Maslakova, 2010b). Other pilidia abandon planktotrophy all together, a phenomenon much more prevalent than traditionally thought (Maslakova and T. Hiebert, 2014).

Until the last decade, the encapsulated Desor's larva of *Lineus viridis* (Desor, 1848), the adelphophagic encapsulated Schmidt's larva of *L. ruber* (Schmidt, 1964), and the free-swimming planula-like Iwata's larva of *Micrura akkeshiensis* (Iwata, 1958), were considered the three exceptions to pilidiophoran planktotrophy (Schwartz and Norenburg, 2005). While they superficially resemble the direct-developing larvae of hoplo- and palaeonemerteans, each of these pilidia develops via imaginal discs derived from the larval epidermis, and at least the larva of *L. viridis* undergoes a distinct metamorphosis wherein the juvenile devours the larval body, as in a typical pilidium (von Döhren, 2011). However, unlike a typical pilidium, the juvenile of Iwata's lava is described to form via five imaginal discs; paired cephalic and trunk discs and an unpaired dorsal disc, which is described to invaginate from the epidermis shortly after the cephalic and trunk discs (Table 2.1). The paired cerebral organ discs (which Iwata did not consider imaginal discs) invaginate from the stomodeum, and the proboscis, reported to arise form the cephalic discs, forms last (Iwata, 1958). The typical pilidium also forms via eight

	Rudiments reported as imaginal discs	Other reported juvenile rudiments	Rudiments reported with uncertain origin	Source	invaginating rudiments	Total # of juvenile rudiments
Micrura akkeshiensis	**5**	**3**		Iwata 1958	**7**	**8**
	Paired cd and td Unpaired dd	Paired cor Unpaired pb			Paired cd, td and cod Unpaired dd	
Lineus ruber	**4**	**1**	**3**	Martîn-Durán	**4**	**5-8**
	Paired cd and td	Unpaired pb	Paired cod Unpaired pb	et al. 2015	Paired cd and td	
	8			Schmidt 1964	**4**	**8**
	Paired cd, td, and cod Unpaired dr and pb				Paired cd and td	
Micrura rubramaculosa	**5**			Schwartz and Norenburg 2005	**?**	**5**
Micrura verrilli	**5**			Schwartz 2009	**?**	**5**
***Micrura sp.* 803**	**6**			Schwartz 2009	**?**	**6**
***Micrura sp.* "dark"**	**6**	**2**		This study	**6**	**8**
	Paired cd, td and cod	Unpaired pb and dr			Paired cd, td and cod	
Maculaura alaskensis	**6**	**2**		Maslakova 2010a	**6**	**8**
	Paired cd, td and cod	Unpaired pb and dr			Paired cd, td and cod	

Table 2.1. Comparison of juvenile rudiment development in lecithotrophic larvae and one typical planktotrophic larva. The first four columns describe juvenile rudiment development reported in the literature. The fifth column identifies which rudiments were reported to invaginate (and/or shown to invaginate in figures), and should be considered imaginal discs. The final column gives the total number of juvenile rudiments. cd—cephalic, discs td—trunk discs, dd—dorsal disc, cor—cerebral organ rudiments, pb—proboscis rudiment, cod—cerebral organ discs, dr—dorsal rudiment

juvenile rudiments, but six are imaginal discs (i.e. paired cephalic, trunk and cerebral organ discs) (Maslakova, 2010a; Table 2.1). Schmidt's larva is described to form from only two pairs of imaginal discs (cephalic and trunk discs), as well as the proboscis rudiment, while the origin of the dorsal side of the juvenile and the cerebral organs is ambiguous (Martîn-Durán et al., 2015; Table 2.1). Notably, the original description of Schmidt's larva identified paired cerebral organ discs and a dorsal disc (Schmidt, 1964; Table 2.1). It appears that at least a few of the reported differences in development of these various lecithotrophic pilidia are perceived rather than real, and simply an artifact of interpretation by different researchers.

In 2005, a fourth lecithotrophic larval form was discovered in *Micrura rubramaculosa* (Schwartz and Norenburg, 2005). It is described as opaque and spherical with both an apical tuft and an equatorial ciliated band, which the authors suggest may be homologous to the ciliated band of the typical pilidium. Its juvenile is thought to develop via five imaginal discs (Schwartz and Norenburg, 2005; Table 2.1). However, the formation and identity of these discs are not described, and were observed through the yolky epidermis. A few years later, three more lecithotrophic pilidia were described by Schwartz (2009). One belongs to the undescribed species Schwartz refers to as *Micrura* sp. 676 and, similar to the larva of *M. rubramaculosa*, it bears an equatorial ciliated band, while the two others, belonging to *M. verrilli* and the undescribed species referred to as *Micrura* sp. 803, are uniformly ciliated (Schwartz, 2009). In all four of these recently described larvae, the AP axes of the juvenile and larva coincide. In *Micrura* sp. 803, the

juvenile is suspected to form via six juvenile rudiments, all described as imaginal discs, while *M. verrilli* may develop via five imaginal discs, but again, their identity and mode of formation is unspecified (Schwartz, 2009; Table 2.1). This brought the number of known lecithotrophic pilidia to seven. As the pattern emerges, it is important to note here, that while each of these lecithotrophic forms are currently assigned to the *Lineus* or *Micrura* genera, these are are poorly defined, and demonstrably non-monophyletic (Schwartz, 2009; Andrade et al., 2012; Kvist et al., 2014). Lecithotrophy likely evolved within Pilidiophora independently at least four times (Schwartz, 2009), and possibly, as many as eight times (T. Hiebert, 2016), so the categorization of these species as *Micrura* or *Lineus* does not suggest merely one or two evolutionary events (Schwartz, 2009; Maslakova and T. Hiebert, 2014).

In 2012, a trochophore-like lecithotrophic larva with two circumferential ciliary bands was reported and dubbed *pilidium nielseni* (Maslakova and von Dassow, 2012) (Figure 2.1A). Soon after, three genetically distinct, uniformly ciliated lecithotrophic larvae with a juvenile AP axis running opposite the larval AP axis were discovered, along with three more *pilidium nielseni* morphotypes, increasing the number of lecithotrophic pilidia to fourteen (Maslakova and T. Hiebert, 2014). Each of the *pilidium nielseni* larval morphotypes displays slight variations on the trochophore-like theme, and are suspected to represent four distinct species, all of which are undescribed (Figure 2.1). Two were genetically matched to their corresponding adults, which are provisionally referred to as *Micrura* sp. “dark” and *Micrura* sp. “albocephala,” in reference to their adult morphology

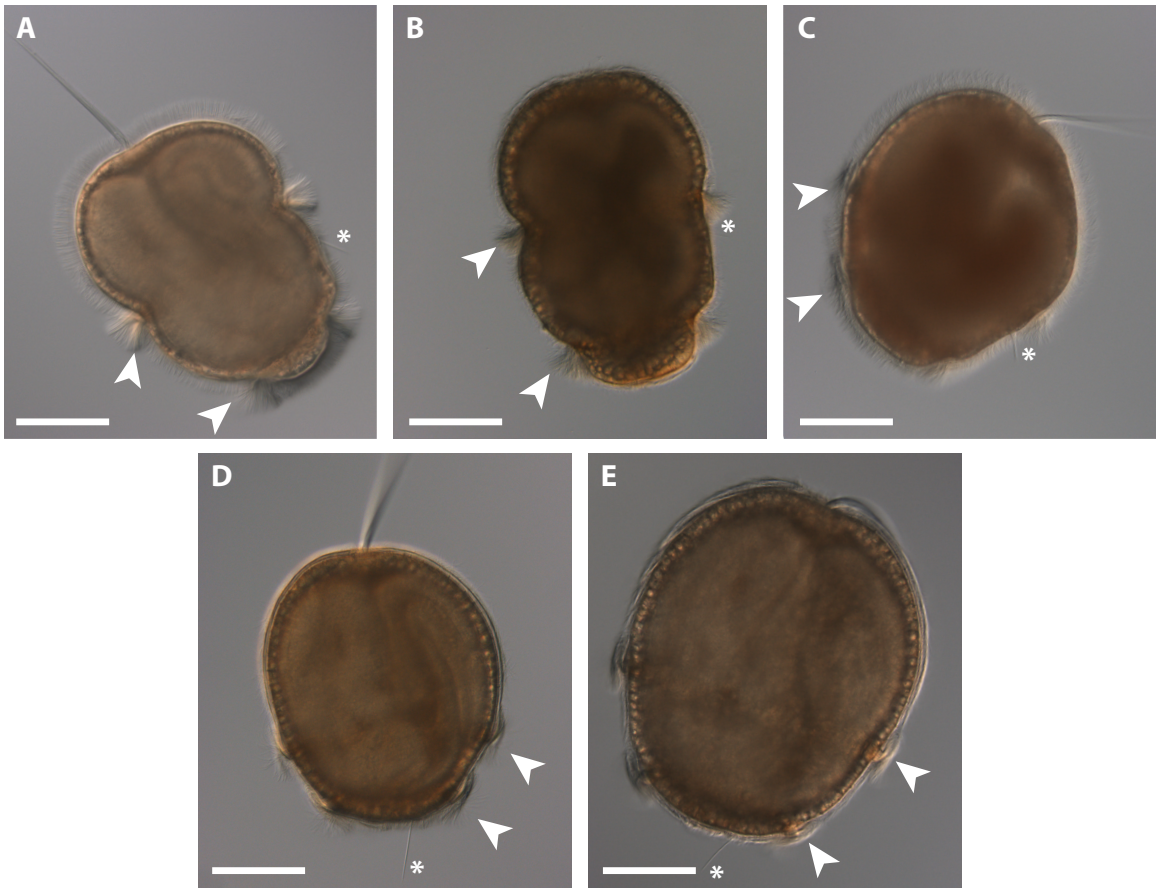

Figure 2.1. *Pilidium nielseni* is found in five different pilidiophoran species from Southern Oregon. DIC images of live larvae of all five species (A-E). Apical tuft is up, juvenile anterior to the left. Transverse ciliary bands are indicated with arrowheads, ciliary cirrus indicated with an asterisk. A. The larva of *Micrura* sp. "dark" with an equatorial "prototroch," and posterior "telotroch." Larval cirrus is located laterally, between the two ciliary bands. B. The larva of *Micrura* sp. 3 with a "prototroch" slightly anterior to the "equator" and a lateral larval cirrus between the two ciliary bands. C. The larva of *Cerebratulus cf. longiceps* with an equatorial "prototroch," and a lateral larval cirrus between the two ciliary bands. D. The larva of *Micrura* sp. "albocephala" with a posterior cirrus and a "prototroch" just posterior to the larval equator. E. The larva of *Micrura* sp. 4, also with a posterior cirrus and a "prototroch" posterior to the equator, is somewhat larger than the larva of *Micrura* sp. "albocephala." Scale bars 100 µm.

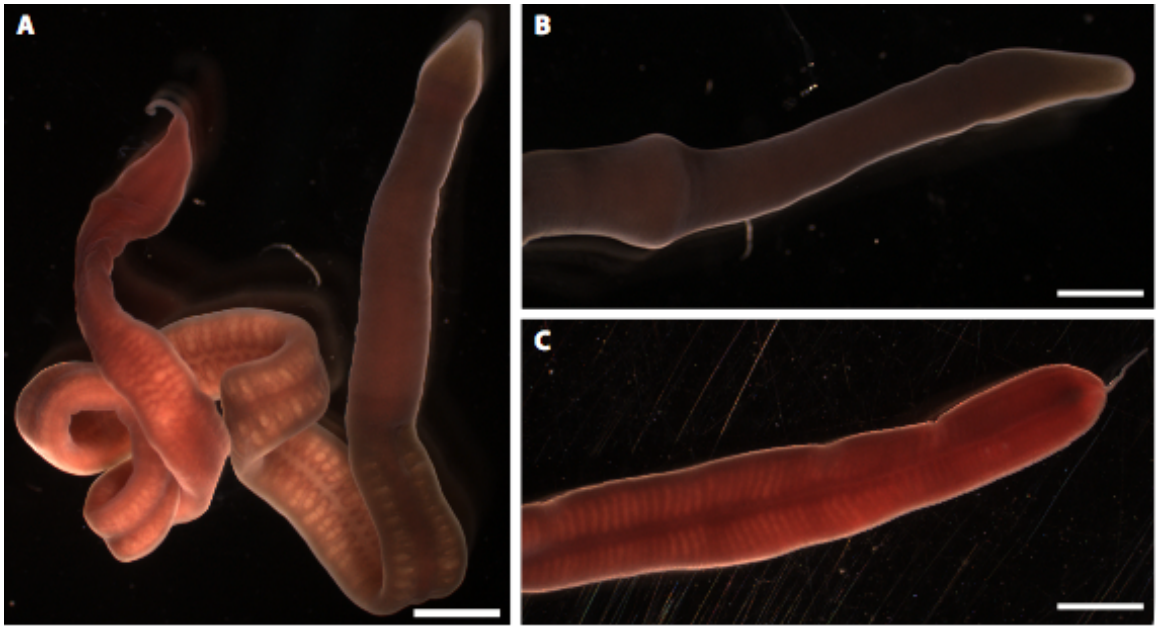

Figure 2.2. Adult morphology of *Micrura* sp. "dark." A. Adult female with characteristically long cirrus and oocytes visible through the epidermis. B. Anterior end demonstrating distinctive peristalsis. C. Posterior end with long cirrus. Scale bars are 2 mm.

(Figure 2.2; see Chapter III). The other two have not been found as adults, and are simply called *Micrura* sp. 3 and and *Micrura* sp. 4.

The larvae of species *Micrura* sp. "albocephala" and *Micrura* sp. 4 both have a larval ciliary cirrus at the posterior end, and a "prototroch" posterior to their "equator," but the larvae of *Micrura* sp. "albocephala" are smaller than those of *Micrura* sp. 4 (Figure 2.1D-E; see Chapter III). Larvae of *Micrura* sp. "dark" have an equatorial "prototroch," and the larval cirrus is located laterally between the "prototroch" and "telotroch" (Figure 2.1A). We have only found two larvae of *Micrura* sp. 3, but they averaged a bit longer than *Micrura* sp. "dark," had a "prototroch" just anterior to the equator, and also had a lateral larval cirrus (Maslakova and T. Hiebert, 2014; Figure 2.1B; see Chapter III). In January of 2014, I discovered a fifth *pilidium nielseni* morphotype

which was pinkish in color, had an "prototroch" shifted slightly posterior to the larval equator, and a lateral cirrus (Figure 2.1C). Sequence data identified it as *Cerebratulus cf. longiceps* (see Chapter III). Most recently, two undescribed, uniformly ciliated lecithotrophic pilidia were reported from Australia (T. Hiebert, 2016). In addition, two undescribed species, Lineidae gen. sp. "large eggs" and *Micrura* sp. "not coei," are reported to have large (200-600 μm) opaque oocytes suggestive of lecithotrophy and, in fact, Lineidae gen. sp. "large eggs" have recently been observed to have encapsulated development (Maslakova and T. Hiebert, 2014; T. Hiebert, 2016; Maslakova, personal communication). In short, the number of known non-feeding pilidia has increased more than sixfold in the last decade. The traditional three exceptions—Desor's larva, Iwata's larva, and Schmidt's larva—are no longer exceptional.

Of all of these, the *pilidium nielseni* larvae are of particular interest because of their superficial resemblance to Nielsen's hypothetical ancestral trochophore; they are ciliated all around, but also bear a long, blade-like apical tuft, and two circumferential ciliary bands composed of longer cilia than those covering the rest of the larva. The two ciliary bands are reminiscent of a spiralian trochophore larva's prototroch and telotroch. However, the equatorial "prototroch" and posterior "telotroch" of *pilidium nielseni* are unlikely to be homologous to the true prototroch and telotroch of other spiralians (e.g. annelids), so these terms are used only as descriptive surrogates, and will therefore remain in quotes. The discovery of a nemertean larva with an apparent "prototroch" and "telotroch" is compelling due to the long-standing controversy surrounding the trochophore larval form. It is commonly believed that the ancestral larval form for many

spiralians, a supraphyletic group which includes the nemerteans, is the trochophore, though the exact form of that ancestral trochophore is debated. Some define the ancestral trochophore as a larva with two ciliary bands that function in opposed-band feeding; the prototroch anterior to the mouth, and the metatroch posterior to the mouth, and in some cases, a posterior telotroch used for locomotion (Nielsen, 1987). Others characterize it by a single pre-oral circumferential band of multi-ciliated cells, the prototroch, which is derived from the primary trochoblast cell lineages (Rouse, 1999). In any case, there is general agreement that the classical trochophore's mouth is posterior to the prototroch, and anterior to the metatroch and telotroch (when these additional bands are present).

Though several lines of evidence, including sequence and ultrastructural data, grouped Nemertea in the Trochozoa (within the Lophotrochozoa/Spiralia), there was a conspicuous lack of evidence for a nemertean trochophore (Turbeville and Ruppert, 1985; Turbeville et al., 1992; Peterson and Eernisse, 2001; Turbeville, 2002; Andrade et al., 2014). Then, in 2004, a vestigial prototroch was discovered in *Carinoma tremaphoros*, a species within the basal nemertean taxon Palaeonemertea (Maslakova et al., 2004a, 2004b). This lends support to the theory that a trochophore larva is ancestral to the nemerteans, and supports its relationship with the trochozoan spiralians (e.g. annelids and mollusks). It would be tempting to consider the *pilidium nielseni* as a return to the ancestral trochophore. However, unlike a true trochophore, the "prototroch" and "telotroch" of *pilidium nielseni* are not on either side of the the blastopore (vestigial mouth); both bands are anterior to the blastopore, which is located at the posterior (vegetal) end of the larva (Figure 2.1). Furthermore, the larva appears to develop

similarly to a classical pilidium, even exhibiting the characteristic catastrophic metamorphosis (Maslakova and von Dassow, 2012). Also, considering that the pilidiophorans are a derived group within Nemertea, and the *pilidium nielseni* represents further derivations from a planktotrophic to a lecithotrophic larval form, it may not be reasonable to draw direct comparisons back to the ancestral form of spiralians at large. Therefore, the *pilidium nielseni'*s trochophore-like appearance is superficial, and arrived at through convergence rather than common ancestry (Maslakova and von Dassow, 2012; Maslakova and T. Hiebert, 2014). To more definitively establish *pilidium nielseni* as an instance of convergence, and determine how much of the pilidial developmental pattern is conserved, I describe and illustrate the development of *pilidium nielseni* produced by *Micrura* sp. "dark" using confocal microscopy, and compare it to that of a typical pilidium.

As of yet, descriptions of lecithotrophic pilidia are scarce, and nearly all have relied on histology (e.g. Hubrecht, 1886; Iwata, 1958; Schmidt, 1964). A few descriptions utilize modern microscopic tools (Schwartz, 2009; von Döhren, 2011), but only one is relatively detailed (Martîn-Durán et al., 2015). Confocal microscopy produces an uninterrupted series of very thin optical sections (0.5-1μm), a significant advantage over the relatively thick (7-8 μm) and often interrupted series of sections provided by traditional histology. Confocal images of *pilidium nielseni* further demonstrate that it is not a trochophore; its development is strikingly similar to that of a typical pilidium. The juvenile develops via three paired imaginal discs and two unpaired juvenile rudiments, then emerges in a catastrophic metamorphosis. *Pilidium nielseni*

even develops transient lobes and lappets in early stages, re-creating the hat-like appearance of a typical pilidium. Also, its "prototroch" and "telotroch" are made up of about six rows of small cells, more like the numerous small cells of the pilidial ciliary band than the large, cleavage arrested cells of a true prototroch (Maslakova et al., 2004b; Maslakova, 2010a; Maslakova and T. Hiebert, 2014). However, it does ultimately alter its body shape and rearrange its ciliary bands, and its developmental timeline is markedly accelerated. Also, *pilidium nielseni* forms one additional transient pair of epidermal invaginations during development, which may correspond to the pilidial anterior axils (Bird et al., 2014). This is one of the first complete descriptions of development of a pilidiophoran with a free-swimming lecithotrophic larva utilizing modern microscopy methods.

Materials and Methods

Collection

Micrura sp. "dark" produces the *pilidium nielseni* first described by Maslakova and von Dassow in 2012. I, along with members of the Maslakova lab and undergraduate volunteers, collected a total of 129 adults in rocky intertidal areas around Cape Arago in Charleston, Oregon (especially Middle Cove, 43.305˚N, 124.400˚ W) during or just prior to their reproductive season. Of these, 33 were collected from October 2013 to March 2014, 41 were collected from July 2014 to February 2015, and 55 individuals were collected from July 2015 to March 2016. The increases in individuals collected from one spawning season to the next are likely due to my improved skill in locating them, rather

than an increase in population. Fertile adults were observed from September through February. Some were fertile when collected, and others (particularly those collected in July and August) developed gametes in the laboratory following collection. Interestingly, despite being kept unfed in the laboratory for a year, a few males developed gametes the next reproductive season. However, I was unable to start cultures with these males, and their sperm appeared somewhat lackadaisical. *Micrura sp.* "dark" were primarily found intertwined with the dense root masses of *Phyllospadix* spp. growing in shell hash, though several individuals were wedged between rocks, or in surf grass rooted in finer sand. Most individuals were collected in root masses of the most dominant surf grass, *Phyllospadix serrulatus,* but also in the root masses of *P. torreyi*, and possibly *P. scouleri.* *Micrura* sp. "dark" may easily be confused with several other local nemertean species, which are similar in size (several centimeters long), pinkish in color, and share the same habitat. Possible misidentifications include the undescribed species *Lineus* sp. "red," which has considerably smaller oocytes than *Micrura* sp. "dark" and develops via a planktotrophic pilidium (T. Hiebert and Maslakova, 2015a), and Lineidae gen. sp. "large eggs," a common co-occurring species with considerably larger oocytes and encapsulated lecithotrophic development (Maslakova and T. Hiebert, 2014; Maslakova, personal observation). *Micrura sp.* "dark" can be distinguished by its nearly constant, pronounced peristaltic motion, which is especially apparent in the foregut region (Figure 2.2B), and by the presence of a distinct caudal cirrus (a tail-like extension of the posterior end, as opposed to the ciliary cirrus in larvae) (Figures 2.2A and 2.2C). One or two of these dramatic anterior to posterior peristaltic waves can be readily observed at nearly any

given time, and their distinct margins conjure up images of a cartoon worm swallowing a series of doughnuts whole.

Initially, individuals were visually identified in the field prior to collection, and subsequently their identity was confirmed via DNA-barcoding. Once I was confident and consistent in my identifications, confirming identification with DNA sequence data was no longer necessary. Adult individuals were photographed, and kept in 150 ml glass dishes in a flow-through sea table at ambient sea temperature, where their water was changed weekly.

Obtaining gametes and rearing larvae

Gametes were dissected from gravid male and female *Micrura* sp. "dark" individuals when reproductive pairs were available. In three instances, sperm was dissected from a male to fertilize naturally spawned oocytes, and in two others, naturally spawned oocytes and sperm were used. The 13 other cultures resulted from dissected oocytes and sperm. Observations are based on eleven embryonic cultures maintained through metamorphosis, including two started with spawned oocytes and one started with both spawned oocytes and sperm, as well as seven other cultures maintained through early developmental stages (two to three days), including one started with spawned oocytes, and another started with spawned oocytes and sperm. Oocytes were fertilized by a dilute suspension of sperm in filtered sea water (0.2 μm), and cultures were maintained in 150 ml glass dishes in flowing sea tables at ambient seawater temperature. The water in their dishes was changed every one to two days. Because the first few cultures

suffered a high mortality rate due to bacterial infestation, subsequent cultures were established and maintained in FSW refiltered through a bottle-top vacuum system (Corning), and an antibiotic solution was added to the cultures. This solution was made up of a mixture of penicillin and streptomycin at a concentration of 5-50 µg/ml each.

Light microscopy

Adult specimens of *Micrura* sp. "dark" were examined and photographed live using a Leica DF400 digital camera mounted to a Leica MZ10F dissecting microscope. Gametes and larval specimens were photographed, trapped between a glass slide and a coverslip supported by clay feet, using a Leica DF400 digital camera mounted to an Olympus BX51 compound microscope equipped with DIC.

Fluorescent labeling and confocal microscopy

Larvae were relaxed in a 1:1 mixture of 0.34 M $MgCl_2$ and FSW for 15 minutes, then in 100% 0.34 M $MgCl_2$ for 15 minutes prior to fixation. They were fixed in 4% paraformaldehyde prepared from 16% or 20% ultrapure paraformaldehyde (Electron Microscopy Sciences) and filtered sea water. Fixed specimens were rinsed in three 10-minute changes of phosphate buffered saline (PBS, pH 7.4, Fisher Scientific), then stored in PBS at 4ºC, or immediately permeabilized and stained. Larvae were permeabilized with three changes of PBS with 0.1% or 0.5% Triton X-100 (PBT) and rinsed in three 10-minute changes of PBS. Specimens were stained with Bodipy FL phallacidin (Molecular Probes) at a concentration of 0.5%, propidium iodide (Sigma) at a 0.1% concentration, or

a combination of both in the same concentrations in 0.1% or 0.5% PBT. Stained specimens were rinsed in three 10-minute changes of PBS, then stored in PBS at 4ºC, or immediately mounted. To view internal structures, specimens were mounted onto Poly-L-lysine (Sigma) coated coverslips, dehydrated through an isopropyl alcohol series (70%, 80%, 90%, 100% I, 100 % II) for 40 seconds-1 minute at each step, then cleared with three 10-minute changes of Murray Clear (a 2:1 mixture of benzyl benzoate and benzyl alcohol). Slides were prepared with strips of foil tape to support the coverslip. After mounting, the coverslips were filled with Murray Clear, which has a refractive index close to that of the immersion oil (~1.5) used during imaging, then sealed with nail polish and imaged immediately, or stored at 4ºC. To view surface structures, stained specimens were placed in a glass bottom dish with PBS, and covered with a coverslip.

Cleared specimens mounted in Murray Clear were imaged with an Olympus Fluoview 1000 laser scanning confocal mounted on an Olympus IX81 inverted microscope with a UPlanFLN 40x 1.3 NA oil lens. Uncleared specimens mounted in PBS were also imaged with the Olympus Fluoview 1000 laser scanning confocal mounted on an Olympus IX81 inverted microscope, but with a UPlanFLN 40x 1.15 water lens. Stacks of 0.65 µm optical sections were imported into ImageJ 1.47v (Wayne Rasband, Nations Institute of Health, Bethesda, MD, USA) for further processing. In figures, I refer to stacks of a subset of optical sections (most often projections of three sections) as “slabs.”

Results

Developmental timeline of pilidium nielseni

I raised eleven cultures of *Micrura* sp. "dark" through metamorphosis, and seven more through the early developmental stages. Reproductive females were readily identified due to the relatively large size of the oocytes, which were visible through the body wall (Figure 2.2A). Whether spawned freely through the gonopores or dissected out, oocytes were ~250 μm in diameter, opaque and pale orange in color, and had a distinct ~265 μm diameter chorion and ~430 μm jelly coat (n=6) (Figure 2.3B). Reproductive males had conspicuously pale gonads. The sperm have a compact head ~5 μm long (n=6), as is typical of species with external fertilization (Stricker and Folsom, 1998; Figure 2.3A). The rate of development was highly dependent on temperature, with cultures at 8ºC requiring at least 20 days to metamorphose, and cultures at 16ºC metamorphosing as early as 9 days after fertilization (Table 2.2). For simplicity, I will focus on describing the order and earliest appearance of significant developments of larvae raised in cultures fertilized at ~16ºC.

I did not observe the formation of polar bodies or germinal vesicle breakdown (GVBD), but in previously studied nemertean species, primary oocytes are released, undergo GVBD upon contact with sea water, and produce polar bodies after fertilization (Maslakova, 2010a). It is unclear how this occurs in *Micrura* sp. "dark." After fertilization, eggs underwent equal spiral cleavage, with a distinct size difference between the animal and vegetal quartets at the eight-cell stage (Figure 2.3D). However, without the polar bodies to indicate which quartet represents the micromeres, it is unclear

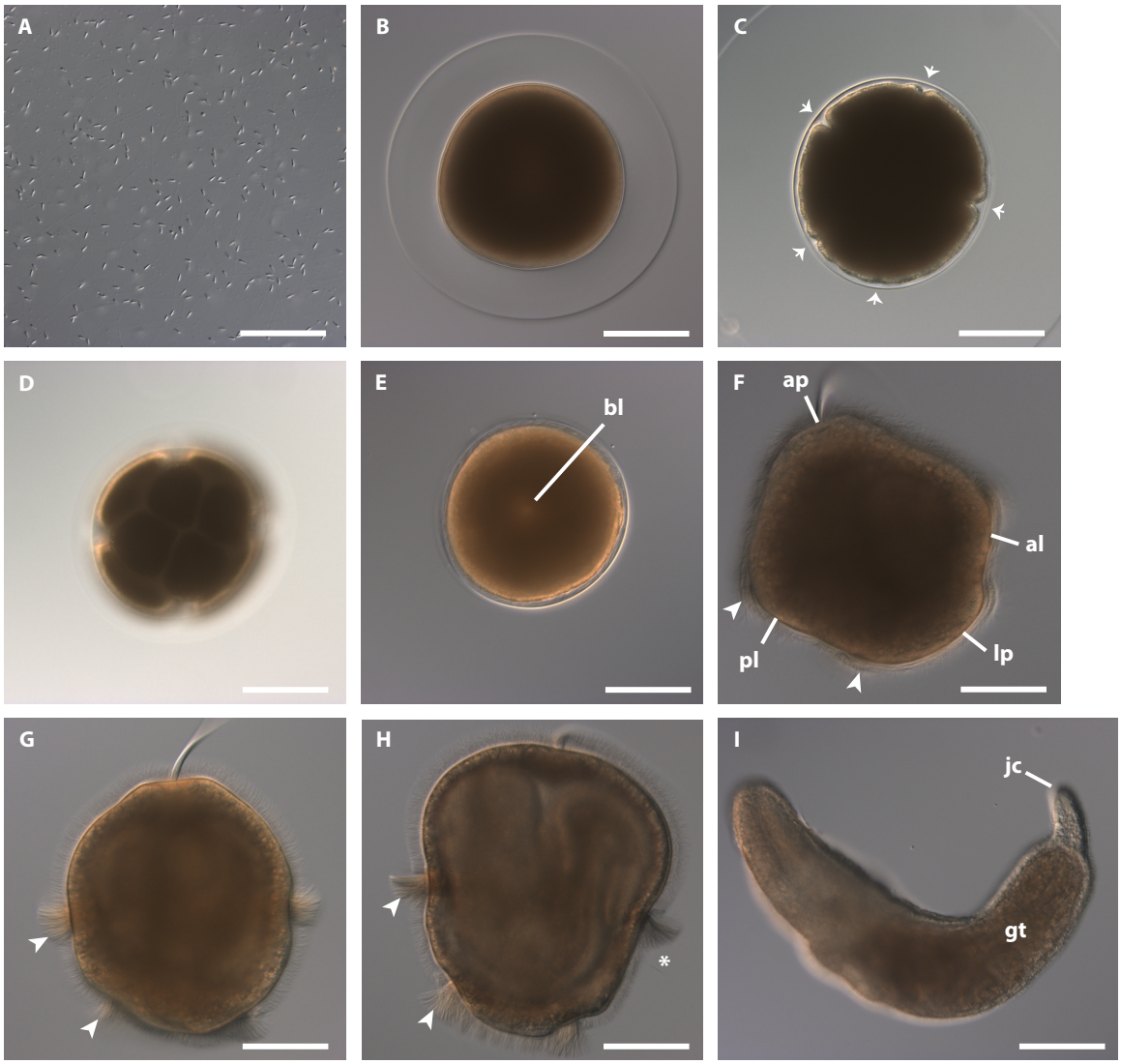

Figure 2.3. Lecithotrophic development of *Micrura* sp. "dark." DIC images. A. Sperm with a compact head. B. Unfertilized oocyte. C. Furrowing prior to cleavage in a fertilized oocyte. Furrows marked with arrows. D. Eight-cell stage demonstrating spiral arrangement of blastomeres. E. Ciliated gastrula with a narrow blastopore (bl). F. Lateral view of "pileus" stage with an apical tuft (ap), transient lateral lappets (lp), anterior (al) and posterior lobes (pl), each fringed with a ciliary band (arrowheads). G. Larva which has lost its lobes and lappets, taking on the characteristic *pilidium nielseni* shape with two transverse circumferential ciliary bands. The cilia are fanned out during a brief arrest of ciliary beat, as is typical in *pilidium nielseni*'s stop-start swimming pattern. H. Lateral view, juvenile anterior to the left, with the larval cirrus (asterisk) in focus. The juvenile body is visible through the larval epidermis. I. A recently metamorphosed juvenile with its larval body in its gut (gt). Juveniles have a long lateral cirrus (jc) at the posterior end. Scale bars 100 µm.

Stage	Description	Earliest appearance (16°C)	Earliest appearance (8°C)
Furrowing	Embryo furrows at five sites (Figure 2.3C)	2.5 hrs	3 hrs
1st Cleavage	Embryo cleaves equally	3 hrs	4 hrs
Blastula	Blastula is slightly flattened along the animal-vegetal axis	15.5 hrs	22 hrs
Gastrula	Gastrula is still somewhat flattened along animal-vegetal axis, becomes ciliated, and develops an apical tuft and vegetal invagination. Gastrulae may swim freely in advanced stages (Figure 2.3E)	20.5 hrs	24 hrs
Cephalic discs	Paired cephalic discs are the first to invaginate (Figure 2.4)	30 hrs	—
Cephalic and trunk discs	Paired trunk discs invaginated shortly after the cephalic discs (Figure 2.4)	42 hrs	—
Pileus stage	Larva develops transient lobes and lappets, the gut curves backward, ciliary bands develop, the paired cerebral organ discs invaginate from the gut, and the proboscis and dorsal rudiment appear. (Figures 2.3F and 2.5). Ciliary bands initially form in four segments which span each transient lobe and lappet. (Figure 2.8)	3 days	3 days
Torus stage	The head and trunk rudiments fuse around the base of the gut (Figure 2.6). Ciliary band segments are re-arranged to form two complete transverse ciliary bands.	4 days	—
Hood stage	The trunk rudiment extends over the proboscis, but has not yet fused with the head rudiment, leaving a dorsal gap (Figure 2.7)	6 days	—
Metamorphosis	The head and trunk rudiments fuse to form a complete juvenile competent to metamorphose (Figure 2.9)	9 days	18 days

Table 2.2. Timeline of developmental stages of *Micrura* sp. "dark" *pilidium nielseni* based on developmental milestones. Uncertain data points are indicated with a dash.

whether the micromeres are larger than the macromeres, as they are in other nemerteans with described development (Maslakova et al., 2004a), or the other way around, as in most appearing as a cross-section of an orange with four relatively equal-sized segments, and a fifth smaller segment, usually about an hour prior to first cleavage (Figure 2.3C; Table 2.2). First cleavage occurred as soon as three hours after fertilization, but most often occurred after four hours (Table 2.2). This relatively large time range may be

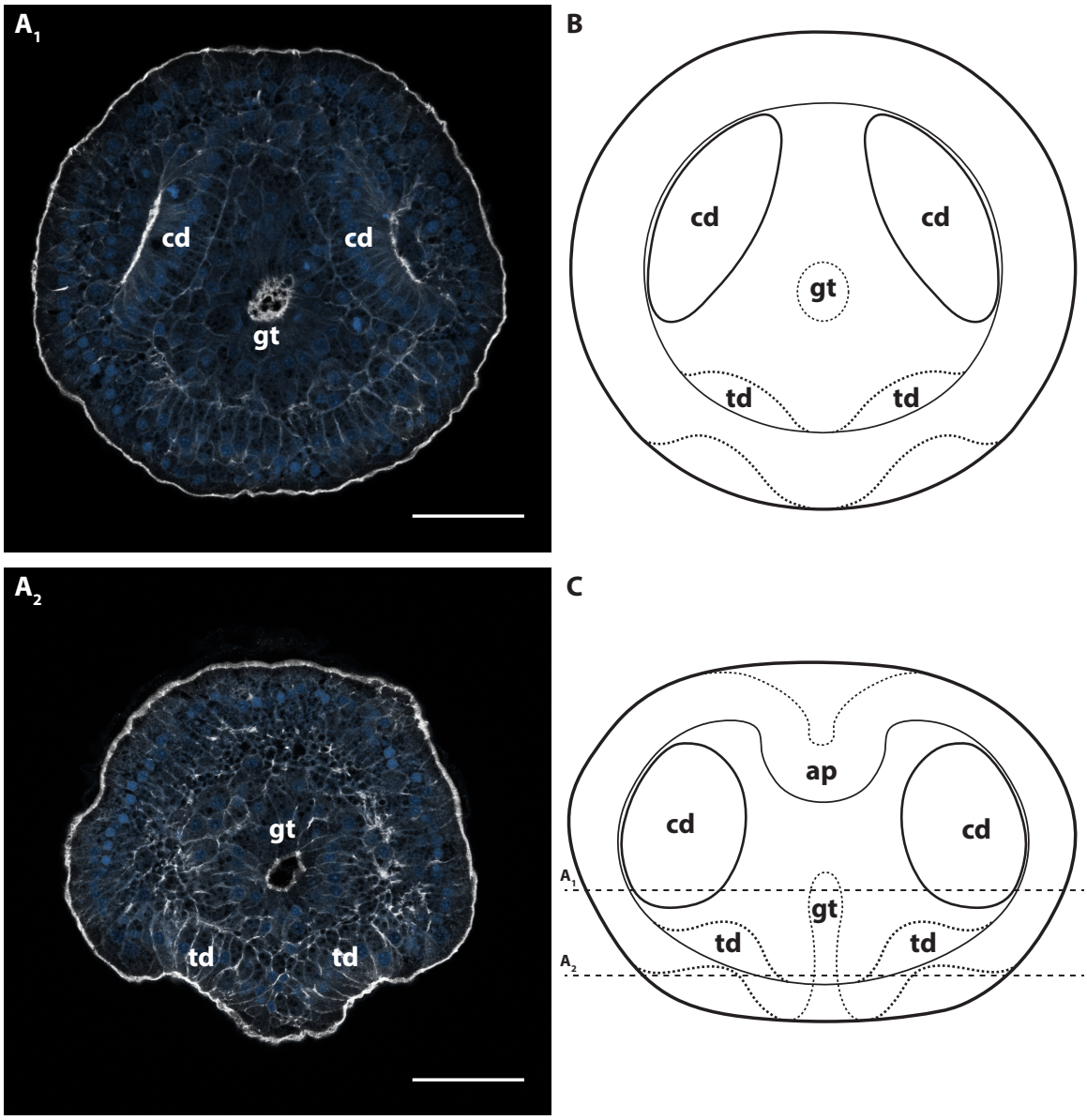

Figure 2.4. Invagination of cephalic and trunk discs in *Micrura* sp. "dark." A_1-A_2 are confocal projections of specimens stained with phalloidin (white) and propidium iodide (blue). Transverse sections (from apical to vegetal), anterior lobe is up. A_1. A 1.95 µm slab showing the cephalic discs (cd) and the gut (gt). A_2. Same individual as on A_1, a 1.95 µm slab showing the trunk discs (td) invaginating from the larval epidermis. B. A diagram (apical view) summarizing A_1-A_2. C. A diagram of the same stage as on A-B, showing a frontal view (apical up). Horizontal lines show approximate levels of the sections in A. Scale bars 50 µm.

attributable to the length of time oocytes were exposed to sea water before insemination. Second cleavage occurred as soon as 30 minutes later, with most cleaving 4.5-5.5 hours post-fertilization, and the 8-cell stage was reached as early as one and a half hours following that, though most cultures required two hours to progress from second to third cleavage. Subsequent cleavage stages were reached every hour, approximately.

The blastula develops within the first day, as early as 15.5 hours after fertilization (Table 2.2). Embryos gastrulate and develop cilia several hours later, as early as 20.5 hours after fertilization (Figure 2.3E, Table 2.2). Larvae hatch from the chorion and begin swimming the next day. The cephalic and trunk disks were apparent before the second day (Figure 2.4). The third day, larvae reach what I call the "pileus" stage, in reference to the type of hat worn in ancient Greece and surrounding regions that the pilidium is named for. In the "pileus" stage, the shape of the *pilidium nielseni* resembles a (reduced) typical pilidium (Figures 2.3F and 2.5); it has stubby lateral lappets and anterior and posterior lobes surrounding the vegetal blastopore. "Pileus"-stage larvae are ciliated over their entire surface, but also have a prominent apical tuft, and its reduced lobes and lappets are fringed with longer cilia. The longer cilia along the margins of the lobes and lappets are organized into four ciliary band segments, one spanning each larval lobe or lappet (Figures 2.3F and 2.8). At the same time, the unpaired proboscis and dorsal rudiments develop, while the cerebral organs invaginate from the basal portion of the gut (near the blastopore) (Figure 2.5). In addition, a tiny pair of invaginations are noticeable between the anterior lobe and lappets, in a position corresponding to the anterior axils (the growth zones) of the pilidium larva (Bird et al., 2014; Figure 2.5C).

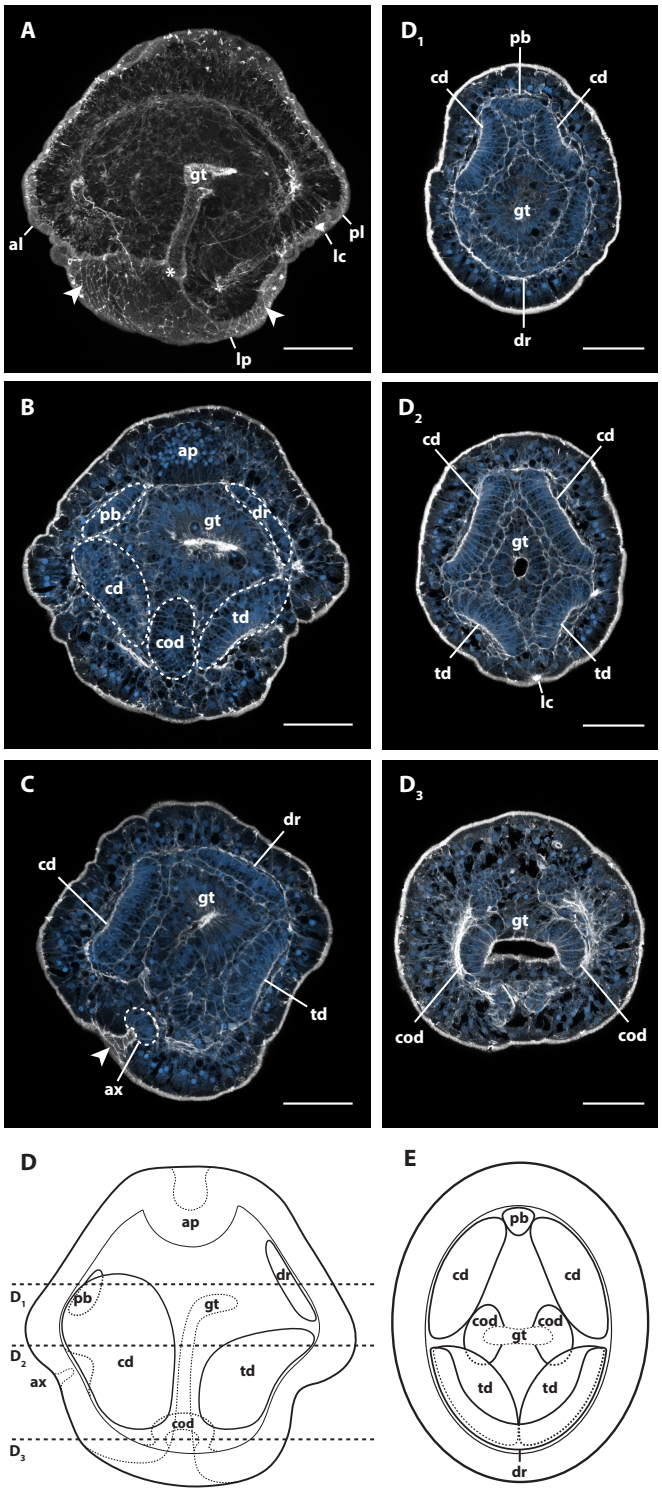

Figure 2.5. Anatomy of the "pileus" stage of *Micrura* sp. "dark." A-C, D_1 -D_3 are confocal projections of specimens stained with phalloidin (A) or phalloidin (white) and propidium iodide (blue). A-C sagittal sections, apical plate up, anterior lobe (al) to the left. D_1-D_3. Transverse sections (from apical to vegetal), anterior lobe is up. A. A 29.9 µm-thick slab showing the opening of the blastopore (asterisk) between the lateral lappets (lp), the lumen of the gut (gt), and the ciliated band (arrowheads) spanning the lateral lappet. Larval ciliary cirrus (lc) visible underneath the posterior lobe. B. Same individual as in A, a 1.95 µm slab showing the apical plate (ap), the gut, and the juvenile rudiments (dashed outlines) inside: one of the cephalic discs (cd), proboscis rudiment (pb), dorsal rudiment (dr), one of the trunk discs (td), and one of the cerebral organ discs (cod). C. A 1.95 µm slab showing the axil (ax, dashed outline), the ciliated band terminating in the axil (arrowhead), cephalic disc, dorsal rudiment, trunk disc and the gut. D. A diagram (lateral view) summarizing A-C. Horizontal lines show approximate levels of the sections on D_1 -D_3. D_1. A 1.95 µm slab showing the proboscis rudiment, paired cephalic discs, gut and dorsal rudiment. D_2. Same individual as in D_1, a 1.95 µm slab showing paired cephalic discs and trunk discs, and the gut. D_3. Same individual as on D_{1-2}, a 1.95 µm slab showing paired cerebral organ discs invaginating from the gut. E. A diagram (apical view) summarizing D_1 -D_3. Scale bars 50 µm.

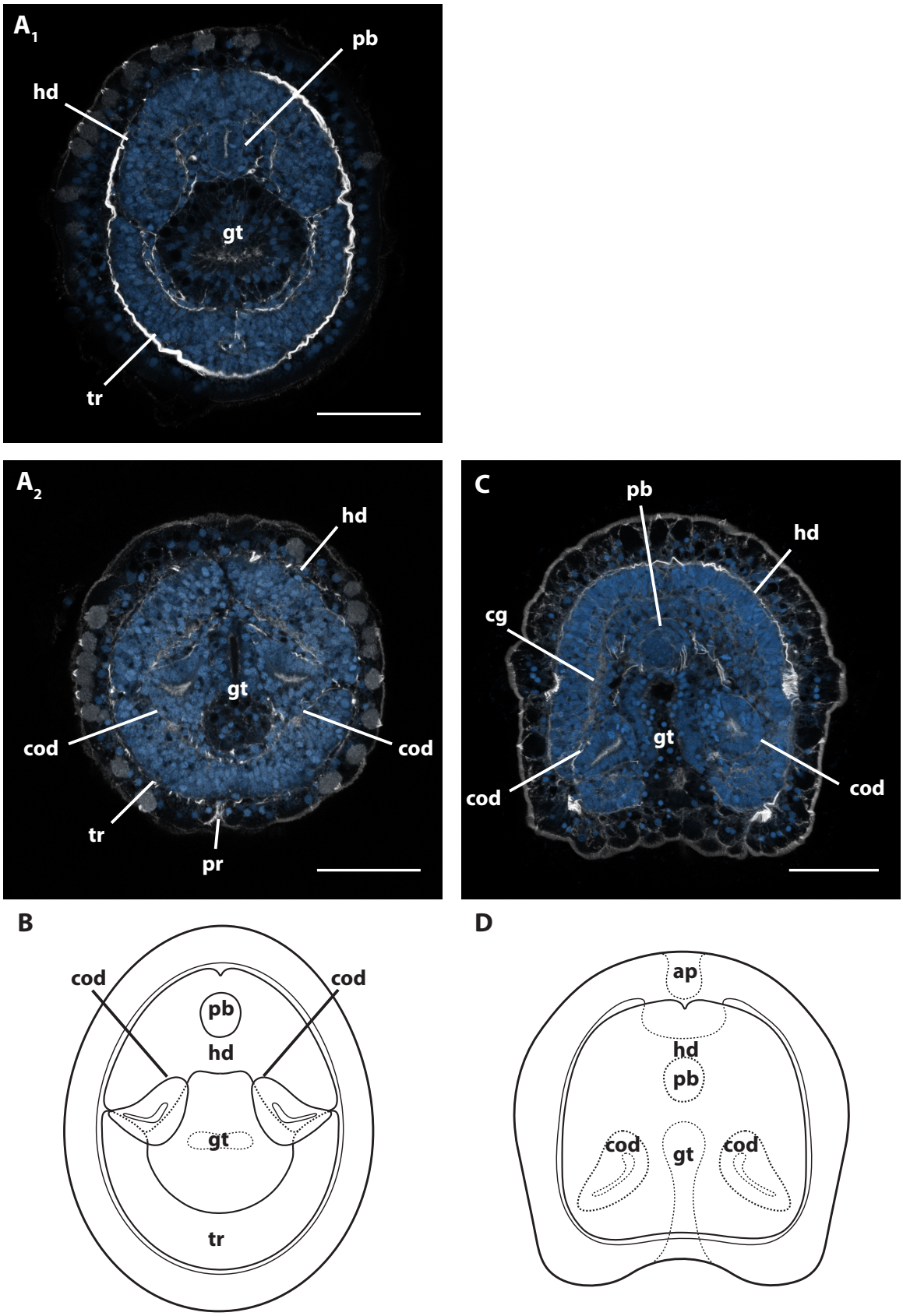
A1
pb
hd
gt
tr
A2
hd
gt
cod
cod
tr
pr
C
pb
hd
cg
gt
cod
cod
B
cod
cod
pb
hd
gt
tr
D
ap
hd
pb
cod
gt
cod

Figure 2.6. Anatomy of the torus stage of *Micrura* sp. "dark." A_1-A_2 and C are confocal projections of larvae stained with phalloidin (white), and propidium iodide (blue). A_1-A_2 are transverse sections (from apical to vegetal), juvenile anterior is up. C is a frontal section (apical is up). A_1. A 1.95 µm slab showing the developing proboscis (pb) and fused pairs of cephalic and trunk discs, forming the head (hd) and trunk rudiments (tr). A_2. The same individual as in A_1. A 1.95 µm slab showing the head and trunk rudiments fused around the gut, forming the characteristic toroid of juvenile tissue. The cerebral organ discs (cod) are closed off from the gut. Note the larval pore (pr), which is associated with the larval cirrus (not visible on this slab). B. A diagram summarizing A_1-A_2. C. A 1.95 µm slab (frontal view) showing the proboscis rudiment, the cerebral organ discs closed off from the gut, and the fibrous core of the right cerebral ganglion (cg). D. A diagram summarizing C. Scale bars 50 µm.

Larval musculature begins to develop, vaguely tracing the lappets. Larvae begin to exhibit a distinctive start-stop swimming behavior between the third and fourth day of development (Figure 2.3G). In this characteristic swimming behavior, *pilidium nielseni* spiral forward led by the apical tuft, then abruptly stop, halting ciliary motion for a brief moment before continuing on. At about the same time, the larval ciliary cirrus and an amniotic "larval pore" develop below what used to be the posterior larval lobe (now located between the two ciliary bands) (Figures 2.5A and 2.5D_2). The larval pore is located just posterior to the larval cirrus, and opens through the larval epidermis to the outside. By the fourth day, typically, the lobes and lappets diminish and become indistinguishable, the ciliary band segments reorganize to form a continuous anterior transverse ciliary band (the "prototroch") and continuous posterior transverse ciliary band (the "telotroch") (Figures 2.3G and 2.8D), and larval musculature develops beneath the "prototroch" and extends into the "telotroch" (Figure 2.10A-B). At the same time the cerebral organ discs close off to the gut, the trunk discs begin to fuse together, and the cephalic discs fuse around the proboscis rudiment (Figure 2.6). The cephalic and trunk

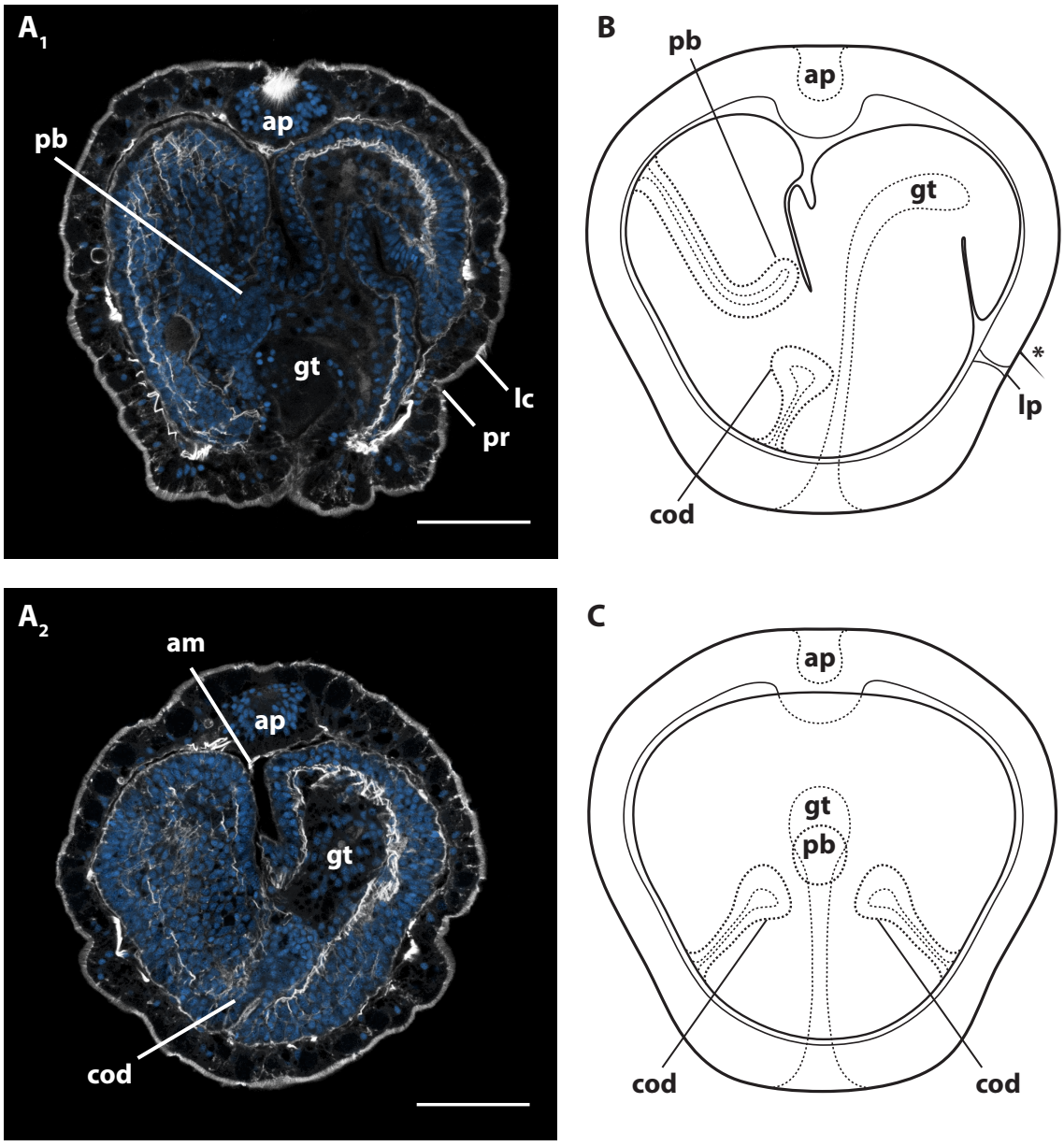

Figure 2.7. Anatomy of the hood stage of *Micrura* sp. "dark." A_1-A_2 are confocal projections of specimens stained with phalloidin (white) and propidium iodide (blue). They are sagittal sections, apical plate (ap) up, juvenile anterior left . A_1. A 1.95 µm slab showing the extension of the proboscis (pb), the larval pore (pr) associated with the larval cirrus (lc), and the lumen of the gut (gt). A_2. A 1.3 µm slab showing cerebral organ disc (cod) opening through the larval epidermis, the apical muscle (am) and the lumen of the gut. B. A diagram summarizing A_1-A_2 . C. A diagram of the same stage from a frontal view. Scale bars 50 µm.

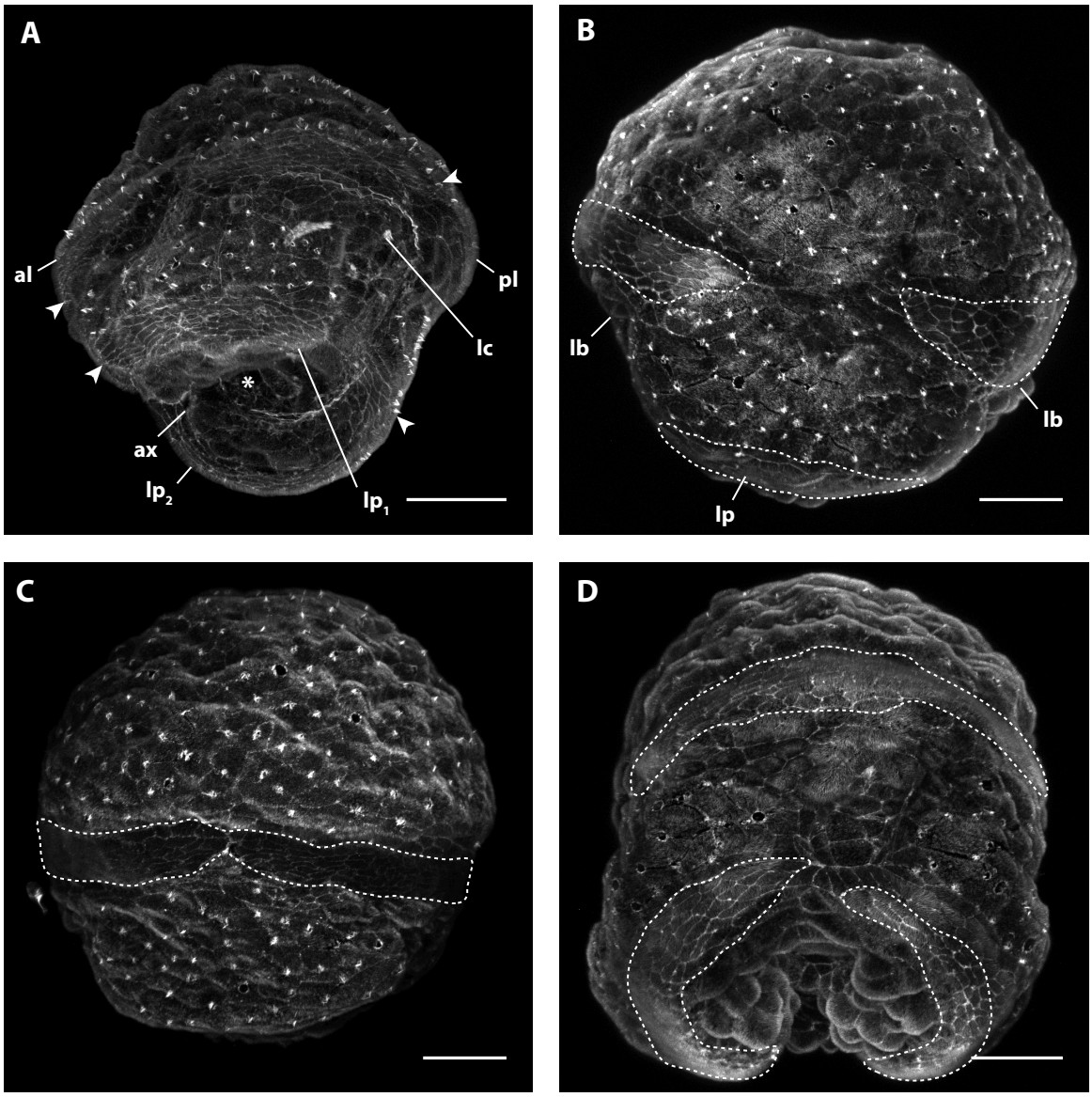

Figure 2.8. Development of the ciliary bands in the *pilidium nielseni* of *Micrura* sp. "dark." Confocal z-projections of 3-5 day old larvae stained with phalloidin, and oriented with the apical plate up. A. A slightly oblique lateral-vegetal view showing of the "pileus" stage (3-day old). Anterior lobe (al) left and posterior lobe (pl) right. Posterior lobe can be identified by the position of the larval cirrus (lc). Shows the two separate segments of the future "telotroch" spanning the two lateral lappets and the two segments of the future "prototroch" spanning the anterior and posterior larval lobes. Blastopore is marked with an asterisk. B. Lateral view of a larva at the "pileus" stage. Shows the lateral gap between the two segments of the future "prototroch." C. Lateral view of a larva several hours past the "pileus" stage. Shows the two "prototroch" segments making contact. D. A larva several hours following the "pileus" stage, rotated 90 along vertical axis showing the the formation of the complete "telotroch." Scale bars 50 μm.

discs fuse with each other on each side of the gut, incorporating the cerebral organ discs into what is now a toroidal juvenile rudiment. This corresponds to the "torus" stage in the development of a planktotrophic pilidium (Maslakova, 2010a). By the next day, the cerebral organ discs penetrate the juvenile epidermis and open laterally (left and right). By day five of development, the circumferential muscle bands underlying the ciliary bands thicken, and the larvae begin to contract at their "trochs," cinching in the larval body like tightening belts (Figures 2.3H and 2.10C). The juvenile lateral nerve cords begin to extend from the head region into the trunk region (Figure 2.11A). About two days after the torus stage, larvae reach what corresponds to the "hood" stage in planktotrophic development (Maslakova, 2010a), where the trunk rudiment, composed of the fused trunk discs and dorsal rudiment, extends over the proboscis rudiment, but has yet to fuse with the head rudiment dorsally (Figure 2.7). By eight days, the head and trunk rudiments fuse dorsally, incorporating the proboscis and gut and forming a complete juvenile (Figures 2.3H and 2.9).

In a few instances, the juvenile was completely formed in six-day-old larvae. At this point, the larvae appear less opaque due to diminishing yolk reserves, so the complete juvenile is visible through the body wall (Figure 2.3H). Approximately one day after the juvenile is completed, its epidermis becomes noticeably ciliated. The circular and longitudinal muscles of the juvenile body wall become obvious first in the posterior, and later in the anterior (Figure 2.12).

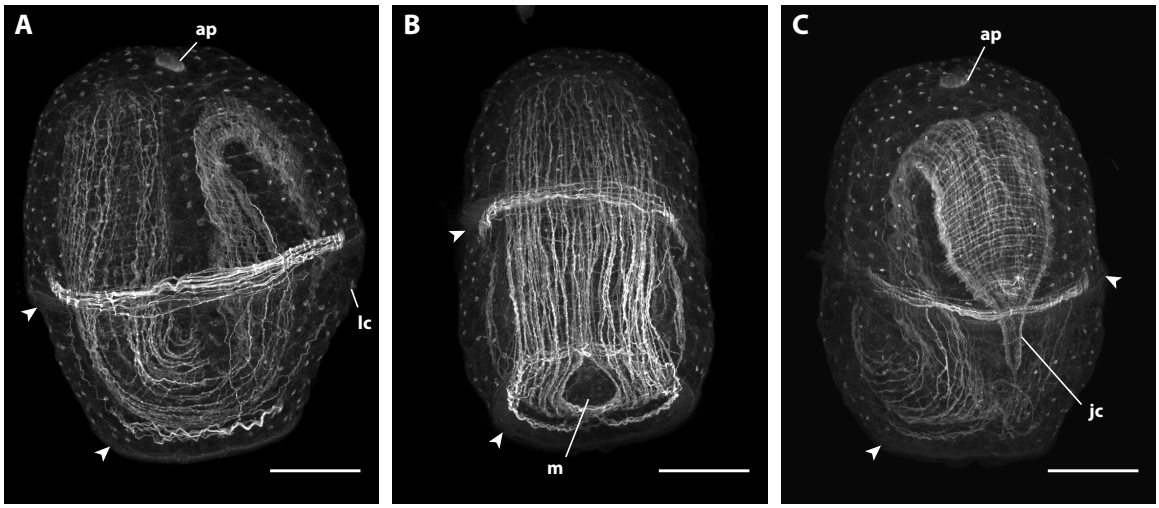

Figure 2.9. Complete juvenile formed within *pilidium nielseni* of *Micrura* sp. "dark." Confocal z-projections of larvae stained with phalloidin; apical organ (ap) up. Larval ciliary bands, with associated circular muscle bands are denoted by arrowheads. A. Lateral view, with juvenile anterior to the left. B. Frontal view showing juvenile anterior with juvenile longitudinal body wall muscles parted around opening of the larval/ juvenile mouth (m). C. Frontal view showing juvenile posterior end folded over, with the juvenile cirrus (jc). Scale bars 50 µm.

In as few as nine days, the brain ring is apparent around the rhynchocoel, and the juvenile begins to move within the larval body, pushing against it, and retracting from it (Figure 2.11B). At the earliest, metamorphosis occurred in only nine days, and most individuals metamorphosed in fewer than 20 days. During its catastrophic metamorphosis, the juvenile extends against the larval body, distorting it, as its tail jabs between the ciliary bands near the lateral cirrus, as described by Maslakova and von Dassow (2012). Confocal imaging exposed the small larval pore open to the outside near the larval cirrus, which suggests that the juvenile may use this pore as an "escape hatch" during metamorphosis (Figures $2.6A_2$, 2.7_A and 2.10F).

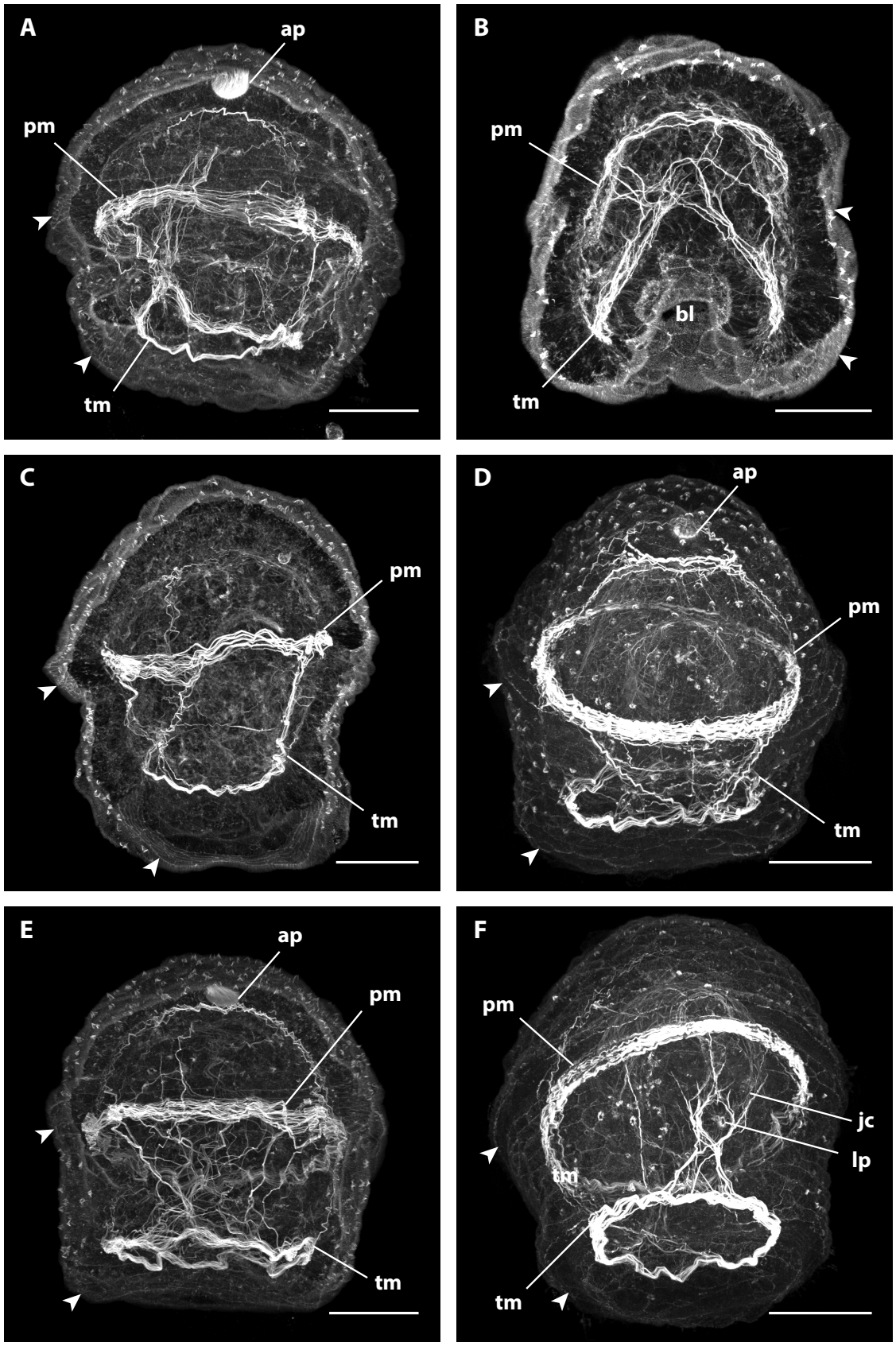
A
ap
pm
tm
B
pm
bl
tm
C
pm
tm
D
ap
pm
tm
E
ap
pm
tm
F
pm
jc
lp
tm
tm

Figure 2.10. Larval muscles in *pilidium nielseni* of *Micrura* sp. "dark." Confocal projections of specimens stained with phalloidin, apical plate up. A, B, and E are slightly oblique lateral views with the anterior end front and left and the posterior back and right. Ciliary bands are marked with arrowheads. A. A 92.95 µm stack (lateral view, apical plate (ap) up), showing "loops" of muscles criss-crossing as they drop into the lappets from either side of the "prototroch" muscle band in the "pileus" stage. B. A 26.0 µm slab showing a frontal (anterior) view of "pileus" stage, with the blastopore (bl) visible. C. A 48.1 µm slab of a specimen one day past the "pileus" stage (lateral view) showing the complete ring of circumferential muscles underlying the "telotroch," formed in part by the "loops" connected to the "prototroch." D. A complete z-projection showing a frontal (anterior) view of a week old specimen with a complete juvenile. Note the ring of muscles underlying the "telotroch" and the ring forming around the apical organ. Extensions of the apical organ muscles are descending towards the "prototroch." E. A 106.6 µm stack (a frontal view) of a larva in the "torus" stage showing the increasing connections between the muscles of the apical ring, the "prototroch," and the "telotroch." F. Complete z-projection of a week old larva with a fully-formed juvenile inside. A frontal (posterior) view showing the muscles around the larval pore (lp), just below the juvenile cirrus (jc). Scale bars 50 µm.

Newly metamorphosed juveniles have a length of ~500-600 µm in gliding, including a distinct caudal cirrus of ~50 µm (Figure 2.3I). The cirrus is sometimes used as a sticky anchor while the juvenile extends its anterior end and writhes in the water. They have a pair of longitudinal cephalic slits, as is characteristic of adults of this species (and the entire family Lineidae), and a slight constriction separates the head from the rest of the body, which can appear somewhat bulbous while the stomach is engorged with the larval body.

Development of the juvenile rudiments

Within two days of development, the embryos develop the first two pairs of imaginal discs. The paired cephalic discs appear first, as early as 30 hours after fertilization, and several hours later, are followed by the paired trunk discs (Figure 2.4).

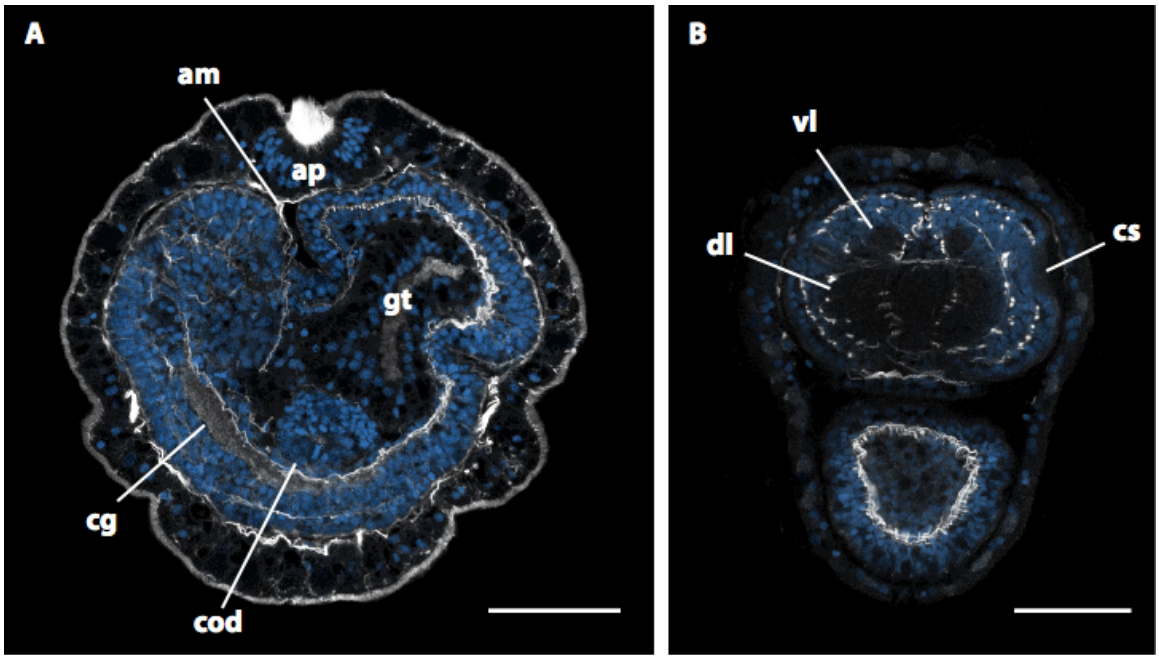

Figure 2.11. Development of the juvenile nervous system in *Micrura* sp. "dark." Confocal projections stained with phalloidin (white) and propidium iodide (blue). A. Sagittal section (1.95 µm) of "hood" stage, apical plate (ap) up, juvenile anterior left. The apical muscle (am) extends alongside the gut to the larval muscles underlying the "telotroch." Note the fibrous core of the left cerebral ganglion (cg), the cerebral organ disc (cod) and the gut (gt). B. Transverse section (apical to vegetal) with the juvenile anterior up, showing the ventral lobe (vl) and dorsal lobe (dl) of the brain ring, and the right cephalic slit (cs). Scale bars 50 µm.

Both pairs of discs are formed by invaginations of the larval epidermis, separating themselves from the larval body wall in an arc curving towards the sagittal plane of the larva. Shortly thereafter, the gut curves backwards over the trunk discs (Figure 2.5A-D). At this point, the cephalic discs are positioned above the transient anterior lobe, while the trunk discs are beneath the backward curve of the gut, along the posterior side of each lappet. Within three days, invaginations of the gut begin to form the cerebral organ discs. The gut first widens near the blastopore, gradually forming two shallow chambers between the developing cephalic and trunk discs on either side of the mid-sagittal plane

(Figure 2.5D). These invaginations of the gut elongate and form the cerebral organ discs. As the gut widens, the dorsal rudiment forms along the inner pilidial epidermis dorsal/ apical to the gut, and the proboscis rudiment forms between the cephalic discs. The origin of these cells is uncertain, but perhaps, as is posited for a typical pilidium, they are mesenchymal (Maslakova, 2010a). The dorsal rudiment becomes bi-layered, and spreads underneath the larval epidermis across the dorsal surface of the gut (Figure 2.5B-C), and the cephalic discs envelop the proboscis rudiment as they fuse around it (Figure 2.5D$_1$). The cephalic discs fuse together near the gut first, then continue to fuse anteriorly and around the proboscis into the fourth day (Figure 2.6). The trunk discs fuse with each other, and with the posterior end of the dorsal rudiment. The dorsal rudiment also extends anteriorly over the gut towards the fusing cephalic discs. The cephalic and trunk discs fuse together around the opening of the gut, enveloping the cerebral organ discs, which have closed off to the gut. The cerebral organs subsequently reopen laterally through the larval epidermis, the proboscis extends posteriorly, and ultimately, all rudiments fuse around the vestigial larval gut to form the complete juvenile.

Anterior invaginations - homologues of anterior pilidial axils?

Around the third or fourth day of development, a small epidermal invagination is noticeable between the anterior lobe and each lappet, below the cephalic discs (Figure 2.5C). The ciliary bands of the lateral lappets extend from these "pits," suggesting that these pits are comparable to the axils (growth zones) described in a planktotrophic pilidium, and give rise to the ciliary bands (Bird et al., 2014; Figure 2.8A).

Ciliary band formation

The ciliary bands extend from the anterior invaginations, appearing as several rows of small cells easily distinguishable from the larger cells of surrounding epidermis (Figures 2.5A and 2.8A). At the "pileus" stage, two halves of the anterior ciliary band span each of the transient lobes, separated by larger epidermal cells (Figure 2.8A-C). The lappets are fringed by the two halves of the posterior ciliary band. The next day, as the lobes and lappets diminish, the corresponding halves of each band begin to make contact with each other (Figure 2.8D-E). Finally, each of the bands integrate fully with their other half, forming the characteristic "prototroch" and "telotroch" of *pilidium nielseni,* while the blastopore remains open to the outside at the vegetal pole.

Larval musculature

The first muscles to form are the circumferential muscles underlying the "prototroch." These develop after the cephalic and trunk discs have invaginated, when larvae are about three days old (at 16ºC). Some of these muscles begin to extend from the "prototroch" into each of the transitory lappets, forming a "loop" of muscle which follows the curve of the lappet, as if two jump ropes of muscle fibers were being held at either side of the "prototroch," and the middle of each was allowed to drop into a lappet (Figure 2.10A-B). As the lappets diminish, the curves at the bottom of "loops" widen, and extend towards each other (like the two handles of each jump rope are being held further apart, towards the handles of the rope on the opposite side), while circumferential muscles underlying the "telotroch" develop between and around them. Eventually, the

sides of the “loops” overlap each other, forming a cross of muscle at either end of the developing juvenile (Figure 2.10A-D). The flattened bottoms of the “loops” are incorporated into developing circumferential muscles underlying the “telotroch” (Figure 2.10C-D). The circumferential muscles forming under both ciliary bands proliferate until they have formed dense bands. At this point, the larva begins its characteristic contractions, wherein the “belt” of muscles underlying the “trochs” tighten and cinch in the larval body (Figure 2.3H). Within five days, circumferential muscles form around the apical organ (Figure 2.10D-E). Some muscles originating around the apical organ begin to extend through the larva behind the cephalic discs, with fibers connecting to the “prototroch” and “telotroch.” These muscles proliferate and form a dense cord of muscle, the apical muscle, which allows the larva to pull in its apical tuft (apical muscle), and will divide the head and trunk regions of the juvenile dorsally in the “hood” stage (Figures 2.7A$_2$ and 2.11A). At about six days, a ring of muscle forms around the larval pore just above the posterior muscle cross (Figure 2.10F). More connections between muscle groups are made as the larva continues to develop, but the muscles encircling the larval pore are the last major muscle group to form (Figure 2.10E-F). When the juvenile nears completion, the apical muscle extending through the larva begins to degrade. This allows the juvenile rudiments to fuse completely, and, presumably, facilitates metamorphosis.

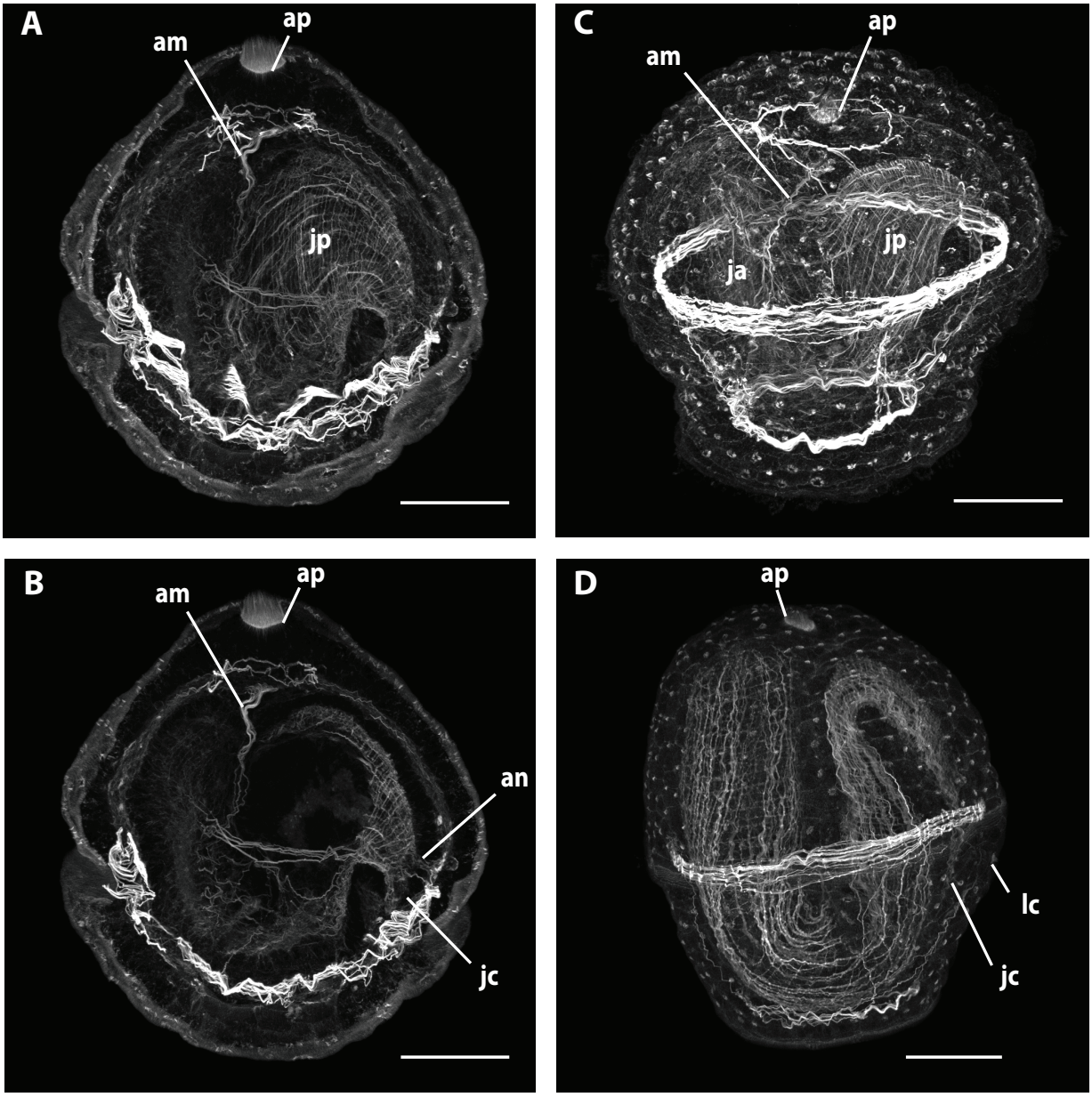

Figure 2.12. Juvenile muscle development of *Micrura* sp. "dark." Confocal z-projections of specimens stained with phalloidin. Apical plate (ap) up, juvenile anterior to the left. A. A 20.2 µm slab of a specimen transitioning from the "torus stage" into the "hood" stage showing the muscles in the juvenile posterior. The apical muscle (am) penetrates through the juvenile body. B. Same specimen as in A. A 36.4 µm slab showing the muscles anchoring (an) the posterior tip of the tail to the larval epidermis. C. A complete z-projection of a specimen in the "hood" stage beginning to develop muscle in the juvenile anterior. D. A complete z-projection of a specimen with a complete, fully formed juvenile with its posterior end oriented towards the larval cirrus (lc). Scale bars are 50 µm.

Juvenile musculature

The juvenile muscles begin to develop before the juvenile is complete, just prior to the "hood" stage. At first, longitudinal and circumferential muscles form at the tip of the posterior end, and expand anteriorly (Figure 2.12A). The trunk becomes muscled first, and remains more muscled than the head. One of the first muscles appears to anchor the posterior end of the juvenile to the larval body wall, just above the larval pore (Figure 2.12B). When the juvenile takes shape at about nine days old, both the head and trunk are muscular, and the juvenile begins to move against the larval body (Figure 2.12C). However, the apical muscle still divides head and trunk ends. When the apical muscle degrades, the juvenile rudiments fuse completely, and the muscular network connects throughout the body (Figure 2.12D).

Juvenile nervous system

After about a week of development, when the juvenile has reached the "torus" stage, the cerebral organ discs are closed off from the gut and open through the juvenile epidermis, and confocal imaging shows the fibrous core of the cerebral ganglia running through the cephalic discs (Figure 2.11A). Within two days, lateral nerve cords extend from the cerebral ganglia into the trunk discs, passing under the cerebral organ discs. It is at this time, at about nine days of development, when the brain ring surrounding the rhynchocoel becomes readily apparent (Figure 2.11B). The brain ring is made up of paired dorsal lobes connected by the dorsal commissure, and paired ventral lobes connected by the ventral commissure.

Digestive system

At 16ºC, gastrulation occurs within 24 hours after fertilization, resulting in an embryo which is somewhat flattened along the animal-vegetal axis, and features a small blastopore (Figure 2.3E). As the larva develops, the gut gradually elongates from the vegetal blastopore towards the apical tuft at the animal pole (Figure 2.4C). After three days, the gut arcs toward the dorsal side over the trunk discs (Figure 2.5A-D). Within five days, the paired cerebral organ discs outpocket from the gut near the blastopore (Figure 2.5D_2), and eventually close off from the gut (Figure 2.6) and open through the juvenile epidermis (Figure 2.7). The gut is first used when the larval body is ingested during metamorphosis.

Discussion

The development of *pilidium nielseni* is consistent with that of a typical planktotrophic pilidium, and its trochophore-like appearance has been arrived at through convergence (Maslakova, 2010a; Maslakova and von Dassow, 2012). Like a typical pilidium, it undergoes spiral cleavage and develops a blade-like apical tuft as it passes through the gastrula stage. Initially, *pilidium nielseni* even takes the form of a highly reduced pilidium, developing transient lobes and lappets, a phenomenon which has not been observed in any other non-feeding pilidium. At this stage, as in a typical pilidium, the ciliary bands span the lobes and lappets (though they do not form a continuous band). The *pilidium nielseni* also shares its method of juvenile development; paired cephalic, trunk and cerebral organ discs, and unpaired proboscis and dorsal rudiments, arise and

fuse together around the larval gut to form the juvenile. The origin of *pilidium nielseni*'s proboscis and dorsal rudiment is uncertain, but in typical pilidia, they have not been observed to invaginate from the epidermis, and it is posited that these unpaired rudiments may be mesenchymal (Maslakova, 2010a). *Pilidium nielseni*'s appear to arise similarly. Once the juvenile is complete, *pilidium nielseni* undergoes catastrophic metamorphosis, a quintessential pilidial trait. During metamorphosis, the juvenile backs out of the larva near (or possibly through) the larval amniotic pore, and draws the larval body into the shared mouth as it escapes (von Dassow and Maslakova, 2012). Similarly, the planktotrophic pilidium of *Maculaura alaskensis* has two amniotic pores underneath its posterior larval lobe (which other species are likely to have these as well), and during metamorphosis, the *M. alaskensis* juvenile often emerges caudal end first at the base of the posterior lobe (Maslakova, 2010a; von Dassow and Maslakova, 2013; Maslakova, personal observation). In the planktotrophic, sock-like *pilidium recurvatum*, there is a single larval pore in a corresponding position, and the juvenile has been observed to emerge near (possibly through) that pore, as well (T. Hiebert et al., 2013). However, as one might imagine, there are some deviations from typical pilidial development in the novel *pilidium nielseni.*

One of the most conspicuous differences between the typical pilidium and *pilidium nielseni*, is, of course, lecithotrophy. In a typical hat-like planktotrophic pilidium, the ciliary bands generate currents while the lobes and lappets perform specialized movements to capture unicellular algae (von Dassow et al., 2013). Likely, other kinds of planktotrophic pilidia, like *pilidium auriculatum* and *pilidium recurvatum*,

have developed feeding mechanisms suited to their particular morphology (von Dassow et al., 2013). The elaborate morphology and feeding mechanisms of planktotrophic pilidia are of no use to non-feeding pilidia, which may explain the simplified body plan of *pilidium nielseni*.

In marine invertebrate groups with both non-feeding and feeding larvae, the feeding larvae are often comparatively complex (Strathmann, 1985; Emlet, 1991; McEdward and Miner, 2001). Larval feeding structures, such as ciliated bands extended on lobes and arms, may decrease swimming ability, but this drawback can be offset by improved feeding efficiency (Emlet, 1991; McEdward and Miner, 2001; von Dassow et al., 2013). The pressure to feed efficiently is removed for non-feeding larvae, and may be replaced by pressure to reduce hydrodynamic drag, thereby improving swimming ability (Emlet, 1991). One would expect that a simpler body plan, like that of a trochophore, would be a suitable solution (Emlet, 1991, 1994; Wray 1996). *Pilidium nielseni* converged on this basic body plan—a prolate spheroid with circumferential ciliary bands —much like the derived non-feeding larvae in other groups (e.g. the doliolaria of holothuroids) (Emlet, 1991, 1994; Wray, 1996; McEdward and Miner, 2001). It reduced its lobes and lappets, which are only discernible in the early stages, and reorganized its ciliary bands, likely improving motility (Emlet, 1994; von Döhren, 2011; Maslakova and von Dassow, 2012). This simplification and loss of feeding structures is also seen in other non-feeding pilidia (Schwartz, 2009; von Döhren, 2011; Maslakova and von Dassow, 2012; Maslakova and T. Hiebert, 2014; Martîn-Durán et al., 2015), and in many instances is probably convergent (Maslakova and T. Hiebert, 2014). The ciliated bands of

the planktotrophic larva are lost, replaced by uniform ciliation, or modified into one or two circumferential bands, which are both patterns of ciliation that are thought to improve swimming ability (Emlet, 1991, 1994). Similar patterns of simplification and modification are seen in the derived non-feeding larvae of groups with ancestral planktotrophy, such as gastropods, annelids, and echinoderms (Emlet, 1991; Lacalli, 1993; Wray, 1996; Moran, 1999; Pernet, 2003; von Döhren, 2011).

Still, the trochophore-like appearance of *pilidium nielseni* is provocative, and there may be an impulse to draw a direct connection to the hypothetical ancestral larva of Spiralia (Lophotrochozoa or Trochozoa, depending on the interpretation). However, the *pilidium nielseni* "prototroch" and "telotroch" are both positioned anterior to the blastopore (i.e. vestigial mouth), which retains its posterior/vegetal position. The prototroch of a true trochophore is anterior to the mouth, and the telotroch, if present, surrounds the anus, which is at the posterior end. The typical planktotrophic pilidium, which is *pilidium nielseni*'s more recent ancestor, feeds using a unique, complex feeding mechanism, which is not homologous to the opposed-band feeding described for some trochophores (Thollesson and Norenburg, 2003; Maslakova and von Dassow, 2012; von Dassow et al., 2013; Maslakova and T. Hiebert, 2014). The "prototroch" and "telotroch" can be ontogenetically linked with the primary ciliary band of a planktotrophic pilidium, as they initially form along the lobes and lappets before wrapping around the larva as two circumferential ciliary bands. Additional substantiation may be provided by a cell lineage study. This would further clarify the relationship between the ciliary bands of

pilidium nielseni and the ciliary band of typical pilidium, and determine if and how the trochoblasts contribute to the formation of the *pilidium nielseni* "trochs."

Pilidium nielseni produced by *Micrura* sp. "dark" have eggs ~250 µm in diameter, much larger than the 75-160 µm eggs of planktotrophic nemertean species (Maslakova and T. Hiebert, 2014; Figure 2.3B). The larger size of these eggs is likely due to the proportionate abundance of yolk, which is later doled out into conspicuous lipid granules dotting the larval epidermis (Maslakova and von Dassow, 2012). The yolk provides enough nutrition for *pilidium nielseni* to develop a complete juvenile without ever needing to feed, but supply is limited, so juvenile development is accelerated (Wray, 1996; McEdward and Miner, 2001; von Döhren, 2011; Maslakova and von Dassow, 2012; Martîn-Durán et al., 2015). Large eggs are characteristic of other non-planktotrophic pilidia, too, and typically fall within the 150-350 µm range (von Döhren, 2011; Schwartz, 2009; Maslakova and T. Hiebert, 2014). Though these yolk-rich, short-lived larvae are energetically expensive to produce, the benefits of avoiding a planktonic feeding stage must outweigh the risks in some cases, as evidenced by the several independent evolutionary events driving pilidiophorans towards lecithotrophy (Schwartz, 2009; von Döhren, 2011; Maslakova and T. Hiebert, 2014). The adult *Micrura* sp. "dark," seem to have a distinct preference for a habitat in dense mats of *Phyllospadix* spp. roots established in shell hash. Perhaps the inherently limited dispersal of relatively short-lived larvae increases the likelihood of encountering this ideal habitat, though more evidence is needed to support this hypothesis.

As described, the development of the juvenile within *pilidium nielseni* seems to align more closely to traditional pilidial development than that of other non-feeding pilidia, but this may be due to the differences in interpretation by different authors, rather than biology. For instance, Iwata's larva is described to develop via five imaginal discs (paired cephalic and trunk discs and a dorsal disc), cerebral organ rudiments which invaginate from the stomodeum, and a proboscis which arises from the cephalic discs (Iwata, 1958). A typical pilidium forms via three paired imaginal discs (formed as epidermal invaginations) and two unpaired juvenile rudiments (possibly mesenchymal) (Maslakova, 2010a). However, it was thought that the proboscis was derived from the cephalic discs in typical pilidia, too, until recent data revealed a separate rudiment (Norenburg and Stricker, 2002; Maslakova, 2010a). Also, the stomodeal invaginations forming the cerebral organs in Iwata's larva are similar to the invaginations of the gut near the blastopore in *pilidium nielseni*, and both are likely homologous to the lateral invaginations of the subumbrellar epidermis/esophagus which form the cerebral organ discs in typical pilidia (Iwata, 1958; Maslakova, 2010a). All of these should be considered imaginal discs. Additionally, Iwata indicates that the dorsal disc invaginates above the paired cephalic discs—not the trunk discs—which is odd, as the dorsal disc typically appears above the trunk discs, then fuses with them to form the trunk rudiment (Iwata, 1958; Maslakova, 2010a). It is possible that a review of *M. akkeshiensis*'s development with modern methods would yield different results, which are more aligned with typical pilidial development.

Schmidt's larva was originally described to form a juvenile via eight imaginal discs—paired cephalic, trunk and cerebral organ discs and unpaired proboscis and dorsal discs—but does not specifically specify which invaginate from the epidermis (Schmidt, 1964). Recent analysis with confocal microscopy shows only two pairs of imaginal discs, the cephalic and trunk discs, and a proboscis rudiment (Martîn-Durán et al., 2015). There is also a cluster of mesenchymal cells where one might expect to find the dorsal rudiment, which may contribute to the dorsal side of the juvenile. Similarly, there appears to be a somewhat undefined region which may form the cerebral organs (Martîn-Durán et al., 2015). *Micrura rubramaculosa* and *M. verrilli* are thought to develop via five and *Micrura* sp. 803 via six imaginal discs, but the discs are not identified and their formation is not described (Schwartz and Norenburg, 2005; Schwartz, 2009). So, while current literature suggests there are many possible departures from typical pilidial development in non-feeding larva, this may be an artifact of the methods employed (e.g. histology vs. confocal microscopy), the depth of study, and interpretation by the author (e.g. which rudiments are counted as imaginal discs and which are not), rather than a representation of true developmental variation.

So, while *pilidium nielseni* looks radically different from a typical pilidium, the differences are not particularly radical. In fact, as more divergent pilidia are discovered, it becomes clear that the modifications in *pilidium nielseni*, like the reduction in feeding structures and altered body shape, are not even unusual. The development of *pilidium nielseni,* which mirrors that of a typical pilidium, demonstrates that this trochophore-like

larval form was converged upon—it does not represent a throwback to the ancestral trochophore.

CHAPTER III

A MULTIFACETED APPROACH TO DELIMITING SPECIES BEARING *pilidium nielseni* LARVAE

Introduction

In December 2011, a few unfamiliar trochophore-like larvae were spotted in a plankton sample from the Charleston boat basin in southern Oregon (Maslakova and von Dassow, 2012). They were ovoid, opaque, and had two circumferential ciliary bands resembling the prototroch and telotroch of a trochophore (Figure 2.1A). However, they also had the blade-like apical tufts and swimming behaviors characteristic of a nemertean pilidium, and, upon closer inspection, a juvenile worm could be seen through the larval epidermis. Ultimately, the juvenile emerged from the trochophore-like larva in a distinctive catastrophic metamorphosis, bursting through the larval epidermis while simultaneously consuming it—just like a typical pilidium. The unfamiliar larvae are lecithotrophic pilidia, which are more common than traditionally thought (Schwartz and Norenburg, 2005; Schwartz, 2009; Maslakova and von Dassow, 2012; Maslakova and T. Hiebert, 2014; see Chapter II). When the trochophore-like larvae were sequenced, they were matched to an adult of an undescribed local species. This adult fit the general criteria of a *Micrura* species, so it is provisionally named *Micrura* sp. "dark" for its dark reddish-gray body (Figure 2.2). Their larvae were dubbed *pilidium nielseni* in honor of a distinguished Danish invertebrate zoologist, Prof. Claus Nielsen, and his theories of

larval evolution, which prominently feature the trochophore (Maslakova and von Dassow, 2012).

Pilidium nielseni were present in plankton samples through the winter, so I, along with other members of the Maslakova lab and Dr. Richard Emlet, collected many additional individuals, which members of the Maslakova lab sequenced. Preliminary analyses of sequence data from the 16S rDNA , 28S rDNA, and Cytochrome Oxidase I Cytochrome Oxidase Subunit I regions from multiple individuals, resulted in four reciprocally monophyletic clades representing four closely-related species, each associated with a particular *pilidium nielseni* morphotype (Hunt, unpublished). These four provisional species formed a well-supported clade on pilidiophoran molecular phylogenies, which was given the moniker "trochonemertes" for their larvae's trochophore-like appearance (T. Hiebert, 2016). The larva of each "trochonemertes" species shares the basic trochophore-like appearance, bearing two circumferential ciliary bands roughly equatorial and posterior (like a "prototroch" and "telotroch" of a trochophore), but the exact position of these bands, the location of the larval ciliary cirrus, and the larval size differed slightly (Maslakova and T. Hiebert, 2014; Figure 2.1).

The larvae of *Micrura* sp. "dark" were reported to be 300 μm long, had an equatorial "prototroch," and a lateral larval cirrus between the "prototroch" and "telotroch" (Maslakova and von Dassow, 2012). A second *pilidium nielseni* morphotype, which had a "prototroch" slightly posterior to the larval equator and a larval cirrus at the posterior end (Figure 2.1D), was also genetically matched to its corresponding adult. It was another undescribed local species, and it met the basic diagnosis of the *Cerebratulus*

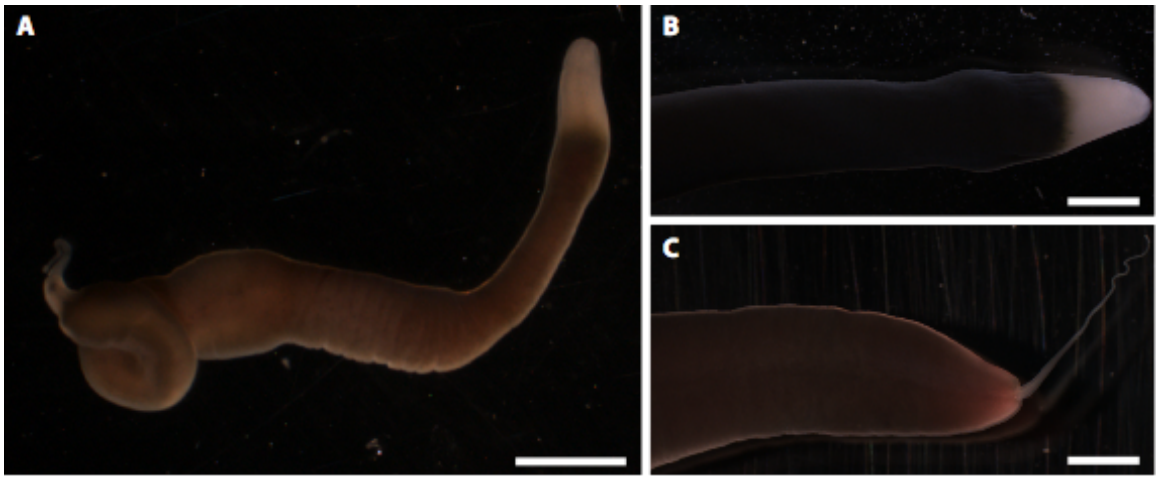

Figure 3.1. Adult morphology of *Micrura* sp. "albocephala." A. Adult with posterior regrowth. B. Anterior end with white tip. C. Posterior end with long cirrus. Scale bars are 2 mm.

genus (T. Hiebert, 2016). However, *Micrura* and *Cerebratulus* are poorly defined, demonstrably non-monophyletic genera (Schwartz, 2009; Andrade et al., 2012; Kvist et al., 2014; T. Hiebert, 2016), so assignments to these groups are more descriptive than phylogenetically meaningful. The *Cerebratulus*-like undescribed species is closely related to *Micrura* sp. "dark," as preliminary and subsequent data show, and is now referred to as *Micrura* sp. "albocephala" for its white head (T. Hiebert, 2016; this study; Figure 3.1). A third morphotype, like the larvae of *Micrura* sp. "albocephala," had a "prototroch" slightly posterior to the larval equator and a posterior larval cirrus, but it is larger. This morphotype is associated with another undescribed species provisionally referred to as *Micrura* sp. 4 (Figure 2.1E). The fourth *pilidium nielseni* morphotype, which represents an undescribed species referred to as *Micrura* sp. 3, was only found once, and this larva was not immediately differentiable from that of the *Micrura sp.* "dark" larvae (Figure 2.1B). Its "prototroch" appeared equatorial, and its cirrus location

was uncertain, but thought to be lateral between the ciliary bands (Maslakova and T. Hiebert, 2014). In this study, I discovered a fifth *pilidium nielseni* morphotype which, to my surprise, was not closely related to the "trochonemertes." It was pinkish, rather than the pale orange of the "trochonemertes" *pilidium nielseni*, its "prototroch" was just posterior to the larval equator, its "telotroch" was slightly more anterior than those of the "trochonemertes," and it had a lateral larval cirrus (Figure 2.1C).

The trochophore-like appearance of these larvae is significant because it could be interpreted as a reversion to the hypothetical ancestral trochophore of lophotrochozoans, or as an instance of convergence on a successful body plan (Maslakova and von Dassow, 2012). Prior to 2004, there was a lack of evidence for a nemertean trochophore, though multiple lines of evidence, such as sequence and ultrastructural data, categorized them as lophotrochozoans (Turbeville and Ruppert, 1985; Turbeville et al., 1992; Peterson and Eernisse, 2001; Turbeville, 2002). Finally, a vestigial prototroch was discovered in *Carinoma tremaphoros*, a species within the basal palaeonemertean clade, which validated the assumption that Nemertea shared an ancestral trochophore larva with other lophotrochozoans (e.g. annelids and mollusks) (Maslakova et al., 2004a, 2004b). However, the pilidiophorans are a highly derived clade within Nemertea, characterized by the pilidium larva, so it seems unlikely that the hypothetical ancestral trochophore would abruptly reappear in this group (Maslakova and von Dassow, 2012). In fact, both of *pilidium nielseni*'s ciliary bands are anterior to the blastopore (vestigial mouth), where a trochophore's would be on either side of the mouth, and (as described in Chapter II) *pilidium nielseni*'s development closely aligns with a typical pilidium's. Convergence on

—not a resurgence of—a successful body plan is the best explanation of *pilidium nielseni'*s superficial similarity to a trochophore larva (Maslakova and von Dassow, 2012; Chapter II of this study).

I show there are five distinct species which share this intriguing larval form—and that it arose independently at least twice—using multiple methods of species delimitation. Species delimitation is the process by which species boundaries are defined, so that species may be identified by empirical data (De Queiroz, 2007; Wiens, 2007). Species boundaries can be determined in a variety of different ways, but results are most convincing if multiple methods (e.g. morphology, development, habitat, molecular phylogenies, etc.) arrive at the same conclusion (e.g. De Queiroz, 2007; Jöger et al., 2012; Zou et al., 2011; Jöger and Schrödl, 2013; T. Hiebert and Maslakova, 2015b). In groups with soft-bodied morphology, and few morphological characters that can be objectively assessed (such as nemerteans), sequence-based approaches are especially useful (e.g. Fontaneto et al., 2015; Strand and Sundberg, 2005; Schwentner et al., 2011; Sundberg, 2015).

Historically, adult morphological characters were the basis for categorizing animals and determining taxonomic relationships, but adult nemerteans have few distinctive external features, and their internal features, identified by time-consuming histological studies, can be ambiguous, and prone to distortion and misinterpretation (e.g. Schwartz and Norenburg, 2001; Turbeville, 2002; Tholleson and Norenburg, 2003; Strand and Sundberg, 2005; Sundberg et al., 2010; Sundberg, 2015). Additionally, cladistic studies have shown that many of the features traditionally used to classify adult

nemerteans have no phylogenetic significance (e.g. Schwartz and Norenburg, 2001; Maslakova and Norenburg, 2001; Thollesson and Norenburg, 2003; Sundberg and Strand, 2010). In fact, new species are often lumped into "mega-genera," huge clades differentiated by subjective assessments of a few morphological characteristics, but which genetic data have shown to be non-monophyletic (e.g. *Lineus, Cerebratulus, Micrura, Amphiporus, Tetrastemma*), or they are assigned to a monotypic genus (over 60% of nemertean genera are monotypic) (Thollesson and Norenburg, 2003; Strand et al., 2014; Sundberg, 2015). Clearly, delimiting nemertean species based on adult morphological characters is an unreliable method, and should not be used to define species on its own. Sequence-based methods, which illuminated this issue, can define species more objectively, identify cryptic species, and determine which morphological characters have phylogenetic significance (Hebert et al., 2003; Thollesson and Norenburg, 2003; Strand and Sundberg, 2005; Barber and Boyce, 2006; Andrade et al., 2014; Maslakova and T. Hiebert, 2014).

With this in mind, I use a multifaceted sequence- and morphology- based approach to define boundaries between species bearing *pilidium nielseni* larvae; I collected both larvae and adults, sequenced them at multiple gene regions, performed multiple analyses on these data, and examined adult and larval morphological characters. These analyses determined there are five distinct species which produce *pilidium nielseni* larvae. Four form a monophyletic clade, the "trochonemertes," which supports preliminary data (T. Hiebert, 2016). Unexpectedly, the fifth species producing *pilidium nielseni* larvae, *Cerebratulus cf. longiceps*, is not closely related to the "trochonemertes,"

but it does group with another species which produces lecithotrophic pilidia (T. Hiebert, 2016; this study). Each of the five species are supported by both genetic and morphological data.

Methods

Larva collection and documentation

I, along with other members of the Maslakova lab and Dr. Richard Emlet, collected *pilidium nielseni* by plankton tows in the Charleston marina with a 150 µm mesh net in late fall and winter of 2011, 2012, 2013, and 2014. I photographed them individually using a Leica DF400 digital camera mounted to an Olympus BX51 compound microscope equipped with DIC while they were trapped between a slide and a coverslip supported by clay feet. Live larvae were kept in 150 ml glass dishes of filtered sea water (FSW, 0.2 µm) and re-photographed as they developed. Larvae were fixed for confocal microscopy, preserved for molecular analysis, and/or reared and photographed through metamorphosis. Larvae were identified to species definitively by DNA sequence data, and less reliably by morphology.

DIC images of each *pilidium nielseni* morphotype were imported into ImageJ64 after their species identity was confirmed by sequence data. I used ImageJ64 software to measure their length from apical organ to posterior end in an un-contracted state, the length of the cilia covering the larval body and the cilia making up the ciliary bands while these cilia were extended, the average diameter of several yolk granules in each individual's epidermis, and the length of the larval cirrus, if visible.

Adult collection and documentation

Micrura sp. "dark" was collected in rocky intertidal areas around Cape Arago in Charleston, Oregon (mostly from Middle Cove, 43.305°N, 124.400° W). I collected 129 *Micrura* sp. "dark" between October 2013 and March 2014, July 2014 and February 2015, and July 2015 to March 2016. *Micrura* sp. "dark" were typically found entangled in dense root masses of *Phyllospadix* spp. growing in shell hash, though several individuals were wedged between rocks, or in surf grass rooted in finer sand. *Micrura* sp. "dark" might be confused with similar-looking local species (e.g. *Lineus* sp. "red" and Lineid gen. sp. "large eggs"), but can be distinguished by their continuous and pronounced peristalsis (T. Hiebert and Maslakova, 2015a).

Micrura sp. "albocephala" was found in the same area as *Micrura* sp. "dark" and in nearby mudflats, one mudflat located in North Bend near the Southwest Oregon Regional Airport, and another in Charleston, Oregon. This species was encountered much less frequently than *Micrura* sp. "dark." I collected a total of five individuals, and included data from two others collected in mudflats prior to this study (in 2011 and 2012). In rocky intertidal areas, where they co-occured with *Micrura* sp. "dark," I found one individual in January 2014, two in January 2015, one in March 2016, and another in April 2016. They are primarily dark greenish-gray to black and have a bright white head, similar to descriptions of *Cerebratulus albifrons*, which has also been collected from local mudflats in Charleston, OR and has been shown to be a separate species by DNA sequence data (T. Hiebert, 2016).

Initially, I visually identified individuals in the field, then confirmed their identities via DNA-barcoding. In later collecting seasons, my identification of *Micrura* sp. "dark" specimens in the field was consistent, so confirming with sequence data was no longer required. Individuals were then photographed, and kept in 150 ml glass dishes in a flow-through sea table at ambient sea temperature, where their water was changed weekly. Within days of their collection, I relaxed 30 *Micrura* sp. "dark" adults and four *Micrura* sp. "albocephala" adults in 0.34M $MgCl_2$ and measured their body length (sans caudal cirrus), width at the esophagus, width at the posterior end, and the length of their caudal cirrus, when present. All three *Micrura* sp. "albocephala" found in January 2014 and 2015 fragmented during collection, so I only measured their body width and cirrus length (when present). The two *Micrura* sp. "albocephala" found in spring 2016 were much smaller and somewhat lighter in color than other specimens, and only one was measured before taking a tissue sample. The two collected prior to this study (in 2011 and 2012) were not measured. Adult specimens of *Micrura* sp. "dark" and *Micrura* sp. "albocephala" were photographed using a Leica DF400 digital camera mounted to a Leica MZ10F dissecting microscope.

Histology of adult specimens

Seventeen adult *Micrura* sp. "dark" and two *Micrura* sp. "albocephala" specimens were relaxed in 0.34 M $MgCl_2$ for 30 min-1 hour, preserved for 24 hours with 10% buffered formalin (Electron Microscopy Sciences), or 10% buffered formalin diluted from concentrated stock in sea water, then post-fixed in Hollande's Bouin fixative

(Electron Microscopy Sciences) for 24-72 hours. Specimens were rinsed in reverse osmosis purified (RO) water, then rinsed in 70% EtOH at least once a day until the solution was clear, which took up to two weeks, then stored in 70% EtOH until processing. Fourteen of the *Micrura* sp. "dark" specimens were processed. Specimens were dehydrated in an increasing EtOH series and then cleared either by hand, or by an automated process in a vacuum tissue processor. When dehydrated by hand, specimens were put through one 80% EtOH rinse for 30 minutes, two 30-minute rinses in 95% EtOH, a 45-minute rinse in 100% EtOH, and a final 100% rinse ranging from 45 minutes to overnight. These specimens were cleared by hand in xylene in three 30 minute steps; one rinse in equal parts xylene and 100% EtOH, followed by two rinses in xylene. In preparation for embedding, half the xylene was exchanged for Fisherfinest Histoplast LP paraffin (Fisher Scientific, 50-54ºC melting point), and the specimen was heated for 30 minutes (~52-56 ºC) until the paraffin solubilized. To remove xylene, the xylene and paraffin mixture was exchanged for paraffin three times, once every 15-30 minutes, then specimens were embedded in paraffin in a histology tray. Specimens dehydrated, cleared and embedded in an automated processes, were dehydrated in two 10-minute steps in 70% EtOH, one 10-minute step in 80% EtOH, two 10-minute steps in 95% EtOH, two 20-minute steps in 100% EtOH, and were cleared by one 20-minute step in xylene followed by followed by another 20-minute step in Clear-Rite 3 (Richard-Allan Scientific), then paraffinized in two 25-minute changes of Paraffin Type 6 (Richard-Allan Scientific), one 25-minute change in Paraffin Type 9 (Richard-Allan Scientific), and a final change of Paraffin Type 9 before being embedded in Paraffin Type 9 (~56ºC melting

point) in a histology tray. Blocks were sliced to form 7 µm thick serial sections, which were mounted onto charged slides in a hot water bath. I developed a staining protocol by modifying Crandall's polychrome method (a combination of Mallory, Gomori, Koneff and Gurr-McConail techniques) to stain thirteen of the mounted specimens. I deparaffinized sections with three four-minute changes in Clear-Rite 3, then hydrated them via a decreasing EtOH series; two 100% EtOH changes at three minutes per step, then 95%, 80%, 70% changes at one minute per step, and finally two three-minute rinses in RO water. I stained sections with Russell's Modified Zenker Solution (EMS) for three minutes, alum mordant (105.40 mM aluminum potassium sulfate) for 10 minutes, Modified Red Stain (34.16 mM acid fuchsin and 21.35 mM chromotrope 2R) for three to four minutes, PTA-PMA (1.74 mM phosphotungstic acid and 2.74 mM phosphomolybdic acid) for two minutes, and finally counter stain (53.69 mM aniline blue, 44.21 mM orange G, 0.69 mM phosphotungstic acid, and 1.10 mM phosphomolybdic acid) for one to two minutes, rinsing with running tap water for 5 minutes followed by a few dips in RO water between the first three steps. The sections were quickly dehydrated in an increasing ethanol series, dipped several times in 85% then 95% EtOH, then three two minute changes in 100% EtOH, and finally submerged in three three-minute changes of xylene. Finally, sections were mounted using Permount (EMS), and imaged with a Leica DFC400 digital camera mounted to an Olympus BX51 compound scope and Leica Application Suite V3.6 software. These data have yet to be analyzed for species descriptions.

Fluorescent labeling and confocal microscopy

Larvae were relaxed in a 1:1 mixture of 0.34 M $MgCl_2$ and FSW for 15 minutes, then in 100% 0.34 M $MgCl_2$ for 15 minutes prior to fixation. They were fixed in 4% paraformaldehyde prepared from 16% or 20% ultrapure paraformaldehyde (Electron Microscopy Sciences). Fixed specimens were rinsed in three 10-minute changes of phosphate buffer solution (PBS), then stored in PBS at 4 ºC, or immediately permeabilized and stained. Larvae were permeabilized with three changes of PBS with 0.1% or 0.5% Triton X-100 (PBT) and rinsed in three 10-minute changes of PBS. Specimens were stained with Bodipy FL phallacidin (Molecular Probes) at a concentration of 0.5%, propidium iodide (Sigma) at a 0.1% concentration, or a combination of both in the same concentrations diluted in 0.1% or 0.5% PBT. Stained specimens were rinsed in three 10-minute changes of PBS, then stored in PBS at 4ºC, or immediately cleared and mounted. Specimens were mounted onto Poly-L-lysine (Sigma) coated coverslips, dehydrated through an increasing isopropyl alcohol series (70%, 80%, 90%, 100% I, 100% II) for 40 seconds-1 minute at each step, then cleared with three 10-minute changes of Murray Clear (a 2:1 mixture of benzyl benzoate and benzyl alcohol which clears yolky eggs). Slides were prepared with strips of foil tape to support the coverslip. After mounting, the coverslips were filled with Murray Clear, which has a refractive index close to that of the immersion oil (~1.5) used during imaging, then sealed with nail polish, and imaged immediately, or stored at 4ºC for up to three days prior to imaging. The stained specimens were imaged with an Olympus Fluoview 1000 laser scanning confocal mounted on an Olympus IX81 inverted microscope with a UPlanFLN

40x 1.3 NA oil lens. Stacks of 0.7 µm optical sections were imported into ImageJ 1.47v (Wayne Rasband, Nations Institute of Health, Bethesda, MD, USA) for further processing.

Molecular analysis

For molecular analysis, I preserved adult and larval tissue in a small volume of FSW in a -80 ºC freezer (cryopreservng it), or in 80% EtOH (stored at -20 ºC). DNA was extracted from adult tissue with a DNEasy Blood and Tissue Kit (Qiagen). DNA from larval samples was extracted using Instagen Matrix (Biorad). Partial sequences of three genes were amplified; mitochondrial markers Cytochrome Oxidase Subunit I (COI) and 16S rDNA, and the nuclear gene 28S rDNA. 16S and COI are useful in nemertean species delimitation because they exhibit a relatively high level of interspecific variation and a low level of intraspecific variation (Thollesson and Norenburg, 2003; Andrade et al., 2012; Kvist et al., 2014; T. Hiebert and Maslakova, 2015b; T. Hiebert, 2016), while the more conserved 28S region is useful in determining broader phylogenetic relationships (Thollesson and Norenburg, 2003; Andrade et al., 2012; Andrade et al., 2014; Kvist et al., 2014). PCR amplification for the COI gene region was carried out with the universal forward primer LCO1490 [5' GGTCAACAAATCATAAAGATATTGG 3'] (Folmer et al., 1994) and a nemertean-specific reverse primer CO1DR [5' GAGAAATAATACCAAAACCAGG 3'] (Norenburg, unpublished). For the 16S PCR amplification, the universal forward primer 16SARL [5' CGCCTGTTTATCAAAAACAT 3'] (Palumbi et al., 1991) and a nemertean-specific reverse primer 16SKR [5'

AATAGATAGAAACCAACCTGGC 3'] (Norenburg, unpublished) were used, or 16SARL was used in combination with the universal reverse primer 16SBRH [5' CCGGTCTGAACTCAGATCACGT 3'] (Palumbi et al., 1991). To amplify the 28S gene region, the universal forward primer LSU5 [5' ACCCGCTGAAYTTAAGCA 3'] (Littlewood. 1994), and the universal reverse primer LSU3 [5' TCCTGAGGGAAACTTCGG 3'] (Littlewood, 1994) were used. PCR reactions were carried out in a 20 µl or 25 µl reactions with 1U/Rx of Go Taq polymerase in buffer solution (Promega), 200 µM dNTPs, 500 nM of each primer, and 2 µl of DNA extract. The cycling parameters for 16S and 28S gene regions were programmed with an initial denaturation step of 95°C for 2 min, followed by 35 cycles at 95°C for 40 sec, 52°C for 40 sec, 72°C for 1 min, then a final extension at 72°C for 2 min. The cycling parameters for the COI gene region were programmed as above, with the exception of the annealing temperature: 95°C for 2 min, followed by 35 cycles at 95°C for 40 sec, 45°C for 40 sec, 72°C for 1 min, and a final extension at 72°C for 2 min. PCR products were purified using the SV Wizard Gel and PCR Cleanup Kit (Promega), quantified using gel Low Molecular Weight DNA Ladder (New England Biolabs), and sequenced in both directions using PCR primers at Sequetech Inc. (Mountain View, CA). Sequences were trimmed, assembled into contigs, and proofread in CodonCode Aligner 4.2.5 (CodonCode Corporation, Dedham, MA). All sequences have been submitted to GenBank (see Appendix for accession numbers). I ran a Basic Local Alignment Search Tool (BLAST) search via CodonCode Aligner 4.2.5 on the 16S sequence for my *Cerebratulus cf. longiceps* larva, which was a 99% match to a *Cerebratulus longiceps* sequence (accession

number EF124872). I then downloaded this 16S sequence from GenBank, and included it in my analysis.

Alignment and phylogenetic analysis

Sequences were aligned in ClustalX2 2.1 (Thompson et al., 1997) using default parameters. I imported aligned sequences into Geneious 8.0.5 (Kearse et al., 2012) for phylogenetic analysis. For species delimitation analysis, I included all available sequences for each "trochonemertes" species, and one *Maculaura alaskensis* sequence for the outgroup (see Appendix for accession numbers). Sequences from 71 individuals made up the 16S alignment, 31 individuals were represented in the COI alignment, and 29 were included in the 28S alignment. To test the monophyly of the "trochonemertes" species, I conducted a separate phylogenetic analysis including a representative subset of sequences for *Micrura* sp. "dark" and *Micrura* sp. "albocephala," all available sequences for *Micrura* sp. 3, *Micrura* sp. 4, and *Cerebratulus cf. longiceps*, a number of other pilidiophoran species, and one *Carinoma mutabilis* sequence as an outgroup (see Appendix for accession numbers). The alignment of 16S sequences included 34 individuals, the alignment of COI sequences represented 34 individuals, and sequences from 36 individuals made up the alignment at the 28S region.

I calculated the uncorrected pairwise genetic distances (*p*-distances) between and within the four proposed "trochonemertes" species and *Cerebratulus cf. longiceps* from the sequence alignments in Geneious 8.0.5 to determine if a barcoding gap was present. I used the same alignments for Automatic Barcode Gap Discovery (ABGD) analysis

(Puillandre et al., 2011) using default parameters (Pmin 0.001, Pmax 0.1, Steps 10, Gap width 0.05–1.5 and JC69 distances). ABGD analysis sorts sequences into hypothetical species based on the presence of barcoding gaps, whereas identifying a barcoding gap via *p*-distances assumes each sequence belongs to a particular hypothesized species, and compares them accordingly. Neighbor-joining (NJ) distance trees for "trochonemertes" were computed in ClustalX at each gene region. Maximally parsimonious trees (MPTs) and strict consensus trees of "trochonemertes" species were computed for all gene regions in PAUP4b10. MPTs were built with 100 replications by holding ten best trees per step, randomly adding sequences to build the initial guide tree for each replicate, and using a tree-bisection-reconnection (TBR) algorithm of branch swapping. Bayesian phylogenetic analyses were conducted in Geneious 8.0.5 using the MrBayes 3.2.6 plugin (Huelsenbeck and Ronquist, 2001). Evolutionary model parameters for each gene region were determined using jModel-Test v 2.1 (Posada, 2008). For analysis of the "trochonemertes" clade, the evolutionary models most appropriate for the data were Hasegawa-Kishino-Yano (HKY) (Hasegawa et al., 1985) with gamma distribution for the 16S and COI gene regions, and Tamura-Nei (TrN) (Tamura Nei, 1993) with gamma distribution for the 28S gene region. For analysis of the Pilidiophora, the most appropriate evolutionary models were the 3-parameter model with unequal frequencies (TPM3uf) (Kimura, 1981), gamma distribution, and invariant sites for the 16S region, TrN (Tamura Nei, 1993) with gamma distribution and invariant sites for the COI region, and the transition model (TIM) (Posada, 2003) with gamma distribution and invariant sites for the 28S region. However, the ideal model parameters were not available in

MrBayes 3.2.6 as implemented in Geneious 8.0.5. Of the available evolutionary models, the General Time Reversible (GTR) evolutionary model (Tavaré, 1986) was the best fit for each gene region, and was run with default parameters. Four chains were run for 1,100,000 generations with a subsampling frequency of 200 and burn-in length of 100,000. Maximum Likelihood phylogenetic analyses were carried out in Geneious 8.0.5 (Kearse et al., 2012) with the PhyML plugin (Guindon and Gascuel, 2003). Clade support was estimated using default parameters with a GTR model and 1,000 bootstrap replicates with the exception of the analysis of Pilidiophora at the 16S gene region, which was analyzed with a TN93 (Tamura Nei, 1993) model using default parameters and 1,000 bootstrap replicates. All trees were viewed in Geneious 8.0.5 and FigTree v 1.3.1 (Rambaut, 2009).

Results

Phylogenetic analysis

Bayesian analyses of the 16S, COI, and 28S datasets all resulted in four well-supported reciprocally monophyletic clades corresponding to the four proposed "trochonemertes" species, *Micrura* sp. "dark," *Micrura* sp. "albocephala," *Micrura* sp. 3, and *Micrura* sp. 4 (Table 3.1, Figure 3.2). When included in a dataset featuring other pilidiophorans, the four "trochonemertes" species formed a monophyletic clade (Figures 3.2B, 3.2D, 3.2E). In all gene regions, analysis showed that *Micrura* sp. "albocephala" and *Micrura* sp. 4 are sister species. The 28S region supported a sister relationship between *Micrura* sp. "dark" and *Micrura* sp. 3, as did the 16S region when other

		Micrura sp. "dark"	*Micrura* sp. "albocephala"	*Micrura* sp. 3	*Micrura* sp. 4	*Cerebratulus cf. longiceps*	Number of species
Morphology	Larva	I	I	I	I	I	5
	Adult	I	I	NA	NA	I	≥3
16S	Reciprocal monophyly	I	I	I	I	I	5
	ABGD	I	I | I | I	I	I	I	7
COI	Reciprocal monophyly	I	I	I	I	NA	≥4
	ABGD	I	I | I | I	I	I	NA	≥6
28S	Reciprocal monophyly	I	I	I	I	I	5
	ABGD	I	I	I	I	I	5

Table 3.1. A comparison of results between different species delimitation methods. The table indicates how many clades each proposed species formed based on the method listed on the left. The column on the right describes the total number of species present as indicated by a particular method.

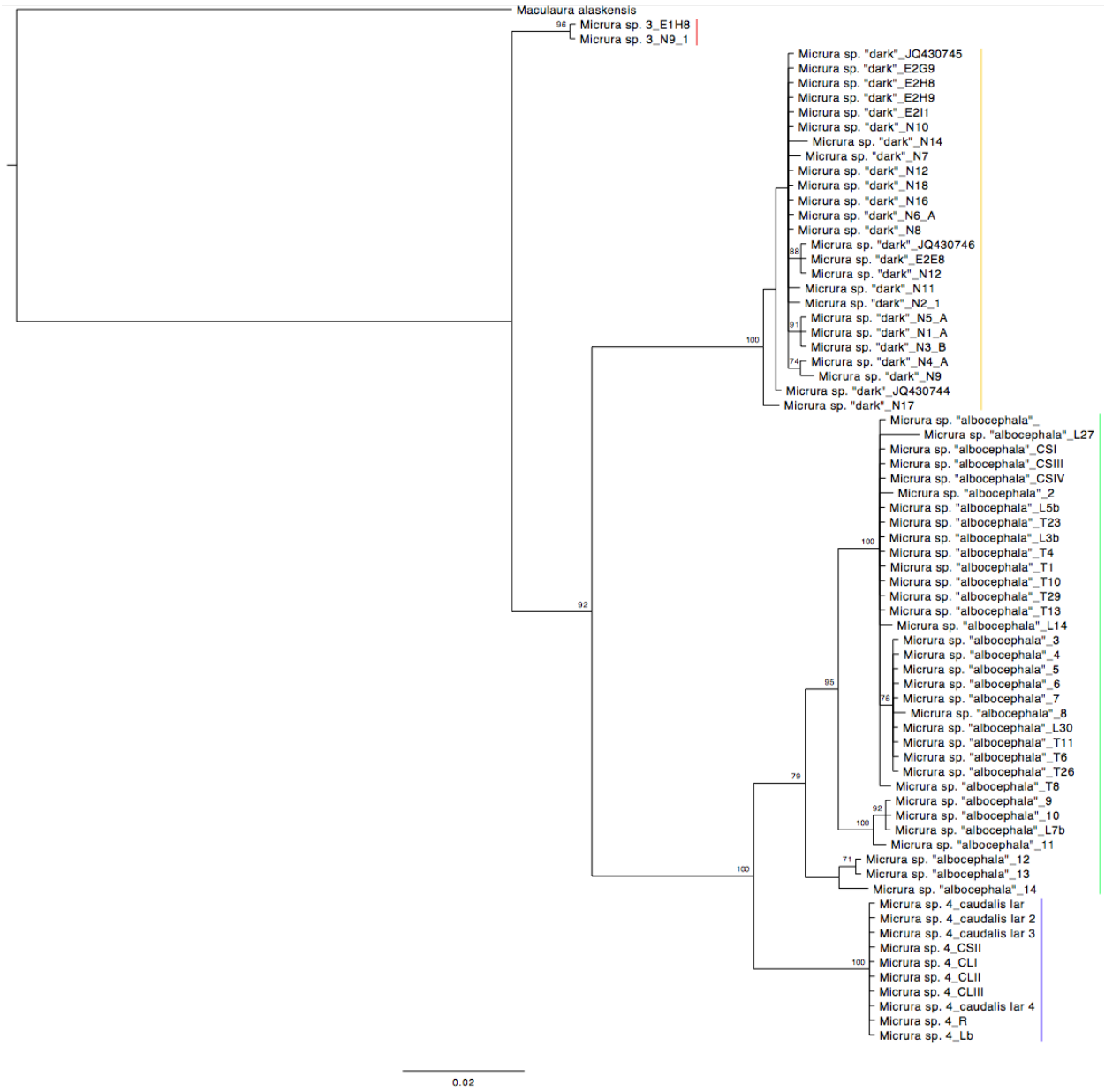

Figure 3.2A. Bayesian phylogeny of 16S sequences of the "trochonemertes" species. Bayesian posterior probabilities ≥70 are indicated above nodes. Monophyletic clades are indicated with a vertical line in a species-specific color. *Maculaura alaskensis*, a pilidiophoran with a typical hat-shaped planktotrophic pilidium, serves as the outgroup.

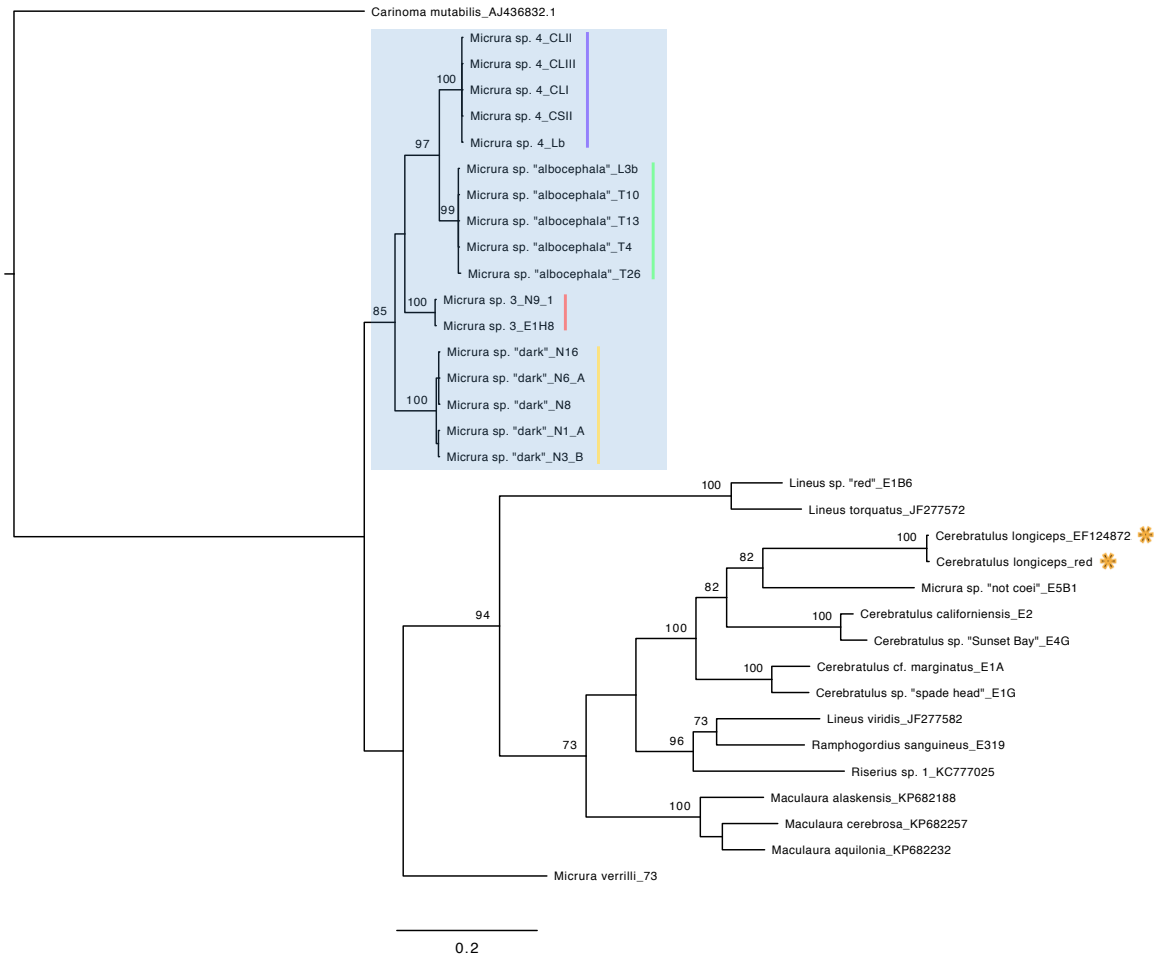

Figure 3.2B. 16S Bayesian phylogeny of the Pilidiophora supports the monophyly of the four "trochonemertes" species. Bayesian posterior probabilities ≥70 are indicated above nodes. The monophyletic "trochonemertes" clade is highlighted in blue, and monophyletic "trochonemertes" clades are indicated with a vertical line in a species-specific color. *Cerebratulus cf. longiceps*, which also bears *pilidium nielseni* larvae, are marked with orange asterisks. *Carinoma mutabilis*, a palaeonemertean, serves as the outgroup.

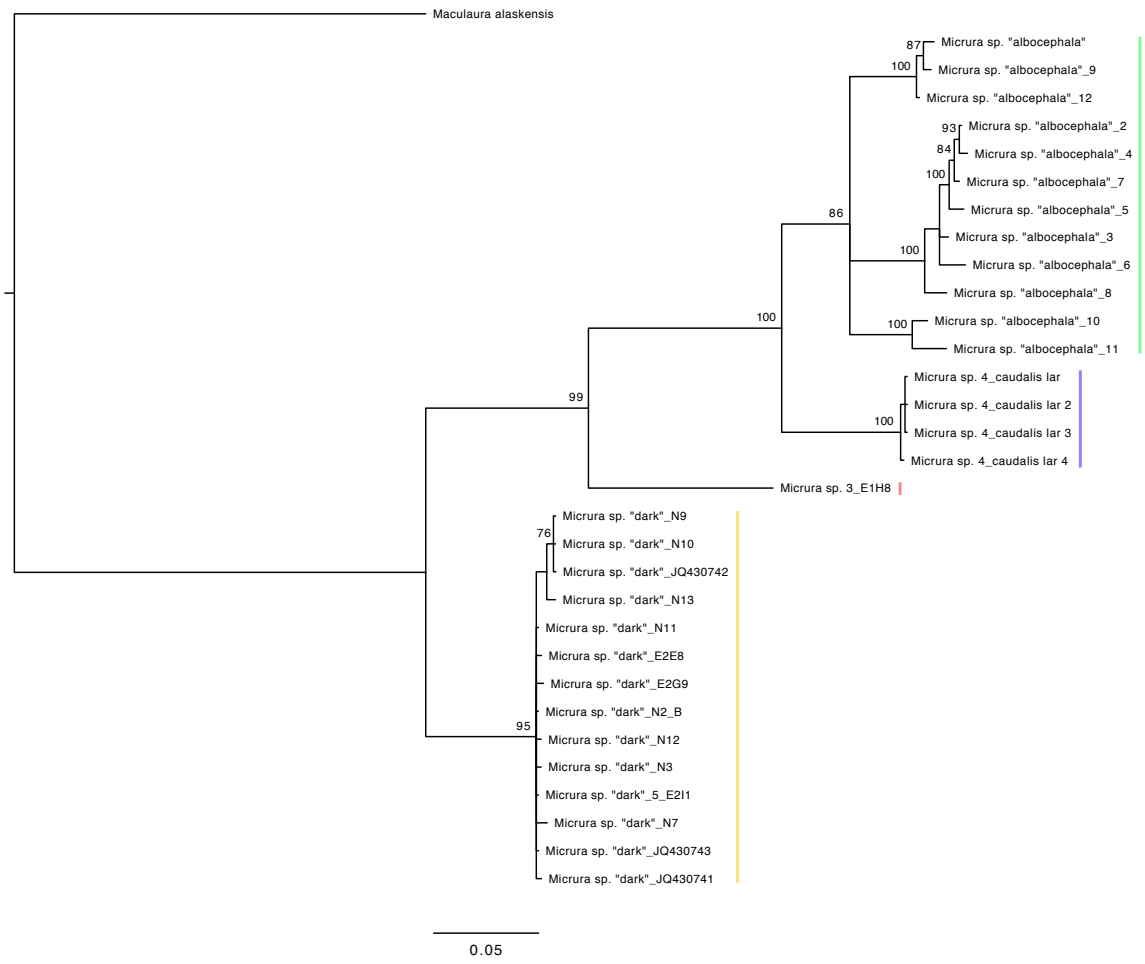

Figure 3.2C. COI Bayesian analysis of "trochonemertes" species. Bayesian posterior probabilities ≥70 are indicated above nodes. Monophyletic clades are indicated with a vertical line in a species-specific color. *Maculaura alaskensis*, a pilidiophoran with a typical hat-shaped planktotrophic pilidium, serves as the outgroup.

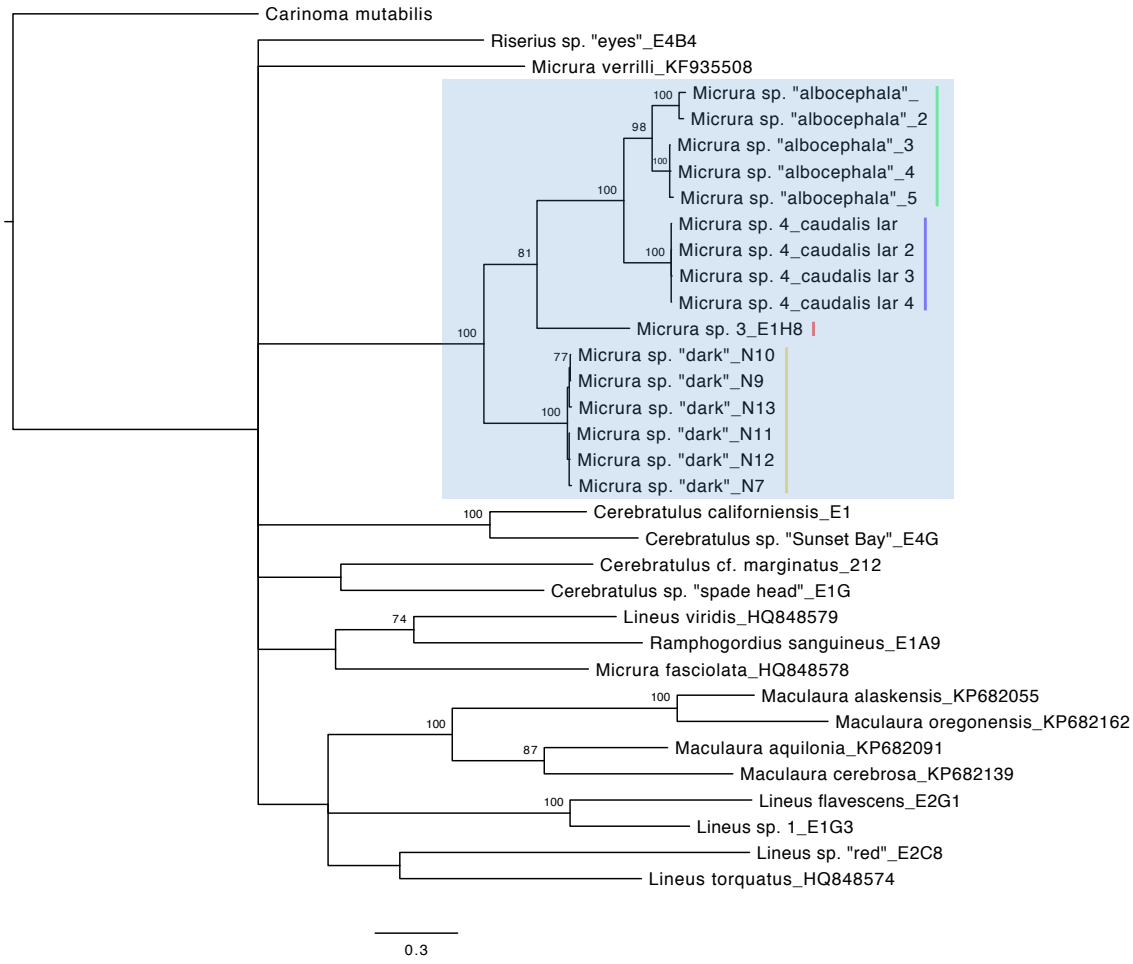

Figure 3.2D. COI Bayesian phylogeny of the Pilidiophora supports the monophyly of the four "trochonemertes" species. Bayesian posterior probabilities ≥70 are indicated above nodes. The monophyletic "trochonemertes" clade is highlighted in blue, and monophyletic "trochonemertes" clades are indicated with a vertical line in a species-specific color. *Carinoma mutabilis*, a palaeonemertean, serves as the outgroup.

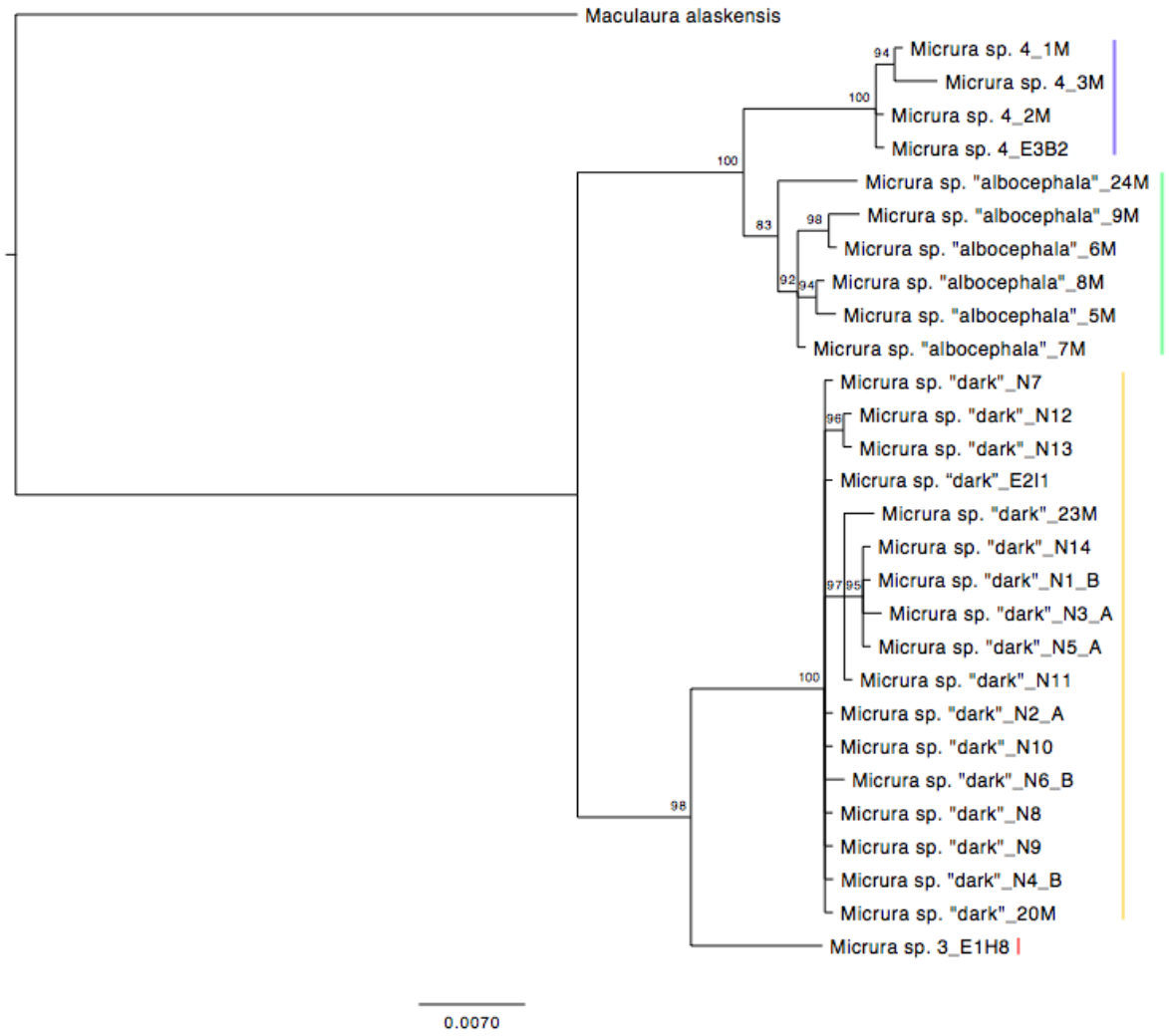

Figure 3.2E. 28S Bayesian analysis of "trochonemertes" species. Bayesian posterior probabilities ≥70 are indicated above nodes. Monophyletic clades are indicated with a vertical line in a species-specific color. *Maculaura alaskensis*, a pilidiophoran with a typical hat-shaped planktotrophic pilidium, serves as the outgroup.

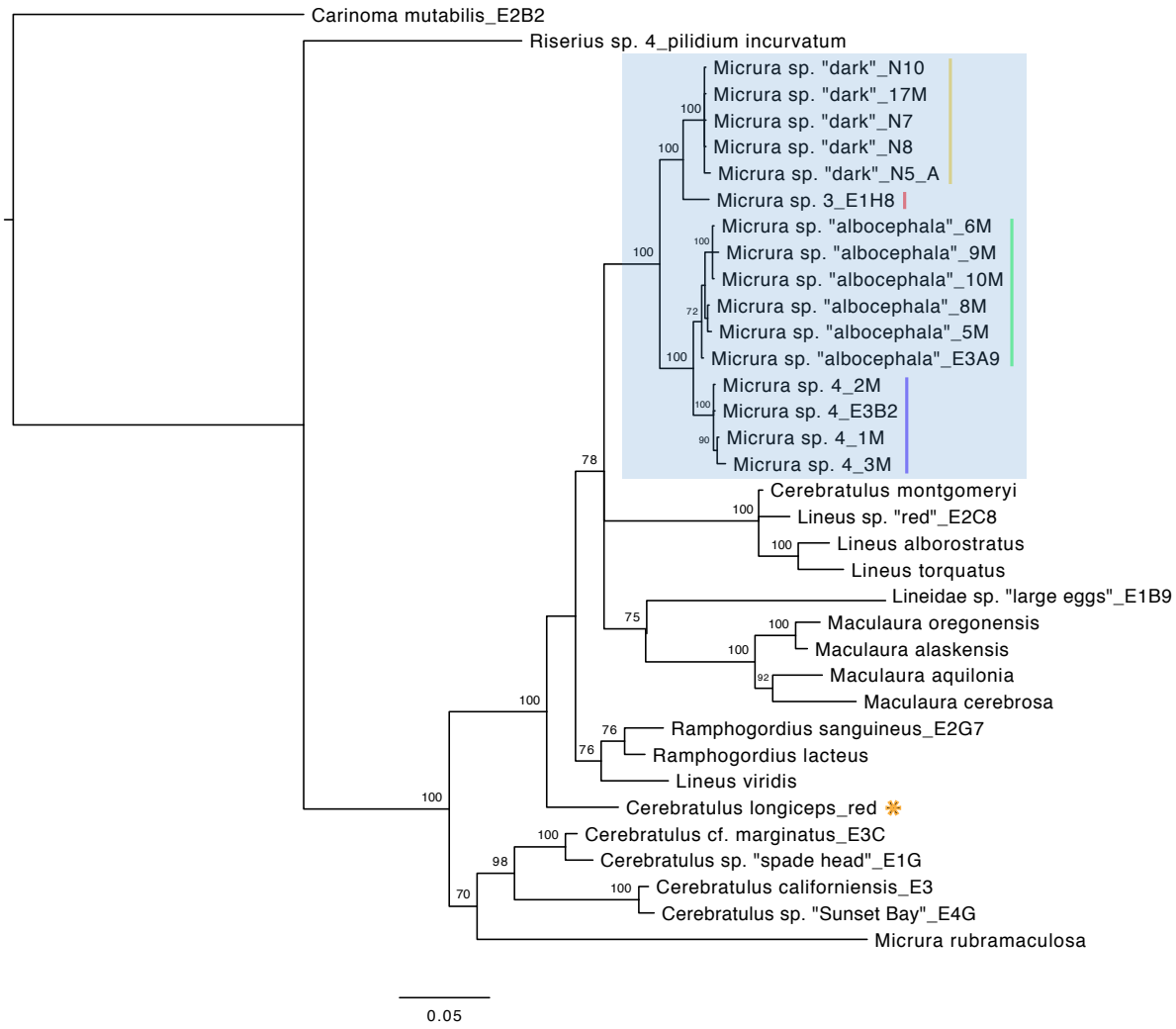

Figure 3.2F. 28S Bayesian phylogeny of the Pilidiophora supports the monophyly of the four "trochonemertes" species. Bayesian posterior probabilities ≥70 are indicated above nodes. The monophyletic "trochonemertes" clade is highlighted in blue, and monophyletic "trochonemertes" clades are indicated with a vertical line in a species-specific color. *Cerebratulus cf. longiceps*, which also bears *pilidium nielseni* larvae, is marked with an orange asterisk. *Carinoma mutabilis*, a palaeonemertean, serves as the outgroup.

pilidiophoran species were included in the analysis (Figures 3.2B, 3.2E-F). In these cases, the sister species *Micrura* sp. "albocephala" and *Micrura* sp. 4 made up the sister clade to the group formed by sister species *Micrura* sp. "dark" and *Micrura* sp. 3. The one *pilidium nielseni* specimen identified as *Cerebratulus cf. longiceps* was sequenced at the 16S and 28S gene regions, and in both cases, did not group with the "trochonemertes" when included in the pilidiophoran dataset. However, at the 16S region, it did group with the undescribed *Micrura* sp. "not coei," which produces yolky eggs suggestive of lecithotrophic development.

Maximum likelihood analysis of the 16S and COI gene regions resulted in reciprocal monophyly for all four proposed species when a subset of "trochonemertes" and pilidiophoran sequences were included in the analysis, but *Micrura* sp. "albocephala" was paraphyletic with respect to *Micrura* sp. 4 in analyses of the "trochonemertes" species. Analysis of 28S data produced four monophyletic clades whether other pilidiophorans were included or not (Table 3.1). In cases where *Micrura* sp. "albocephala" is monophyletic, maximum likelihood data supports a sister relationship with *Micrura* sp. 4. Analysis of the 28S gene region supported a sister relationship between *Micrura* sp. "dark" and *Micrura* sp. 3, and, when other pilidiophorans were included in the analysis, 16S data also supported this relationship. In these three cases, the sister species *Micrura* sp. "dark" and *Micrura* sp. 3 formed a clade sister to the clade formed by sister species *Micrura* sp. "albocephala" and *Micrura* sp. 4. *Cerebratulus cf. longiceps* did not group with the "trochonemertes" at the 16S and 28S gene regions when

included in the pilidiophoran dataset. At the 16S gene region, it grouped with *Micrura* sp. "not coei," which likely produces lecithotrophic larvae (trees not shown).

Neighbor-joining trees at every gene region resulted in four reciprocally monophyletic clades representing each "trochonemertes" species (Table 3.1). Analysis of the 16S and 28S gene regions supported a sister relationship between *Micrura* sp. "dark" and *Micrura* sp. 3, as well as *Micrura* sp. "albocephala" and *Micrura* sp. 4. Analysis of COI data only supported a sister relationships for *Micrura* sp. "albocephala" and *Micrura* sp. 4 (trees not shown).

Maximum parsimony analysis of each gene region showed that each of the four "trochonemertes" species formed a monophyletic clade (Table 3.1). Similarly to the neighbor-joining distance trees, both of the previously described sister relationships were supported by 16S and 28S data, but COI data only supported the sister relationship between *Micrura* sp. "albocephala" and *Micrura* sp. 4. The 16S alignment included 533 characters, including 74 parsimony-informative characters. Maximum parsimony analysis resulted in 150 most parsimonious trees (MPTs) with a tree length of 229, a consistency index (CI) of 0.8384, and a homoplasy index (HI) of 0.2761, and strict consensus tree supports the reciprocal monophyly of the four species. The COI alignment was 697 bp long, 147 of which were parsimony-informative. Maximum parsimony analysis resulted in 100 MPTs with a tree length of 399, a CI of 0.6992, and HI of 0.3008. The 28S alignment was 1072 total bp long, and 52 were informative. Maximum parsimony analysis produced a single MPT with a length of 160, a CI of 0.8228 and an HI of 0.1772 (trees not shown).

Barcoding gap

Average uncorrected intra- and interspecific distances supported the presence of five distinct species (Tables 3.1 and 3.2). The average intraspecific variation in both *Micrura* sp. "dark" and *Micrura* sp. 4 is less than 0.6% for all three gene regions. Intraspecific variation in *Micrura* sp. "albocephala" is less than 1% at the 16S and 28S gene regions, and just under 5% at the COI gene region. There was no difference between the two available *Micrura* sp. 3 sequences, and a 0.41% difference between the two *Cerebratulus cf. longiceps* sequences at the 16S region. Only one *Micrura* sp. 3 individual was sequenced at the COI and 28S regions, and only one *Cerebratulus cf. longiceps* was sequenced at the 28S region, so intraspecific variation at these regions could not be determined for these species. The interspecific variation between *Micrura* sp. "albocephala" and *Micrura* sp. 4, sister species, averaged 4.65% at the 16S gene region, 9.20% at the COI region, and 1.68% at the 28S gene region. *Micrura* sp. "dark" and *Micrura* sp. 3, also sister species, varied by 7.26%, 13.77%, and 2.51% at the 16S, COI, and 28S gene regions, respectively. The interspecific variation between *Cerebratulus cf. longiceps* and each of the "trochonemertes" species, was about 24% at the 16S gene region, and 8% at the more conserved 28S gene region. When maximum intraclade uncorrected *p*-distances are compared to minimum interclade uncorrected *p*-distances, there is a barcoding gap of 0.40 % (28S) to 0.51% (COI) (Table 3.3). If *Micrura* sp. "albocephala," which displays the highest intraspecific variation, is removed from the dataset, there is a gap of 1.79% (28S), 6.62% (16S), and 10.9% (COI) between maximum intraspecific and minimum interspecific divergences in the other three species.

	***Micrura* sp. "dark"**	***Micrura* sp. "albocephala"**	***Micrura* sp. 3**	***Micrura* sp. 4**	***Cerebratulus cf. longiceps***
***Micrura* sp.**	0.29				
"dark"	**0.57**				
	0.23				
***Micrura* sp.**	9.52	0.99			
"albocephala"	**14.17**	**4.90**			
	3.91	*0.49*			
***Micrura* sp. 3**	7.26	8.30	0.00		
	13.77	**13.87**	**NA**		
	2.51	*3.65*	*NA*		
***Micrura* sp. 4**	10.24	4.65	8.40	0.00	
	13.24	**9.20**	**12.16**	**0.08**	
	4.19	*1.68*	*3.99*	*0.21*	
Cerebratulus	24.00	24.33	23.48	24.90	0.41
cf. longiceps	**NA**	**NA**	**NA**	**NA**	**NA**
	8.57	*7.84*	*8.42*	*8.36*	*NA*

Table 3.2. Average uncorrected p-distances showing intra- and interspecific variation in the 16S gene region, COI gene region (bold), and 28S gene region (italics).

Gene region	Intraspecific p-distance	Interspecific p-distance
16S	0-3.21	3.66-24.90
COI	0.15-8.15	8.66-13.37
28S	0.40-0.98	1.38-8.57

Table 3.3. Range of divergence of inter- and intraspecific variation as uncorrected *p*-distances.

Automatic Barcode Gap Discovery analysis of each species bearing *pilidium nielseni* larvae, identified gaps between *Micrura* sp. "dark," *Micrura* sp. 3, *Micrura* sp. 4, and *Cerebratulus cf. longiceps* consistently across all tested gene regions, but oversplit *Micrura* sp. "albocephala" into three groups using 16S and COI data (Table 3.1).

Species delimitation based on larval morphology

The larvae of *Micrura* sp. "dark" collected from the plankton averaged 308 µm from the apical organ to the posterior end, with measurements ranging from 293 µm to 325 µm (n=8) (Table 3.4). Their anterior ciliary band is equatorial, and their posterior ciliary band encircles the larval posterior (Figure 2.1A). They have a lateral larval cirrus between the two ciliary bands near the juvenile posterior. These were about 40 µm, ranging from 32 µm to 46 µm. The yolk granules embedded in the larval epidermis were about 6 µm in diameter. Larvae cultured in lab had similar measurements: an average body length of 310 µm, a 45 µm cirrus, and 6 µm diameter yolk granules (n=22). Just posterior to the larval cirrus, confocal microscopy revealed a larval pore between the ciliary bands near the tip of the juvenile's posterior end in cultured *Micrura* sp. "dark" larvae (Figure 3.3A). *Pilidium nielseni* with a lateral cirrus collected from the plankton also had a lateral larval pore, but their identity is uncertain, because DNA of individuals preserved for confocal microscopy (in formaldehyde) cannot be easily extracted and sequenced.

Micrura sp. 3 larvae appear similar to the larvae of *Micrura* sp. "dark," sharing a lateral cirrus between the ciliary bands, but the "prototroch" is shifted slightly more

	Length (μm)	Length of cirrus (μm)	Diameter of yolk granules (μm)	Length of body cilia (μm)	Length of cilia in ciliary band (μm)
***Micrura* sp. "dark" (n=8)**	308	40	6	20	36
***Micrura* sp. "albocephala" (n=19)**	325	22	9	21	37
***Micrura* sp. 3 (n=2)**	311	62	9	22	34
***Micrura* sp. 4 (n=6)**	347	50	10	22	36
***Cerebratulus cf. longiceps* (n=1)**	290	30	6	21	31

Table 3.4. Average measurements of each *pilidium nielseni* morphotype.

anteriorly compared to *Micrura* sp. "dark" (Figure 2.1B) They also average a bit larger than *Micrura* sp. "dark," around 325 μm (n=2) (Table 3.4). However, this is still within the size range of *Micrura* sp. "dark." Their yolk granules averaged 9 μm in diameter, while all measured *Micrura* sp. "dark" larvae had yolk granules of 7 μm or less. The lateral cirrus of *Micrura* sp. 3 larvae were almost half as long as those of *Micrura* sp. "dark," measuring at 22 μm. However, the lengths of their cilia and cirrus were only measured for one individual, and the rest of the data was averaged from two individuals. Additionally, no known *Micrura* sp. 3 larvae were fixed and stained for confocal analysis, so I cannot compare internal larval morphology.

Micrura sp. "albocephala" larvae have a posterior larval cirrus, an anterior ciliary band shifted posteriorly from the larval equator, and a posterior ciliary band surrounding the larval posterior (Figure 2.1D). They averaged about 311 μm long, ranging from 280

µm to 343 µm (n=19) (Table 3.4). The cirrus averaged about 62 µm, but ranged from 43 µm to 72 µm. Their yolk granules were about 9 µm across.

The larvae of *Micrura* sp. 4 are similar to those of *Micrura* sp. "albocephala" (Figure 2.1E). They have a posterior larval cirrus, an anterior ciliary band shifted posteriorly from the equator, and a posterior ciliary band around the larval posterior. However, they average 347 µm, ranging from 300 to 383 µm (n=6) (Table 3.4). There is an overlap in size ranges for *Micrura* sp. "albocephala" and *Micrura* sp. 4, but *Micrura* sp. 4 larvae are generally larger. The average *Micrura* sp. 4 length is 36 longer than *Micrura* sp. "albocephala." Their yolk granules are about 10 µm. The length of the larval cirrus averages 50 µm, 12 µm shorter than the average for *Micrura* sp. "albocephala."

I also compared measurements of cilia, both the cilia uniformly covering the body and those which make up the ciliary bands. Body cilia are about 21 µm in each "trochonemertes" species, and those making up the ciliary bands are about 36 µm (Table 3.4).

I fixed 21 *pilidium nielseni* with a posterior larval cirrus and stained them for confocal analysis (Figures 3.3B-C). Analysis of confocal images revealed that 15 of these had a posterior cirrus extending from the perimeter of the blastopore on the same side as the juvenile's posterior end (Figure 3.3B). The other six had a second opening beside the blastopore (Figure 3.3C). This amniotic pore was open through the larval epidermis, and located between the posterior ciliary band and blastopore, vegetal to the

trunk of the juvenile. Its associated cirrus was just outside the larval pore along the posterior region of its perimeter (relative to the juvenile posterior).

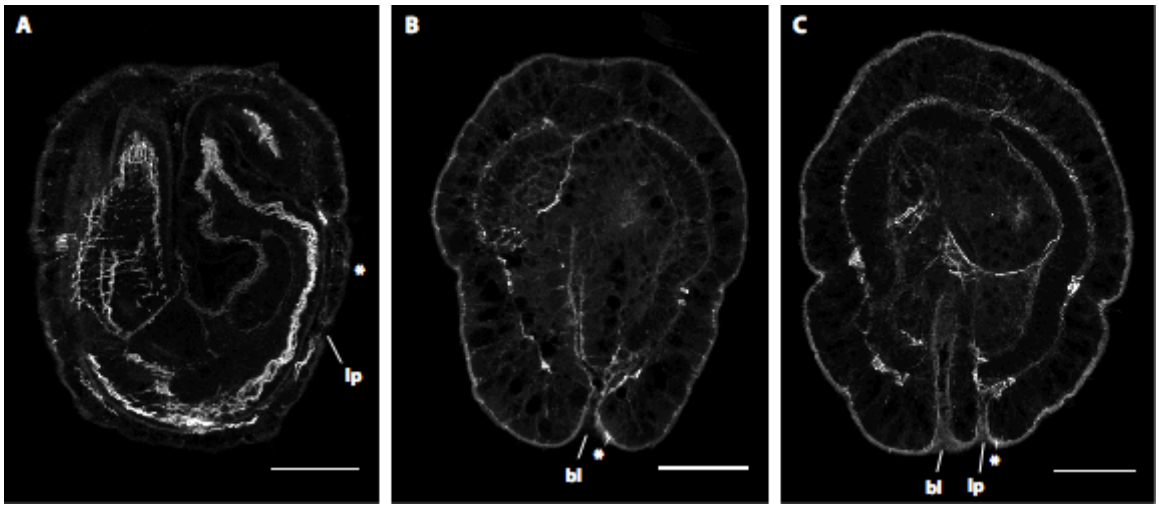

Figure 3.3. Larval pore and cirrus of three morphotypes of *pilidium nielseni*. Confocal z-projections of specimens stained with phalloidin. Sagittal sections, apical plate up, juvenile anterior to the left. A. A 3.25 µm slab from the left side of *Micrura* sp. "dark" larva showing a lateral larval pore (lp) and lateral larval cirrus (asterisk) between the two ciliary bands. B. A 3.25 µm slab from the right side of a *Micrura* sp. "albocephala" larva showing a posterior larval cirrus just outside the blastopore (bl). C. A 5.85 µm slab from the right side of a *Micrura* sp. 4 larva showing a posterior larval pore and larval cirrus. Scale bars are 50 µm.

I only collected one *pilidium nielseni* belonging to *Cerebratulus cf. longiceps*, and sequenced it rather than fixing it for confocal analysis, so I do not know if it has a larval pore. Like *Micrura* sp. "dark" and *Micrura* sp. 3, it has a lateral cirrus, but its anterior ciliary band is just posterior to the larval equator, and its posterior ciliary band appears to be slightly more anterior than the posterior bands in any of the "trochonemertes" (Figure 2.1C) It measured 290 µm long, its lateral cirrus was 30 µm long, and the diameter of its yolk granules was 6 µm (n=1) (Table 3.4). Like the "trochonemertes," the cilia covering

the body was about 21 µm, but the cilia making up the ciliary bands was 31 µm, about 5 µm shorter than average for the "trochonemertes," and longer than its cirrus. It is pinkish color, as opposed to the "trochonemertes" *pilidium nielseni* which are all a pale orange.

Species delimitation based on adult morphology

Micrura sp. "dark" adults have gray to dark gray heads, and in lighter-colored individuals, appear pinkish in the brain region (Figure 2.2). They have typical lineid longitudinal cephalic slits and lack ocelli. Most of the body is gray to dusty pink, but the posterior end is usually a bright cranberry and tapers to a long caudal cirrus, a thin "tail" of tissue (as opposed to the ciliary larval cirrus). Specimens averaged 7 cm long when relaxed in 0.34 $MgCl_2$, and typically ranged from about 5 to 9 cm long. Their cirri were about 3 mm long when relaxed, but I observed one active specimen with a cirrus stretched to 1 cm. The posterior end is somewhat dorsoventrally flattened with an average width of 2 to 3 mm, while the anterior is more rounded, with a diameter of about 2 mm. When ripe, the body coloration appears lighter because gametes are visible through the body wall. In glide, the tip of the head is narrowed and moves side to side as the rest of the body is led forward. Their characteristic, nearly constant peristaltic motion distinguishes it from other co-occuring, similarly-sized, reddish nemertean species, such as the undescribed species *Lineus* sp. "red" and Lineid gen. sp. "large eggs" (T. Hiebert and Maslakova, 2015a). At almost any given time, one or two peristaltic waves can be observed; they are most apparent in the anterior region of the body (head and foregut region), and move from anterior to posterior (Figure 2.2B). The well-defined margins of

the wave give the worms a cartoonish appearance, looking as though they are gulping down a series of doughnuts whole. The peristaltic waves are somewhat lessened in females engorged with (~250 μm in diameter) eggs. When disturbed, the worms will contract and loosely coil, halting their distinctive peristalsis. They are easily fragmented during collection, but rarely fragment when handled gently in lab. If they are damaged, the posterior end and cirrus will regenerate within a few days, but the anterior end does not regenerate.

Micrura sp. "albocephala" adults are predominantly dark gray to black with greenish undertones, though smaller (possibly younger) specimens tend to have somewhat lighter coloration (Figure 3.1). Their bodies are rounded anteriorly, but are dorsoventrally flattened in the posterior region, which ends in a long caudal cirrus. They have a bright white, ovate head with longitudinal cephalic slits and lack ocelli, resembling the rarely-encountered, co-occurring *Cerebratulus albifrons,* a genetically distinct species found in southern Oregon (T. Hiebert, 2016). Like *Micrura* sp. "dark," *Micrura* sp. "albocephala" are more likely to fragment during collection than when handled in lab. I collected all three of the *Micrura* sp. "albocephala" found in January of 2014 and 2015 as fragments, and was only able to collect the smallest specimens, those collected in the spring of 2016, intact. I measured the body width and cirrus length (when present) of those collected in January, and all three measured 4-5 mm across. Two had a cirrus, with one measuring at 2 mm, and the other at 5 mm. The much smaller, but complete specimen collected in March 2016, was 16 mm long and 1 mm wide with a 3.5 mm long cirrus. Two specimens collected from mudflats prior to this study, in 2011 and

2012, were not measured. Like *Micrura* sp. "dark," *Micrura* sp. "albocephala" can regenerate their posterior end and cirrus.

Despite several years of continuous collection and sequencing of adult nemerteans in local intertidal habitats, adult specimens of *Micrura* sp. 3 and *Micrura* sp. 4 have yet to be discovered (see T. Hiebert, 2016).

Cerebratulus longiceps (Coe, 1901) is described as having a length of up to 30 cm and a width up to 6 mm (Roe et al., 2007). It is darkly colored dorsally, appearing brownish-black to purplish, with a paler ventral side. Its head, which is described as long, flat and pointed, is also paler in color, as are the borders of its cephalic slits (Roe et al., 2007). Adults have not been encountered locally. The *Cerebratulus longiceps* 16S sequence in GenBank I matched my pinkish *pilidium nielseni* larva to, belonged to an adult specimen collected from subtidal shell rubble (70-80 m) by dredging at Rocky Point near San Juan Island, in Puget Sound, Washington by Drs. Maslakova, Norenburg, and Schwartz in 1998 (both 16S and COI are available in GenBank, see Appendix for 16S). It fit this description, and was provisionally identified as *Cerebratulus longiceps*, but it had two ocelli-like spots at the tip of its head, which were not mentioned in the original description (Coe, 1901; Maslakova, personal communication).

Adult ecology

All adult *Micrura* sp. "dark" specimens were collected in the rocky intertidal areas of Cape Arago in Charleston, Oregon. Most were found in dense root masses of *Phyllospadix scouleri, P. serratus,* and *P. torreyi* in shell hash in the mid and low

intertidal zones, though several individuals were found wedged between rocks, or in surf grass rooted in finer sand. They often co-occured with a variety of polychaetes, small ophiuroids, isopods, and other nemertean species, including *Maculaura cerebrosa* (T. Hiebert and Maslakova, 2015a), *Tetrastemma* spp., *Paranemertes peregrina*, and two undescribed lineiform species referred to as Lineid gen. sp. "large eggs," which has encapsulated development (Maslakova and T. Hiebert, 2014; Maslakova, personal communication.), and *Lineus* sp. "red," which have planktotrophic pilidium larva (T. Hiebert and Maslakova, 2015a). *Micrura* sp. "dark" is reproductive in the late fall and winter, as early as August and as late as February, though I only observed their larvae in plankton tows from October to January.

Adult *Micrura* sp. "albocephala" were encountered much less frequently, but often in the same habitat as *Micrura* sp. "dark." The first two were discovered in nearby mudflats; one from a Charleston mudflat in fall of 2011, and a second from North Bend near the Southwest Oregon Regional Airport in January 2012. The rest were found in the rocky intertidal area of Middle Cove, Cape Arago. *Micrura* sp. "albocephala" also inhabit dense root masses of surf grass rooted in shell hash, but I usually found them in lower intertidal areas than I found *Micrura* sp. "dark." They are also winter spawners. Their larvae were collected in plankton tows in December and January, and the only adult observed with gametes was a female engorged with eggs, collected in January 2014.

Cerebratulus longiceps (Coe 1901) was originally described from Alaska, and is reported to have a range from Alaska to California, but adults have yet to be encountered

in southern Oregon (Roe et al., 2007; T. Hiebert, 2016). The *pilidium nielseni* collected in this study is the first *Cerebratulus cf. longiceps* specimen found in this region.

Discussion

Traditionally, nemertean species were distinguished by adult morphology, but this has been problematic. Rather than relying on a description of the adult as the sole or primary method of species delimitation, I have used a multifaceted approach, including sequence- and morphology-based methods with both larval and adult specimens. The consistency of the results across methods strengthens their conclusion; there are four distinct, but closely-related species which produce a *pilidium nielseni* larva, forming the monophyletic "trochonemertes" clade, and a fifth species, *Cerebratulus cf. longiceps*, which is not included in the "trochonemertes" (Table 3.1, Figure 3.3).

Phylogenetic analyses of "trochonemertes" data resulted in four reciprocally monophyletic clades representing each of the proposed species at 16S, COI, and 28S regions in all but two cases, where maximum likelihood analyses determined that *Micrura* sp. "albocephala" was paraphyletic at the 16S and COI regions (Table 3.1, Figure 3.2). The only gene region to resolve each species into a monophyletic clade with every analyses was the 28S region, which is unsurprising, as it is the most conserved of the three regions. Reciprocal monophyly takes time to achieve, so this data suggests the "trochonemertes" are unlikely to have diverged recently (Knowles and Carstens, 2007; van Velzen et al,. 2012). Additionally, these analyses support sister relationships between *Micrura* sp. "albocephala" and *Micrura* sp. 4, and, less consistently, between *Micrura* sp.

"dark" and *Micrura* sp. 3. Only one *Micrura* sp. 3 individual was sequenced at the 28S and COI regions, and only two at the 16S region, so additional data may clarify its relationship to *Micrura* sp. "dark." *Cerebratulus cf. longiceps* did not group with the "trochonemertes" at the 16S or 28S regions, but at the 16S region, did group with *Micrura* sp. "not coei," which also has lecithotrophic development. This suggests it arrived at its *pilidium nielseni* morphology independently from the "trochonemertes." This conclusion is based on genetic data from one larval specimen, but is supported by the fact that I immediately recognized it as morphologically distinct from other *pilidium nielseni*.

The average uncorrected intra- and interspecific *p*-distances identified five distinct species (Tables 3.1, 3.2 and 3.3). The intraspecific *p*-distances are low, as one would expect within a species, and there is no overlap in average intra- and interspecific *p*-distances for any species at any gene. The lack of overlap provides a clear distinction between species, and signifies the presence of a barcoding gap. Some would argue that barcoding based on average values can hide the overlap between maximum intraclade and minimum interclade values (e.g. Meyer and Paulay, 2005). While much smaller, a barcoding gap still exists between maximum intraspecific and minimum interspecific values. Automated Barcode Gap Discovery analysis produced similar results. *Micrura* sp. "albocephala," which has the largest intraspecific variation, was overspilt into three groups using both 16S and COI data, but ABGD identified a barcoding gap between all species at the 28S region. The discrepancy between this and the *p*-distance data, can be attributed to the fact that ABGD analysis does not assume that a sequence belongs to any

particular species, but instead, sorts sequences into species based on the differences between them. Taken together, the results of the ABGD analysis and the barcoding gap between *p*-distances support each of the five species bearing *pilidium nielseni* larvae. However, intraspecific divergences could not be ascertained for *Micrura* sp. 3 at the COI and 28S regions, because it is represented by one sequence, and divergence at the 16S region is based on a comparison of only two sequences. Intraspecific variation in *Cerebratulus cf. longiceps* at the COI and 28S regions could not be determined, because it was not sequenced at the COI region, and only one individual was sequenced at the 28S gene region. Values for *Cerebratulus cf. longiceps* and *Micrura* sp. 3's interspecific divergences should also be considered preliminary, and require more data to definitively determine.

Overall, analysis of the sequence data supports the presence of five distinct clades divergent enough from each other to represent separate species. Together, four species form a strongly supported monophyletic clade, the "trochonemertes," and the fifth, *Cerebratulus cf. longiceps*, is more distantly related. These results agree with and expand on preliminary assessments (Maslakova and T. Hiebert, 2014; T. Hiebert, 2016; Maslakova et al., unpublished).

Each of the five species revealed by the sequence data is corroborated by larval morphology, findings which align with previous studies (Maslakova and T. Hiebert, 2014; T. Hiebert, 2016; Maslakova et al., unpublished; Figures 2.1 and 3.4). A unique *pilidium nielseni* morphotype is produced by each species, and sister species are most morphologically similar. *Micrura* sp. "dark" and *Micrura* sp. 3 share an equatorial ciliary

band (though *Micrura* sp. 3's may be shifted anteriorly slightly) and a lateral cirrus, but can be distinguished from each other based on body length, cirrus length, and the diameter of the yolk granules dotting the surface of the larval epidermis (Figure 2.1A-B, Table 3.4). The *Micrura* sp. 3 larvae are longer than *Micrura* sp. "dark" (though there is some overlap between the longest *Micrura* sp. "dark" and shortest *Micrura* sp. 3 larvae), *Micrura* sp. "dark" has a cirrus averaging almost twice as long as that of *Micrura* sp. 3, and the yolk granules in *Micrura* sp. "dark" were consistently smaller in diameter than those in *Micrura* sp. 3. However, the *Micrura* sp. 3 measurements are based on only two individuals. Analysis of confocal data showed that lab-raised *Micrura* sp. "dark" larvae develop a lateral pore associated with their cirrus three to four days post-fertilization (Figure 3.3A; see Chapter II). I also fixed and stained 12 wild-caught *pilidium nielseni* with a lateral cirrus, and I was able to identify a lateral larval pore in most of these specimens, but without definitively identifying any of these as *Micrura* sp. 3 or *Micrura* sp. "dark" larvae, I cannot determine whether they share this trait. Overall, the lack of data for *Micrura* sp. 3 makes it difficult to recognize and define cutoff points for quantifiable morphological characteristics between these sister species. Differences in cirrus length and yolk granule size seem like the most promising distinguishing features, but this assertion requires support from a larger dataset.

The second pair of sister species, *Micrura* sp. "albocephala" and *Micrura* sp. 4, both have an anterior ciliary band shifted slightly posterior to the equator and a posterior larval cirrus, but differ in body and cirrus length (Figure 2.1D-E, Table 3.4). *Micrura* sp. 4 averages 36 µm longer than *Micrura* sp. "albocephala," but has a cirrus averaging 12

μm shorter. However, there was overlap between maximum and minimum measurements. That said, these general size differences can still help distinguish between species, especially when comparing proportions; *Micrura* sp. "albocephala" produce a relatively small larva with a long posterior cirrus, while *Micrura* sp. 4 produce a relatively large larva with a short posterior cirrus.

Another possible difference between *Micrura* sp. "albocephala" and *Micrura* sp. 4 larvae is the location of the larval pore (Figure 3.3B-C). Of the 21 *pilidium nielseni* with a posterior cirrus I fixed and stained for confocal analysis, I tentatively identified one relatively large larva as *Micrura* sp. 4, and three relatively small larvae as *Micrura* sp. "albocephala." Confocal images revealed that the larva I identified as *Micrura* sp. 4 had a posterior larval pore associated with its cirrus, while the three I identified as *Micrura* sp. "albocephala" lacked an amniotic pore and, instead, the cirrus was associated with the blastopore. Based on my preliminary judgements and the fact that larvae without a larval pore were more abundant, I suspect that *Micrura* sp. "albocephala" lack a separate larval pore, while *Micrura* sp. 4 have an amniotic pore just outside the blastopore.

Straightaway, I was struck by the pink hue of the *pilidium nielseni* of *Cerebratulus cf. longiceps,* because "trochonemertes" larvae are a pale orange (Figure 2.1). I also noticed that it took on a different shape than the "trochonemertes" *pilidium nielseni* when the muscles underlying the ciliary bands contracted; it looked more bulb-like, with a narrower posterior end, which I attribute to the "telotroch" being positioned slightly more anteriorly than that of the "trochonemertes" *pilidium nielseni*. It had a lateral cirrus, and the cilia making up the ciliary bands were a bit shorter than those in the

"trochonemertes," on average (Figure 2.1C, Table 3.4). Sequence data confirmed my suspicions—it did not match to any "trochonemertes" sequences. Because of its distinctive coloration, this *pilidium nielseni* is the only one recognizable without the aid of a compound microscope—and it is the only one (so far) not closely related to the others.

It would be helpful to compare *pilidium nielseni* of known ages, and in future studies, larvae should be relaxed prior to being photographed. My data are based on images of unrelaxed specimens, as I did not originally plan to take these measurements, so when larvae swam or altered their position, there was some variation between photographs of the same individual. Also, *pilidium nielseni* collected from the plankton were of unknown age, which may account for some of the overlap in measurements between species. For instance, *Micrura* sp. "dark" raised in laboratory cultures were almost 25% longer than the diameter of their eggs once the larvae took on their characteristic trochophore-like form (see Chapter II). It is reasonable to assume that *pilidium nielseni* of other species also elongate as they develop, so it is possible that younger individuals of a generally larger species (like *Micrura* sp. 4) would be shorter than older individuals of a generally smaller species (like *Micrura* sp. "albocephala").

There are obvious differences between *Micrura* sp. "dark" and *Micrura* sp. "albocephala" adults, which further support their separation into different species (Figures 2.2 and 3.1). In fact, they were initially lumped into different megagenera, with *Micrura* sp. "dark" meeting the basic definition of a *Micrura* species, and *Micrura* sp. "albocephala" presenting more like a *Cerebratulus*. *Micrura* sp. "dark" is long and

slender with a dark gray anterior and bright cranberry posterior, while *Micrura* sp. "albocephala" is generally larger and wider with a white head and black body. They do co-occur in rocky intertidal areas, entangled in surf grass roots growing in shell hash, but *Micrura* sp. "albocephala" tend to be in lower intertidal zones. Additionally, *Micrura* sp. "albocephala" have been found in mudflats, while *Micrura* sp. "dark" never have. Adult ecology and external morphology clearly distinguish them from each other, but internal morphology has yet to be described for either of these species. *Micrura* sp. 3 and *Micrura* sp. 4 adults have never been found, but it would be helpful to compare their adult characters as well. Adult *Cerebratulus cf. longiceps* have not been located locally, but the presence of their larvae suggests they are nearby, and are described as low intertidal to subtidal species (Roe et al., 2007). Measuring up to 30 cm long, they are larger than both known "trochonemertes" adults. Their coloration is also distinct, described as dark on the dorsal side, with a pale head and ventral side (Roe et al., 2007). The particular specimen in GenBank which matched to my pinkish *pilidium nielseni* fit this description (Maslakova, personal communication).

Alone, the traditional method of defining species based on adult morphological characters would have been inadequate. Without collecting, sequencing and examining larvae, *Micrura* sp. 3 and *Micrura* sp. 4 would still be undiscovered, and we would not know *Cerebratulus cf. longiceps* is present locally, or that it produces lecithotrophic larvae. Sequence data, but not external adult morphology, could identify *Micrura* sp. "dark" and *Micrura* sp. "albocephala" as closely related species, but the synapomorphy of the *pilidium nielseni* larva—arguably their most interesting characteristic—would be

unknown. As this study demonstrates, collecting, characterizing, and sequencing both larvae and adults allows one to identify and delimit species more completely and confidently.

In the future, ideally, *Micrura* sp. "albocephala," *Micrura* sp. 3, *Micrura* sp. 4, and *Cerebratulus cf. longiceps*, would be collected as adults and spawned in lab, just as *Micrura* sp. "dark" was (see Chapter II). This would allow for comparisons between *pilidium nielseni* of known age and identity. It would also be useful to compare gamete morphology, and metamorphoses. *Micrura* sp. "dark" juveniles push through the larval epidermis with their posterior end, near the lateral larval pore and cirrus (Maslakova and von Dassow, 2012). I observed several *pilidium nielseni* with a posterior cirrus metamorphose, and their juveniles seemed to emerge through the posterior end. Variance in metamorphosis may be phylogenetically significant, and related to the location of the larval pore. Additionally, the discovery of *Micrura* sp. 3 and *Micrura* sp. 4 adults would augment sequence data, and permit a comparison of adult morphologies, as well as proper species descriptions. While the infrequency of *Micrura* sp. 3 and *Micrura* sp. 4 larvae's appearance in plankton samples suggests they are the most rare of the "trochonemertes" species, it is also possible that adults have not been encountered yet because collection has focused on the more accessible intertidal regions. Perhaps they—as well as *Cerebratulus cf. longiceps* adults—will be found subtidally.

Even without these data, using a multifaceted approach, I have uncovered multiple lines of evidence supporting the existence of five distinct species which produce *pilidium nielseni* larvae. I have shown that four of these species form the monophyletic

"trochonemertes" clade, characterized by the novel trochophore-like *pilidium nielseni,* while the fifth species, *Cerebratulus cf. longiceps*, represents an independent convergence on this larval form. I have also demonstrated that each species produces a unique *pilidium nielseni* morphotype, supporting the notion that, when possible, larval characters should be included in species descriptions (Lacalli, 2005; Barber and Boyce, 2006; De Queiroz, 2007).

CHAPTER IV

CONCLUSION

I have described the development of *pilidium nielseni*, an intriguingly—but superficially—trochophore-like pilidium. This is one of the first complete descriptions of development for a lecithotrophic pilidium using modern methods (Schwartz, 2009; von Döhren, 2011; Martîn-Durán et al., 2015). I have demonstrated that the novel *pilidium nielseni* larva develops very similarly to a typical, hat-shaped planktotrophic pilidium, despite its radically different outward appearance (Maslakova, 2010a).

The transition to lecithotrophy often results in predictable modifications, including larger eggs, accelerated development, rearrangement of the ciliary bands, and a more streamlined body form (Strathmann, 1985; Emlet, 1991; McEdward and Miner, 2001). These types of adjustments have been seen in other lecithotrophic pilidia, and in lecithotrophic larvae derived from planktotrophic larvae in other phyla, including Mollusca, Annelida, and Echinodermata (Emlet, 1991; Wray, 1996; Moran, 1999; Pernet, 2003). Each of these groups have independently converged on a simpler, ovoid larva with transverse ciliary bands (or uniform ciliation) multiple times (Emlet, 1991), and nemerteans have converged on the trochophore-like *pilidium nielseni* at least twice, as demonstrated by its appearance in both the "trochonemertes" clade and *Cerebratulus cf. longiceps* (T. Hiebert, 2016; this study). So, despite the impulse to view *pilidium nielseni* as a reversion to the hypothetical ancestral trochophore, its appearance is convincingly explained as a convergence on a successful body plan. Once the need to feed was removed, *pilidium nielseni* likely evolved to optimize swimming ability by reducing and

repurposing extraneous feeding structures inherited from its planktotrophic ancestor (Emlet, 1994; von Döhren, 2011; Maslakova and von Dassow, 2012).

This novel larval type is produced by at least five species, which I determined using a combination of morphological and sequence data. These efforts consistently demonstrated that *pilidium nielseni* are produced by four distinct, but closely related species forming a monophyletic pilidiophoran clade, the "trochonemertes," as well as a fifth species, *Cerebratulus cf. longiceps*, which is not included in this clade.

Multiple phylogenetic analyses of sequence data from two different mitochondrial gene regions, 16S rDNA and Cytochrome Oxidase I, and one nuclear region, 28S rDNA, resulted in four reciprocally monophyletic clades representing each of the four proposed "trochonemertes" species: *Micrura* sp. "dark," *Micrura* sp. "albocephala," *Micrura* sp. 3, and *Micrura* sp. 4. When these species were included in a larger pilidiophoran dataset, they consistently formed a monophyletic clade, the "trochonemertes." At the tested gene regions (16S and 28S), *Cerebratulus cf. longiceps* did not group with the rest of the *pilidium nielseni*-bearing species. Uncorrected pairwise distances quantified sequence divergences, and showed no overlap between maximum intraspecific and minimum interspecific *p*-distances. These "barcoding gaps" further support the presence of five distinct species.

The distinction between species is also corroborated by larval morphology. Each of the five species corresponds to a unique *pilidium nielseni* morphotypes. *Micrura* sp. "dark" and *Micrura* sp. 3 are sister species, and both produce *pilidium nielseni* with a lateral larval cirrus and a roughly equatorial "prototroch." Body length, cirrus length, and

yolk diameter may differ between species, but this differentiation is based on the only two *Micrura* sp. 3 *pilidium nielseni* that were collected, measured, and sequenced. The second set of sister species, *Micrura* sp. "albocephala" and *Micrura* sp. 4, also produce *pilidium nielseni* morphotypes which are similar to each other. Each have a "prototroch" slightly posterior to the larval equator, and a posterior larval cirrus. They can be distinguished by size, cirrus length, and possibly the presence of a posterior larval pore. Confocal data suggests that *Micrura* sp. 4 may have a posterior larval pore associated with its cirrus, while *Micrura* sp. "albocephala" lacks a larval pore, and instead, its posterior cirrus is associated with the blastopore. Each distinct morphotype is unique to a particular species, and the similarity between pairs of morphotypes mirrors the sister relationships defined by sequence data. *Cerebratulus cf. longiceps* produces a *pilidium nielseni* readily distinguishable from the "trochonemertes" by its pinkish color, as all other *pilidium nielseni* are a pale orange. It also has a "telotroch" which is slightly more anterior than the "telotrochs" of "trochonemertes" larvae. If the one *Cerebratulus cf. longiceps* larva I collected is typical for the species, it is the easiest *pilidium nielseni* to pick out from the rest, and its readily observable differences support the conclusions reached by analysis of the sequence data—*Cerebratulus cf. longiceps* converged on this larval form independently.

Data related to adult morphology is minimal. Only *Micrura* sp. "dark" and *Micrura* sp. "albocephala" have been found locally as adults, and neither have been thoroughly examined. A histological study of any and all adult "trochonemertes" species could elucidate adult synapomorphies to define the clade, as well as identify and

differentiate species among adult specimens. It would also allow for a complete species description. Notably, species delimitation traditionally relied on identifying distinguishing characteristics in adult organisms, but this study demonstrates the effectiveness of taking a broader approach (Thollesson and Norenburg, 2003; De Queiroz, 2007; Maslakova and T. Hiebert, 2014; Sundberg, 2015).

This study has established that at least five species produce a *pilidium nielseni* larva, each bearing its own unique morphotype. Together, four species form a monophyletic clade within Pilidiophora characterized by the *pilidium nielseni* synapomorphy, while the fifth converged on its trochophore-like body form independently. Collecting and analyzing both larvae and adults, employing sequence- and morphology-based species delimitation methods, and sequencing specimens at multiple gene regions, revealed unknown nemertean diversity and a novel nemertean larval form, allowed me to delimit four closely-related undescribed species, revealed that *Cerebratulus cf. longiceps* produces a *pilidium nielseni* larva, and identified phylogenetically significant morphological characters.

APPENDIX

SPECIMENS AND SEQUENCES USED

Species		GenBank Accession # (s)			Study	Life Stage	Collection Information
		16S	COI	28S			
Carinoma mutabilis	-	AJ436832	-	-	Thollesson and Norenburg 2003		San Juan Island, WA USA
Carinoma mutabilis	-	-	AJ436942	-	Thollesson & Norenburg 2003		San Juan Island, WA USA
Cerebratulus longiceps	-	EF124872	-	-	Schwartz and Norenburg	adult	Rocky Point, San Juan Island, WA USA
Cerebratulus californiensis	E1D7	-	KU197718	-	T. Hiebert 2016		Charleston, OR (T. Hiebert)
Cerebratulus californiensis	E2B6	KU197378	-	-	T. Hiebert 2016		Charleston, OR (T. Hiebert)
Cerebratulus californiensis	E3G5	-	-	KU365682	T. Hiebert 2016	adult	Charleston, OR (T. Hiebert and S. Maslakova)
Cerebratulus cf. longiceps	Red	KX296733	-	KX342095	This study	larva	Charleston, OR USA (M. Hunt)
Cerebratulus cf. marginatus	212	-	KU197734	-	T. Hiebert 2016		Charleston, OR USA (G. von Dassow)
Cerebratulus cf. marginatus	E1A1	KU197402	-	-	T. Hiebert 2016	adult	North Cove, Cape Arago, OR (T. Hiebert and S. Maslakova)
Cerebratulus cf. marginatus	E3C3	-	-	KU365683	This study	adult	Charleston, OR (T. Hiebert)
Cerebratulus montgomeryi	-	-	-	EF178489	Schwartz and Norenburg, unpublished	adult	Canada
Cerebratulus sp. “spade head”	E1G2	KU197425	KU197751	-	T. Hiebert 2016		Charleston, OR (T. Hiebert)
Cerebratulus sp. “spade head”	E1G5	-	-	KU365686	T. Hiebert 2016		Charleston, OR (T. Hiebert)
Cerebratulus sp. “Sunset Bay”	E4G9	KU197428	KU197755	KU365687	T. Hiebert 2016	larva	Charleston, OR (T. Hiebert and S. Maslakova)
Lineidae sp. “large eggs”	E1B9	-	-	KU365699	T. Hiebert 2016	adult	Charleston, OR USA (S. Maslakova)

APPENDIX

SPECIMENS AND SEQUENCES USED

Species		GenBank Accession # (s)			Study	Life Stage	Collection Information
		16S	COI	28S			
Lineus alborostratus	-	-	-	AJ436877	Thollesson and Norenburg 2003	adult	Vostok Bay, Sea of Japan, Russia
Lineus flavescens	E2G1	-	KU197784	-	T. Hiebert 2016	adult	Middle Cove, Cape Arago, OR (T. Hiebert and S. Maslakova)
Lineus sp. "red"	E1B6	KU197520	-	-	T. Hiebert 2016	adult	Middle Cove, Cape Arago, OR (T. Hiebert and S. Maslakova)
Lineus sp. "red"	E2C8	-	KU197819	KU365704	T. Hiebert 2016	larva	Charleston, OR USA (T. Hiebert)
Lineus sp. 1	E1G3	-	KU197799	-	T. Hiebert 2016	larva	Charleston, OR USA (T. Hiebert)
Lineus torquatus	-	JF277572	HQ848574	HQ856856	Andrade et al. 2012	adult	Akkeshi Bay, Japan
Lineus viridis	-	JF277582	HQ848579	HQ856854	Andrade et al. 2012	adult	Sylt Island, Germany
Maculaura alaskensis	E3B7	-	-	KU365705	T. Hiebert and Maslakova 2015b	adult	Gearhart, OR USA (T. Hiebert)
Maculaura alaskensis	F1_M19	KP682206	KP682082	-	T. Hiebert and Maslakova 2015	adult	False Bay, Friday Harbour (S. Maslakova)
Maculaura alaskensis	OR_C1 _M17	-	KP682055	-	T. Hiebert and Maslakova 2015	adult	Charleston, OR USA
Maculaura alaskensis	E2H6	KP682188	-	-	T. Hiebert et al. 2013	adult	Middle Cove, Charleston, OR USA (T. Hiebert and S. Maslakova)
Maculaura aquilonia	AK_J2_ J11	-	KP682091	-	T. Hiebert and Maslakova 2015	adult	Auke Creek, Juneau, AK (T. Hiebert)
Maculaura aquilonia	AK_J6_ J52	KP682232	-	-	T. Hiebert and Maslakova 2015	adult	Outer Point Douglas, Juneau, AK (T. Hiebert)
Maculaura aquilonia	E2G3	-	-	KU365706	T. Hiebert and Maslakova 2015b	adult	Charleston, OR USA

APPENDIX

SPECIMENS AND SEQUENCES USED

Species		GenBank Accession # (s)			Study	Life Stage	Collection Information
		16S	COI	28S			
Maculaura cerebrosa	E1A8	-	-	KU365707	T. Hiebert and Maslakova 2015b	adult	Crescent City, CA USA
Maculaura cerebrosa	OR_C13_M11	-	KP682139	-	T. Hiebert and Maslakova 2015	adult	Charleston, OR USA
Maculaura cerebrosa	OR_C5_173	KP682257	-	-	T. Hiebert and Maslakova 2015	adult	Charleston, OR USA
Maculaura oregonensis	E4A2	-	-	KU365709	T. Hiebert and Maslakova 2015b	adult	Charleston, OR USA (T. Hiebert)
Maculaura oregonensis	OR_C10_M28	-	KP682162	-	T. Hiebert and Maslakova 2015	adult	Colder Cove, Charleston, OR
Micrura fasciolata	-	-	HQ848578	-	Andrade et al. 2012		Tjärnö, Koster, Sweden
Micrura rubramaculosa	-	-	-	KF935349	Schwartz and Norenburg 2005		Bacos del Toro, Panama
Micrura sp. "dark"	E2G9_20M	KU197583	KU197860	-	T. Hiebert 2016	larva	Charleston, OR USA (T. Hiebert)
Micrura sp. "dark"	-	-	JQ430741	-	Maslakova and von Dassow 2012	larva	Charleston, OR USA (S. Maslakova)
Micrura sp. “albocephala”	125	KU197564	-	-	T. Hiebert 2016		Charleston, OR USA (A. Bird)
Micrura sp. “albocephala”	142	KU197565	KU197842	-	T. Hiebert 2016		Charleston, OR USA (S. Maslakova)
Micrura sp. “albocephala”	145	KU197566	-	-	T. Hiebert 2016		Charleston, OR USA (S. Maslakova)
Micrura sp. “albocephala”	146	KU197567	KU197843	-	T. Hiebert 2016		Charleston, OR USA (S. Maslakova)
Micrura sp. “albocephala”	184_6M	-	-	KX352451	This study	adult	Charleston, OR USA

APPENDIX

SPECIMENS AND SEQUENCES USED

Species		GenBank Accession # (s)			Study	Life Stage	Collection Information
		16S	COI	28S			
Micrura sp. "albocephala"	CSI	KX296707	-	-	This study	larva	Charleston, OR USA (M. Hunt)
Micrura sp. "albocephala"	CSIII	KX296708	-	-	This study	larva	Charleston, OR USA (M. Hunt)
Micrura sp. "albocephala"	CSIV	KX296709	-	-	This study	larva	Charleston, OR USA (M. Hunt)
Micrura sp. "albocephala"	E1D6	KU197568	KU197844	-	T. Hiebert 2016		Charleston, OR (T. Hiebert)
Micrura sp. "albocephala"	E1H2_9M	-	-	KX352454	This study	larva	Charleston, OR (T. Hiebert)
Micrura sp. "albocephala"	E1H2_9M	KU197569	KU197845	-	T. Hiebert 2016	larva	Charleston, OR (T. Hiebert)
Micrura sp. "albocephala"	E2C2_8M	-	-	KX352453	This study	larva	Charleston, OR (T. Hiebert)
Micrura sp. "albocephala"	E2C2_8M	KU197570	KU197846	-	T. Hiebert 2016	larva	Charleston, OR (T. Hiebert)
Micrura sp. "albocephala"	E2C3_7M	-	-	KX352452	This study	larva	Charleston, OR (T. Hiebert)
Micrura sp. "albocephala"	E2C3_7M	KU197571	-	-	T. Hiebert 2016	larva	Charleston, OR (T. Hiebert)
Micrura sp. "albocephala"	E2C4	KU197572	KU197847	-	T. Hiebert 2016		Charleston, OR (T. Hiebert)
Micrura sp. "albocephala"	E2C5_5M	-	-	KX352450	This study	larva	Charleston, OR (T. Hiebert)
Micrura sp. "albocephala"	E2C5_5M	KU197573	KU197848	-	T. Hiebert 2016	larva	Charleston, OR (T. Hiebert)
Micrura sp. "albocephala"	E3A9_24 M	-	-	KU197849	This study	larva	Charleston, OR (T. Hiebert and S. Maslakova)
Micrura sp. "albocephala"	E3A9_24 M	KU197574	KU197849	-	T. Hiebert 2016	larva	Charleston, OR (T. Hiebert and S. Maslakova)

APPENDIX

SPECIMENS AND SEQUENCES USED

Species		GenBank Accession # (s)			Study	Life Stage	Collection Information
		16S	COI	28S			
Micrura sp. "albocephala"	E3B1	KU197575	KU197850	-	T. Hiebert 2016		Charleston, OR (T. Hiebert and S. Maslakova)
Micrura sp. "albocephala"	E3B3	KU197576	KU197851	-	T. Hiebert 2016		Charleston, OR (T. Hiebert and S. Maslakova)
Micrura sp. "albocephala"	E5A9	KU197577	KU197852	-	T. Hiebert 2016		Charleston, OR USA (M. Hunt)
Micrura sp. "albocephala"	L14	KX296710	-	-	This study	larva	Charleston, OR USA (M. Hunt)
Micrura sp. "albocephala"	L27	KX296711	-	-	This study	larva	Charleston, OR USA (M. Hunt)
Micrura sp. "albocephala"	L30	KX296712	-	-	This study	larva	Charleston, OR USA (M. Hunt)
Micrura sp. "albocephala"	L3b	KX296713	-	-	This study	larva	Charleston, OR USA (M. Hunt)
Micrura sp. "albocephala"	L7b	KX296715	-	-	This study	larva	Charleston, OR USA (M. Hunt)
Micrura sp. "albocephala"	MMB106	-	KU197853	-	T. Hiebert 2016		Charleston, OR (T. Hiebert and S. Maslakova)
Micrura sp. "albocephala"	T1	KX296719	-	-	This study	larva	Charleston, OR USA (M. Hunt)
Micrura sp. "albocephala"	T10	KX296716	-	-	This study	larva	Charleston, OR USA (M. Hunt)
Micrura sp. "albocephala"	T11	KX296717	-	-	This study	larva	Charleston, OR USA (M. Hunt)
Micrura sp. "albocephala"	T13	KX296718	-	-	This study	larva	Charleston, OR USA (M. Hunt)
Micrura sp. "albocephala"	T23	KX296720	-	-	This study	larva	Charleston, OR USA (M. Hunt)
Micrura sp. "albocephala"	T26	KX296721	-	-	This study	larva	Charleston, OR USA (M. Hunt)

APPENDIX

SPECIMENS AND SEQUENCES USED

Species		GenBank Accession # (s)			Study	Life Stage	Collection Information
		16S	COI	28S			
Micrura sp. "albocephala"	T29	KX296722	-	-	This study	larva	Charleston, OR USA (M. Hunt)
Micrura sp. "albocephala"	T4	KX296723	-	-	This study	larva	Charleston, OR USA (M. Hunt)
Micrura sp. "albocephala"	T6	KX296724	-	-	This study	larva	Charleston, OR USA (M. Hunt)
Micrura sp. "albocephala"	T8	KX296725	-	-	This study	larva	Charleston, OR USA (M. Hunt)
Micrura sp. "dark"	-	-	JQ430741	-	Maslakova and von Dassow 2012		Charleston, OR USA
Micrura sp. "dark"	-	-	JQ430742	-	Maslakova and von Dassow 2012		Charleston, OR USA
Micrura sp. "dark"	-	-	JQ430743	-	Maslakova and von Dassow 2012		Charleston, OR USA
Micrura sp. "dark"	68	JQ430746	-	-	Maslakova and von Dassow 2012	adult	North Cove, Cape Arago, OR (S. Maslakova)
Micrura sp. "dark"	126	JQ430744	-	-	Maslakova and von Dassow 2012		Charleston, OR USA (S. Maslakova)
Micrura sp. "dark"	147_ 23M	-	-	KX342097	This study	juvenile	Charleston, OR USA (T. Hiebert)
Micrura sp. "dark"	E2E8	KU197582	KU197859	-	T. Hiebert 2016	adult	Middle Cove, Cape Arago, OR (T. Hiebert)
Micrura sp. "dark"	E2G9 _20M	-	-	KX342096	This study	larva	Charleston, OR USA (T. Hiebert)
Micrura sp. "dark"	E2H8	KU197584	-	-	T. Hiebert 2016	adult	Middle Cove, Cape Arago, OR (T. Hiebert and M. Hunt)
Micrura sp. "dark"	E2H9	KU197585	-	-	T. Hiebert 2016	adult	Middle Cove, Cape Arago, OR (T. Hiebert and M. Hunt)

APPENDIX

SPECIMENS AND SEQUENCES USED

Species		GenBank Accession # (s)			Study	Life Stage	Collection Information
		16S	COI	28S			
Micrura sp. "dark"	E2I1	KU197586	KU197858	KU365713	T. Hiebert 2016	adult	Middle Cove, Cape Arago, OR (T. Hiebert and M. Hunt)
Micrura sp. "dark"	N1_A	KX296698	-	-	This study	adult	Charleston, OR USA (M. Hunt)
Micrura sp. "dark"	N1_B	-	-	KX342103	This study	adult	Charleston, OR USA (M. Hunt)
Micrura sp. "dark"	N10	KX296690	KX342087	KX342098	This study	larva	Charleston, OR USA (M. Hunt)
Micrura sp. "dark"	N11	KX296691	KX342088	KX342099	This study	larva	Charleston, OR USA (M. Hunt)
Micrura sp. "dark"	N12	KX296692	KX342089	KX342100	This study	larva	Charleston, OR USA (M. Hunt)
Micrura sp. "dark"	N12_1	KX296693	-	-	This study	larva	Charleston, OR USA (M. Hunt)
Micrura sp. "dark"	N13	-	KX342090	KX342101	This study	larva	Charleston, OR USA (M. Hunt)
Micrura sp. "dark"	N14	KX296694	-	KX342102	This study	larva	Charleston, OR USA (M. Hunt)
Micrura sp. "dark"	N16	KX296695	-	-	This study	larva	Charleston, OR USA (M. Hunt)
Micrura sp. "dark"	N17	KX296696	-	-	This study	larva	Charleston, OR USA (M. Hunt)
Micrura sp. "dark"	N18	KX296697	-	-	This study	larva	Charleston, OR USA (M. Hunt)
Micrura sp. "dark"	N2_A	-	-	KX342104	This study	adult	Charleston, OR USA (M. Hunt)
Micrura sp. "dark"	N2_B	KX296699	KX342091	-	This study	adult	Charleston, OR USA (M. Hunt)

APPENDIX

SPECIMENS AND SEQUENCES USED

Species		GenBank Accession # (s)			Study	Life Stage	Collection Information
		16S	COI	28S			
Micrura sp. "dark"	N3_B	KX296700	-	-	This study	adult	Charleston, OR USA (M. Hunt)
Micrura sp. "dark"	N4_A	KX296701	-	-	This study	adult	Charleston, OR USA (M. Hunt)
Micrura sp. "dark"	N4_B	-	-	KX342106	This study	adult	Charleston, OR USA (M. Hunt)
Micrura sp. "dark"	N5_A	KX296702	-	KX342107	This study	adult	Charleston, OR USA (M. Hunt)
Micrura sp. "dark"	N6_A	KX296703	-	-	This study	adult	Charleston, OR USA (M. Hunt)
Micrura sp. "dark"	N6_B	-	-	KX342108	This study	adult	Charleston, OR USA (M. Hunt)
Micrura sp. "dark"	N7	KX296704	KX342093	KX342109	This study	larva	Charleston, OR USA (M. Hunt)
Micrura sp. "dark"	N8	KX296705	-	KX342110	This study	larva	Charleston, OR USA (M. Hunt)
Micrura sp. "dark"	N9	KX296706	KX342094	KX342111	This study	larva	Charleston, OR USA (M. Hunt)
Micrura sp. "dark"	-	-	JQ430743	-	Maslakova and von Dassow 2012	adult	North Cove, Cape Arago, OR (S. Maslakova)
Micrura sp. "dark"	-	JQ430745	-	-	Maslakova and von Dassow 2012		Charleston, OR USA (G. von Dassow)
Micrura sp. "not coei"	E5B1	KU197392	-	-	T. Hiebert 2016		Middle Cove, Cape Arago, OR (M. Hunt)
Micrura sp. 3	E1H8	KU197563	KU197841	KU365710	T. Hiebert 2016	larva	Charleston, OR USA (T. Hiebert)
Micrura sp. 3	N9_1	KX296726	-	-	This study	larva	Charleston, OR USA (M. Hunt)

APPENDIX

SPECIMENS AND SEQUENCES USED

Species		GenBank Accession # (s)			Study	Life Stage	Collection Information
		16S	COI	28S			
Micrura sp. 4	143_3M	-	-	KX342114	This study	larva	Charleston, OR USA (S. Maslakova)
Micrura sp. 4	143_3M	KU197578	KU197854	-	T. Hiebert 2016	larva	Charleston, OR USA (S. Maslakova)
Micrura sp. 4	144_2M	-	-	KX342113	This study	larva	Charleston, OR USA (S. Maslakova)
Micrura sp. 4	144_2M	KU197579	KU197855	-	T. Hiebert 2016	larva	Charleston, OR USA (S. Maslakova)
Micrura sp. 4	148_1M	-	-	KX342112	This study	larva	Charleston, OR USA (S. Maslakova)
Micrura sp. 4	148_1M	KU197580	KU197856	-	T. Hiebert 2016	larva	Charleston, OR USA (S. Maslakova)
Micrura sp. 4	CLI	KX296728	-	-	This study	larva	Charleston, OR USA (M. Hunt)
Micrura sp. 4	CLII	KX296729	-	-	This study	larva	Charleston, OR USA (M. Hunt)
Micrura sp. 4	CLIII	KX296730	-	-	This study	larva	Charleston, OR USA (M. Hunt)
Micrura sp. 4	CSII	KX296727	-	-	This study	larva	Charleston, OR USA (M. Hunt)
Micrura sp. 4	E3B2	KU197581	KU197857	KU365711	T. Hiebert 2016	larva	Charleston, OR USA (T. Hiebert)
Micrura sp. 4	L5b	KX296714	-	-	This study	larva	Charleston, OR USA (M. Hunt)
Micrura sp. 4	Lb	KX296731	-	-	This study	larva	Charleston, OR USA (M. Hunt)
Micrura sp. 4	R	KX296732	-	-	This study	larva	Charleston, OR USA (M. Hunt)

APPENDIX

SPECIMENS AND SEQUENCES USED

Species		GenBank Accession # (s)			Study	Life Stage	Collection Information
		16S	COI	28S			
Micrura verrilli	73	KU197527	-	-	T. Hiebert 2016		Cattle Pt, San Juan Island, WA (MMB 09)
Micrura verrilli	-	-	KF935508	-	Kvist et al. 2014	adult	USA (M. Schwartz)
Ramphogordius lacteus	-	-	-	HQ856850	Andrade et al. 2012		Brittany, France
Ramphogordius sanguineus	E1A9	-	KU197836	-	T. Hiebert 2016		Charleston, OR USA (G. von Dassow)
Ramphogordius sanguineus	E2G7	-	-	KU365717	T. Hiebert 2016	adult	Brown's Cove (T. Hiebert)
Ramphogordius sanguineus	E3I9	KU197555	-	-	T. Hiebert 2016	larva	Charleston, OR (T. Hiebert)
Riserius sp. "eyes"	E4B4	-	KU197840	-	T. Hiebert 2016		Charleston, OR USA (T. Hiebert)
Riserius sp. 1	156	KC777025	-	-	T. Hiebert et al. 2013	larva	Charleston, OR USA
Riserius sp. 4	-	E4H6	-	KU365718	T. Hiebert 2016	larva	Vostok Bay, Sea of Japan, Russia (A. Chernyshev)

REFERENCES CITED

Andrade, S.C.S., Strand, M., Schwartz, M., Chen, H., Kajihara, H., von Döhren, J., Sun, S., Junoy, J., Thiel, M., Norenburg, J.L., Turbeville, J.M., Giribet, G., & Sundberg, P. (2012). Disentangling ribbon worm relationships: multi-locus analysis supports traditional classification of the phylum Nemertea. *Cladistics* 28:141–159.

Andrade, S. C. S., H. Montenegro, M. Strand, M. L. Schwartz, H. Kajihara, J. L. Norenburg, J. M. Turbeville, Sundberg, P., & Giribet, G. (2014). A transcriptomic approach to ribbon worm systematics (Nemertea): resolving the Pilidiophora problem. *Mol Biol Evol* 31:3206-3215.

Appeltans, W., Ahyong, S.T., Anderson, G., Angel, M.V., Artois, T., Bailly, N., Bamber, R., Barber, A., Bartsch, I., Berta, A., Błazewicz-Paszkowycz, M., Bock, P., Boxshall, G., Boyko, C.B., Brandão, S.N., Bray, R.A.,.Bruce, N.L., Cairns, S.D., Chan, T-Y., Cheng, L., Collins, A., Cribb, T., Curini-Galletti, M., Dahdouh-Guebas, F., Davie, P.J.F., Dawson, M.N., De Clerck, O., Decock, W., De Grave, S., deVoogd, N.J., Domning, D.P., Emig, C.C., Erséus, C., Eschmeyer, W., Fauchald, K., Fautin, D.G., Feist, S.W., Fransen, C.H.J.M., Furuya, H., Garcia-Alvarez, O., Gerken, S., Gibson, D., Gittenberger, A., Gofas, S., Gómez-Daglio, L., Gordon, D.P., Guiry, M.D., Hernandez, F., Hoeksema, B.W., Hopcroft, R.R., Jaume, D., Kirk, P., Koedam, N., Koenemann, S., Kolb, J.B., Kristensen, R.M., Kroh, A., Lambert, G., Lazarus, D.B., Lemaitre, R., Longshaw, M., Lowry, J., Macpherson, E., Madin, L.P., Mah, C., Mapstone, G., McLaughlin, P.A., Mees, J., Meland, K., Messing, C.G., Mills, C.E., Molodtsova, T.N., Mooi, R., Neuhaus, B., Ng, P.K.L., Nielsen, C., Norenburg, J., Opresko, D.M., Osawa, M., Paulay, G., Perrin, W., Pilger, J.F., Poore, G.C.B., Pugh P., Read, G.B., Reimer, J.D., Rius, M., Rocha R.M., Saiz-Salinas, J.I., Scarabino, V., Schierwater, B., Schmidt-Rhaesa, A., Schnabel, K.E., Schotte, M., Schuchert, P., Schwabe, E., Segers, H., Self-Sullivan, C., Shenkar, N., Siegel, V., Sterrer, W., Stöhr, S., Swalla, B., Tasker, M.L., Thuesen, E.V., Timm, T., Todaro, M.A., Turon, X., Tyler, S., Uetz, P., van der Land, J., Vanhoorne, B., van Ofwegen, L.P., van Soest, R.W.M., Vanaverbeke, J., Walker-Smith, G., Walter, T.C., Warren, A., Williams, G.C., Wilson, S.P. & Costello, M.J. (2012). The Magnitude of Global Marine Species Diversity. *Curt Biol* 22: 2189–2202.

Barber, P. & Boyce, S.L. (2006). Estimating diversity of Indo-Pacific coral reef stomatopods through DNA barcoding of stomatopod larvae. *Proc Roy Soc B Biol Sci* 273: 2053-2061.

Bird, A. M., von Dassow, G., & Maslakova, S. A. (2014). How the pilidium larva grows. *EvoDevo* 5:10.

Chernyshev, A.V. (2001). The larvae of unarmed nemerteans in Peter the Great Bay (Sea of Japan). *Russ J Mar Biol* 27(1): 58-61.

Coe, W. R. (1901). Papers from the Harriman Alaska Expedition, 20 The nemerteans. *Proc Wash Acad Sciences* 3: 1-110

Davidson, E. H., Peterson, K. J., & Cameron, R. A. (1995). Origin of bilaterian body plans- evolution of developmental regulatory mechanisms. *Science* 270:1319-1325.

Dawydoff, C. (1940). Les formes larvaires de polyclades et de némertes du plankton Indochinois. [Larval forms of polyclads and nemerteans of Indochinese plankton]. *Bull Biol Fr Belg* 4:443–496.

De Queiroz, K. (2007). Species concepts and species delimitation. *Syst Biol* 56:879-886.

Desor, E. (1848). Embryology of Nemertes. *Proc Boston Nat Hist Soc* 6:1-18.

Emlet, R.B. (1991). Functional constraints on the evolution of larval forms of marine invertebrates: experimental and comparative evidence. *Am Zool* 31(4):707-725.

Emlet, R.B. (1994). Body form and patterns of ciliation in non-feeding larvae of echinoderms: functional solutions to swimming in plankton? *Am Zool* 34:570–585.

Folmer, O., Black, M., Hoeh, W., Lutz, R., & Vrijenhoek R. (1994). DNA primers for amplification of mitochondrial cytochrome c oxidase subunit I from diverse metazoan invertebrates. *Mol Mar Biol Biotech* 3:294–299.

Fontaneto, D., Flot, J. & Tang, C. Q. (2015). Guidelines for DNA taxonomy, with a focus on the meiofauna. *Mar Biodiv* 45:433-451.

Guindon, S. & Gascuel, O. (2003). A simple, fast, and accurate algorithm to estimate large phylogenies by maximum likelihood. *Syst Biol* 52(5):696-704.

Hasegawa, M., Kishino, K. & Yano, T. (1985). Dating the human-ape splitting by a molecular clock of mitochondrial DNA. *J Mol Evol* 22:160-174

Hebert, P.D.N., Cywinska, A., Ball, S.L., & deWaard, J.R. (2003). Biological identifications through DNA barcodes. *Proc R Soc* Lond. B 270:313–321.

Henry, J.Q. (2014). Spiralian model systems. *Int J Biol* 58:389-401.

Hiebert, T. C., G. von Dassow, L. S. Hiebert, & S. A. Maslakova. (2013). The peculiar nemertean larva pilidium recurvatum belongs to Riserius sp., a basal heteronemertean that eats *Carcinonemertes errans*, a hoplonemertean parasite of Dungeness crab. *Invert Biol* 132(3): 207-225.

Hiebert, L.S. & Maslakova, S.A. (2015). Hox genes pattern the anterior-posterior axis of the juvenile but not the larva in a maximally-indirect developing invertebrate, *Micrura alaskensis* (Nemertea). *BMC Biol* 13:23

Hiebert, T.C. (2016). New diversity discovered in the Northeast Pacific using surveys of both planktonic larvae and benthic adults. Oregon Institute of Marine Biology. Ph.D thesis. University of Oregon, Eugene, OR.

Hiebert, T.C. & Maslakova, S.A. (2015a). The pilidiophoran development of two NE Pacific nemertean species, an undescribed member of the Lineidae and *Micrura wilsoni* (Heteronemertea; Lineidae). *Biol Bull* 229(3): 265-275.

Hiebert, T.C. & Maslakova, S.A. (2015b). Integrative taxonomy of the *Micrura alaskensis* Coe, 1901 species complex (Heteronemertea; Nemertea), with descriptions of a new genus *Maculaura* gen. nov. and four new species from the NE Pacific. *Zool Sci* 32(5).

Hiebert, T.C., von Dassow, G., Hiebert, L.S., & Maslakova, S.A. (2013). The peculiar nemertean larva *pilidium recurvatum* belongs to *Riserius* sp., a basal heteronemertean that eats *Carcinonemertes errans*, a hoplonemertean parasite of Dungeness crab. *Invert Biol* 132(3): 207-225.

Hubrecht, A. A. W. (1886). Contributions to the embryology of nemerteans. *QJ Micr Sci* 26:417-448.

Huelsenbeck, J.P. & Ronquist, F. (2001). MRBAYES: Bayesian inference of phylogenetic trees. *Bioinformatics* 17(8):754-755.

Iwata, F. (1958). On the development of the nemertean *Micrura akkeshiensis*. *Embryologia* 4:103– 131.

Jörger, K.M., Norenburg, J.L., Wilson, N.G., & Schrödl, M. (2012). Barcoding against a paradox? Combined molecular species delineations reveal multiple cryptic lineages in elusive meiofaunal sea slugs. BMC *Evol. Biol* 12:245.

Jörger, K.M. & Schrödl, M. (2013). How to describe a cryptic species? Practical challenges of molecular taxonomy. *Front. Zoo.* 10:59

Kajihara, H., Chernyshev, A.V., Sun, S., Sundberg, P., & Crandall, F. (2008). Checklist of nemertean genera and species published between 1995 and 2007. *Species Div* 13:245–74.

Kearse, M., Moir, R., Wilson, A., Stones-Havas, S., Cheung, M., Sturrock, S., Buxton, S., Cooper, A., Markowitz, S., Duran, C., Thierer, T., Ashton, B., Meintjes, P., & Drummond, A. (2012). Geneious basic: an integrated and extendable desktop software platform for the organization and analysis of sequence data. *Bioinformatics* 28(12):1647-1649.

Kimura, M. (1981). Estimation of evolutionary distances between homologous nucleotide sequences. *Proc Nat Acad Sci USA* 78:454-458.

Knowles, L.L. & Carstens, B.C. (2007). Delimiting species without monophyletic gene trees. *Syst Biol* 56(6):887–895.

Kvist, S., Laumer, C. E., Junoy, J., & Giribet, G. (2014). New insights into the phylogeny, systematics and DNA barcoding of Nemertea. *Invert Systematics* 28: 287-308.

Lacalli, T. C. (1993). Ciliary bands in echinoderm larvae: evidence for structural homologies and a common plan. *Acta Zool* 74(2):127-133.

Lacalli, T. (2005). Diversity of form and behaviour among nemertean pilidium larvae. *Acta Zool* 86:267-276.

Littlewood, D.T. (1994). Molecular phylogenetics of cupped oysters based on partial 28S rRNA gene sequences. *Mol Phylo Evol* 3: 221-229.

Martîn-Durán, J.M., Vellutini, B.C., & Hejnol, A. (2015). Evolution and development of the adelphophagic, intracapsular Schmidt's larva of the nemertean *Lineus ruber*. *EvoDevo* 6:28

Maslakova, S.A. (2010a). Development to metamorphosis of the nemertean pilidium larva. *Front Zool* 7:30.

Maslakova, S.A. (2010b). The invention of the pilidium larva in an otherwise perfectly good spiralian phylum Nemertea. *Integ Comp Biol* 50: 734-743.

Maslakova, S.A. & Hiebert, T.C. (2014). From trochophore to pilidium and back again - a larva's journey. *Int J Devel Biol* 58: 585-591.

Maslakova, S.A., Martindale, M.Q., & Norenburg, J.L. (2004a). Fundamental properties of the spiralian developmental program are displayed by the basal nemertean *Carinoma tremaphoros* (Palaeonemertea, Nemertea). *Dev Biol* 267(2): 342-360.

Maslakova, S.A., Martindale, M.Q., & Norenburg, J.L. (2004b). Vestigial prototroch in a basal nemertean, *Carinoma tremaphoros* (Nemertea; Palaeonemertea). *Evol Dev* 6:219– 226.

Maslakova, S.A. & Norenburg, J.L. (2001). Phylogenetic study of pelagic nemerteans (Pelagica, Polystilifera). *Hydrobiologia* 456:111-132.

Maslakova, S.A. & von Dassow, G. (2012). A lecithotrophic pilidium with apparent prototroch and telotroch. *J Exp Zool B Mol Dev Evol* 10:47.

McDermott, J. J. & Roe, P. (1985). Food, Feeding Behavior and Feeding Ecology of Nemerteans. *Amer Zool* 25(1):113-125.

McEdward, L.R. & Miner, B.G. (2001). Larval and life-cycle patterns in echinoderms. *Can J Zool* 79:1125-1170.

Meyer, C.P. & Paulay, G. (2005). DNA barcoding: error rates based on comprehensive sampling. *PLoS Biol* 3(12): 2229-2238.

Mora, C., Tittensor, D.P., Adl, S., Simpson, A.G.B. & Worm, B. (2011). How many species are there on Earth and in the ocean? *PLoS Biol* 9(8).

Moran, A.L. (1999). Intracapsular feeding by embryos of the gastropod genus *Littorina*. *Biol Bull* 196:229-244.

Nielsen, C. (1987). Structure and function of metazoan ciliary bands and their phylogenetic significance. *Acta Zool* 68(4):205-262.

Norenburg, J. L. & Stricker, S. A. (2002). Phylum Nemertea. Pp. 163-177 *in* C. M. Young, M. A. Sewall, and M. E. Rice, eds. Atlas of Marine Invertebrate Larvae. Academic Press, San Diego.

Palumbi, S., Martin, A., Romano, S., McMillan, W.O., Stice, L., & Grabowski, G. (1991). The simple fools guide to PCR Version 2.0. Honolulu, HI: Department of Zoology Kewalo Marine Laboratory, University of Hawaii.

Pernet, B. (2003). Persistent ancestral feeding structures in nonfeeding annelid larvae. *Biol Bull* 205: 295–307.

Peterson, K.J. & Eernisse, D.J. (2001). Animal phylogeny and the ancestry of bilaterians: inferences from morphology and 18S rDNA gene sequences, *Evol Dev* 3(3): 170-205.

Posada, D. (2003). Using Modeltest and PAUP* to select a model of nucleotide substitution (In) Current Protocols in Bioinformatics (Baxevanis, A.D., Davison, D.B., Page, R.D.M., Petsko, G.A., Stein, L.D., & Stormo, G.D., Ed.). New York: John Wiley & Sons.

Posada, D. (2008). jModelTest: Phylogenetic model averaging. *Mol Biol Evol* 25(7): 1253-1256.

Puillandre, N., Lambert, A., Brouillet, S., & Achaz, G. (2011). ABGD, automatic barcode gap discovery for primary species delimitation. *Mol Ecol* 21:1864–1877

Rambaut, A. (2009). FigTree version 1.4.2 [http://tree.bio.ed.ac.uk/software/figtree/]

Roe, P., Norenburg, J.L. & Maslakova, S.A. (2007). Nemertea (In) The Light and Smith Manual: Intertidal Invertebrates from Central California to Oregon 4th Edition (Carlton, JT, Ed). University of California Press, Berkeley.

Rouse, G.W. (1999). Trochophore concepts: ciliary bands and the evolution of larvae in spiralian Metazoa. *Biol J Linn Soc* 66(4):411-464.

Schmidt, G.A. (1964). Embryonic development of littoral nemertines *Lineus desori* (Mihi, species nova) and *Lineus ruber* (O. F. Mülleri, 1774, G. A. Schmidt, 1945) in connection with ecological relation changes of mature individuals when forming the new species *Lineus ruber*. *Zool Pol* 14: 76-122.

Schwartz, M.L. (2009). Untying a Gordian Knot of Worms: Systematics and Taxonomy of the Pilidiophora (phylum Nemertea) from Multiple Data Sets. Columbian College of Arts and Sciences. Ph.D thesis. The George Washington University, Washington, DC.

Schwartz, M. L. & Norenburg, J. L. (2001). Can we infer heteronemertean phylogeny from available morphological data?. *Hydrobiologia* 456:165-174.

Schwartz, M. L. & Norenburg, J. L. (2005). Three new species of *Micrura* (Nemertea: Heteronemertea) and a new type of heteronemertean larva from the Caribbean Sea. *Caribb J Sci* 41:528-543.

Schwentner, M., Timms, B.V., & Richter, S. (2011). An integrative approach to species delineation incorporating different species concepts: a case study of *Limnadopsis* (Branchiopoda: Spinicaudata). *Biol J Linnean Soc* 104:575-599.

Strand, M., Herrera-Bachiller, A., Nygren, A., & Kanneby, T. (2014). A new nemertean species – What are the useful characters for ribbon worm descriptions? *J Mar Biol Assoc UK* 94(2): 317-330

Strand, M., Hjelmgren, A., & Sundberg, P. (2005). Genus *Baseodiscus* (Nemertea: Heteronemertea): Molecular identification of a new species in a phylogenetic context. *J Nat Hist* 39(44): 3785-3793.

Strand, M. & Sundberg, P. (2005). Delimiting species in the hoplonemertean genus *Tetrastemma* (phylum Nemertea): morphology is not concordant with phylogeny as evidence from mtDNA sequences. *Biol J Linn Soc* 86: 201–212.

Strathmann, R.R. (1985). Feeding and nonfeeding larval development and life-history evolution in marine invertebrates. *Annu Rev Ecol Syst* 16: 339–361.

Stricker, S. A. & Folsom, M. W. (1998). A comparative ultrastructural analysis of spermatogenesis in nemertean worms. *Hydrobiologia* 365: 55-72.

Sundberg, P. (2015). Thirty-five years of nemertean (Nemertea) research—past, present, and future. *Zool Sci* 32(6):501-506.

Sundberg, P., Chernyshev, A.V., Kajihara, H., Känneby, T. & Strand, M. (2009). Character-matrix based descriptions of two new nemertean (Nemertea) species. *Zool J Linnean Soc 157:264-294.*

Sundberg, P. & Strand, M. (2010). Nemertean taxonomy — time to change lane? *J Zool Syst Evol Res* 48(3):283-284.

Sundberg, P.E., Thuroczy Vodoti, E., & Strand, M. (2010). DNA barcoding should accompany taxonomy – the case of Cerebratulus spp (Nemertea). *Mol Ecol Resour* 10:274–281.

Tamura, K. & Nei, M. (1993). Estimation of the number of nucleotide substitutions in the control region of mitochondrial DNA in humans and chimpanzees. *Mol Biol Evol* 10:512-526.

Tavaré, S. (1986). Some probabilistic and statistical problems in the analysis of DNA sequences. *Lectures Math Life Sci* 17:57-86.

Thollesson, M. & Norenburg, J.L. (2003). Ribbon worm relationships—a phylogeny of the phylum Nemertea. *Biol Sci* 270:407-415.

Thompson, J.D., Gibson, T.J., Plewniak, F., Jeanmougin, F., & Higgins, D.G. (1997). The CLUSTAL_X Windows interface: flexible strategies for multiple sequence alignment aided by quality analysis tools. *Nucleic Acids Res* 25(24):4876-4882.

Turbeville, J.M. (2002). Progress in Nemertean Biology: Development and Phylogeny. *ICB* 42(3):692-703.

Turbeville, J. M., Field, K. G., & Raff, R. A. (1992). Phylogenetic position of phylum Nemertini, inferred from 18S-ribosomal-RNA sequences - molecular-data as a test of morphological character homology. *Mol Biol Evol* 9:235-249.

Turbeville, J. M. & Ruppert, E. E. (1985). Comparative ultrastructure and the evolution of nemertines. *Am Zool* 25:53-71.

van Velzen R, Weitschek E, Felici G, Bakker FT. (2012). DNA barcoding of recently diverged species: relative performance of matching methods. *PLoS ONE* 7(1):e30490.

von Dassow, G., Emlet, R.B., & Maslakova, S.A. (2013). How the pilidium larva feeds. *Front Zool* 10:47.

von Dassow, G. & Maslakova, S.A. (2013). How the pilidium larva pees. *ICB* 53:E386.

von Döhren, J. (2011). The fate of the larval epidermis of the Desor-larva of *Lineus viridis* (Pilidiophora, Nemertea) displays a historically constrained functional shift from planktotrophy to lecithotrophy. *Zoomorphology* 130(3): 189-196.

Wiens, J.J. (2007). Species delimitation: new approaches for discovering diversity. *Syst Biol* 56(6):875-878.

Wray, G.A. (1996). Parallel evolution of non-feeding larvae in echinoids. *Syst Biol* 45:308–322.

Zou S, Li Q, Kong L, Yu H, Zheng X. (2011). Comparing the usefulness of distance, monophyly and character-based DNA barcoding methods in species identification: a case study of neogastropoda. *PLoS ONE* 6(10):e26619.